

**BACK-END NUCLEAR FUEL CYCLE
OPTIONS: EFFECTS ON HIGH LEVEL WASTE
MANAGEMENT AND DISPOSAL**

**REAKTÖR SONRASI NÜKLEER YAKIT
ÇEVİRİMİ SEÇENEKLERİ: YÜKSEK AKTİVİTELİ
ATIK İDARESİ VE TASFİYESİ
ÜZERİNDEKİ ETKİLER**

BANU BULUT ACAR

Prof. Dr. H. OKAN ZABUNOĞLU

Supervisor

Submitted to Institute of Sciences of Hacettepe University
as a Partial Fulfilment to the Requirements
for the Award of the Degree of Doctor of Philosophy
in Nuclear Engineering

2013

This work named “**Back-end Nuclear Fuel Cycle Options: Effects on High Level Waste Management and Disposal**” by **BANU BULUT ACAR** has been approved as a thesis for the Degree of **DOCTOR of PHILOSOPHY in NUCLEAR ENGINEERING** by the below mentioned Examining Committee Members.

Head

Prof. Dr. C. Niyazi SÖKMEN

Supervisor

Prof. Dr. H. Okan ZABUNOĞLU

Member

Prof. Dr. Mehmet TOMBAKOĞLU

Member

Doç. Dr. Ayhan YILMAZER

Member

Doç. Dr. İlker TARI

This thesis has been approved as a thesis for the Degree of **DOCTOR of PHILOSOPHY in NUCLEAR ENGINEERING** by Board of Directors of the Institute for Graduate Studies in Science and Engineering.

Prof. Dr. Fatma SEVİN DÜZ

Director of the Institute of
Graduate Studies in Science
and Engineering

ETHICS

In this thesis study, prepared in accordance with the spelling rules of Institute of Graduate Studies in Science of Hacettepe University,

I declare that

- all the information and documents have been obtained in the base of the academic rules,
- all audio-visual and written information and results have been presented according to the rules of scientific ethics,
- in case of using others Works, related studies have been cited in accordance with the scientific standards,
- all cited studies have been fully referenced,
- I did not do any distortion in the data set,
- and any part of this thesis has not been presented as another thesis study at this or any other university.

.. /.. /2013

Banu BULUT ACAR

ABSTRACT

BACK-END NUCLEAR FUEL CYCLE OPTIONS: EFFECTS ON HIGH LEVEL WASTE MANAGEMENT AND DISPOSAL

Banu BULUT ACAR

Doctor of Philosophy, Department of Nuclear Engineering

Supervisor: Prof. Dr. H. Okan ZABUNOĞLU

December 2013, 112 pages

In this thesis, back end fuel cycle options for Pressurized Water Reactor are discussed in terms of effects on high level waste management and, more specifically, on geological disposal. Once-through and alternative closed nuclear fuel cycles for a typical Pressurized Water Reactor are compared with respect to waste disposal densities (waste disposal area required for spent fuel and high level waste) in a permanent geological repository and radiological toxicities of resultant wastes. In the first part of the study, utilizing the code MONTEBURNS, relevant compositions and decay heats of wastes generated in the considered fuel cycles are obtained for several selected burnup values. Then, using the code ANSYS, thermal analyses are performed for a reference repository concept and disposal areas needed for waste types under consideration are determined. A sensitivity analysis is also performed for evaluating the effect of variations in thermal properties of reference repository components on waste disposal densities. Results are expressed in terms of “total electrical energy (MWe-yr) produced per unit waste disposal area (m^2)”, which is taken as the decisive parameter to compare the cycles. As an alternative parameter to assess the effect of back end fuel cycle options on waste management and disposal, radiotoxicities of wastes generated in fuel cycles are also compared. The results of the disposal

density analysis indicates that: the once-through cycle displays an advantage up to nearly a burnup of 40000 MWd/t with regard to waste (spent fuel and high-level waste) disposal density; however, at higher burnups, the closed cycle with standard reprocessing is better than once-through and other closed fuel cycles. According to results of radiotoxicity analysis, closed cycle with MOX recycling is more advantageous than once-through and other closed cycles.

Keywords: Fuel cycle, Spent fuel, Repository, Monteburns, Ansys

ÖZET

REAKTÖR SONRASI NÜKLEER YAKIT ÇEVİRİMİ SEÇENEKLERİ: YÜKSEK AKTİVİTELİ ATIK İDARESİ VE TASFİYESİ ÜZERİNDEKİ ETKİLER

Banu BULUT ACAR

Doktora, Nükleer Enerji Mühendisliği Bölümü

Tez Danışmanı: Prof. Dr. H. Okan ZABUNOĞLU

Aralık 2013, 112 sayfa

Bu tezde, Basınçlı Su Reaktörü tipi bir reaktör için reaktör sonrası yakıt çevrimi seçenekleri yüksek aktiviteli atık idaresi, özellikle de jeolojik bertaraf üzerindeki etkileri yönünden irdelenmiştir. Açık yakıt çevrimi ile alternatif kapalı yakıt çevrimleri, oluşan atıkların jeolojik bertaraf yoğunlukları (kullanılmış yakıt ve yüksek seviyeli atığın tasfiyesi için gereken alan) ve radyolojik toksisiteleri açısından karşılaştırılmıştır. Çalışmanın ilk bölümünde, seçilmiş yanma miktarları için, yakıt çevrimlerinde oluşan atıkların kompozisyonları ve bozunma ısıları MONTEBURNS kodu kullanılarak elde edilmiştir. Daha sonra, ANSYS kodu kullanılarak bir referans jeolojik bertaraf tesisi tasarımı için ısı analizler yapılmış ve her bir atık tipi için gerekli bertaraf alanları belirlenmiştir. Referans bertaraf tasarımındaki bileşenlerin ısı özelliklerindeki değişimlerin atık bertaraf yoğunluğu üzerindeki etkisini değerlendirmek amacıyla ısı analizler farklı ısı özellikler kullanılarak tekrarlanmıştır. Sonuçlar, yakıt çevrimlerinin karşılaştırılması için belirleyici bir parametre olan “birim atık bertaraf alanı (m^2) başına üretilen toplam elektrik enerjisi (MWe-yr)” cinsinden ifade edilmiştir. Yakıt çevrimi seçeneklerinin atık yönetimi ve jeolojik bertaraf üzerindeki etkisini değerlendirmede alternatif bir

parametre olarak oluřan radyoaktif atıkların radyolojik toksisiteleri de karřılařtırılmıřtır. Atık bertarafı yoęunluęu ile ilgili analizlerin sonuęları 40000 MWd/t yanma oranına kadar aık yakıt evriminin avantajlı olduęunu gstermiřtir. Daha yksek yanma oranlarında ise standart yeniden iřleme uygulanan yakıt evrimi dięer yakıt evrimlerine gre daha avantajlı olmaktadır. Radyotoksosite analizlerinin sonuęlarına gre MOX yakıtının yeniden iřlendięi kapalı yakıt evrimi dięer kapalı yakıt evrimleri ve aık evrime gre daha avantajlıdır.

Anahtar Kelimeler: Yakıt evrimi, Kullanılmıř yakıt, Jeolojik bertaraf alanı, Monteburns, Ansys

ACKNOWLEDGEMENTS

I would like to express my deepest gratitude to my supervisor Prof. Dr. H. Okan Zabunođlu for his invaluable guidance and encouragement throughout this study.

I would like to express my special thanks to Prof. Dr. C. Niyazi Sökmen, Prof. Dr. Mehmet Tombakođlu, Assoc. Prof. Ayhan Yilmazer and Assoc. Prof. İlker Tarı for their valuable suggestions and comments as the examining committee members.

Finally, I would like to thank my husband Hakan and my parents for their support and understanding throughout this study.

TABLE OF CONTENTS

	<u>Page</u>
1. INTRODUCTION.....	1
2. THE NUCLEAR FUEL CYCLE	4
2.1. FRONT END OF THE NUCLEAR FUEL CYCLE	4
2.1.1. Uranium Mining and Milling.....	4
2.1.2. Conversion.....	4
2.1.3. Enrichment.....	5
2.2. BACK END OF THE NUCLEAR FUEL CYCLE	6
2.2.1. Spent Fuel Storage and Cooling	6
2.2.2. Reprocessing of Spent Fuel.....	6
2.2.3. Permanent Disposal.....	7
3. LITERATURE REVIEW	9
4. NUCLEAR FUEL CYCLE: ALTERNATIVES AND GENERATED WASTE FORMS	14
4.1. NUCLEAR FUEL CYCLE ALTERNATIVES	14
4.1.1. Once-through Cycle	14
4.1.2. Closed Cycle.....	14
4.1.2.1. Standard Reprocessing Cycle	15
4.1.2.2. Complete Co-processing Cycle	16
4.1.2.3. Partial Co-processing Cycle	17
4.1.2.4. Closed Cycle with Spent MOX: Standard Reprocessing and Recycling	17
4.2. DETERMINATION OF CHARACTERISTICS (COMPOSITIONS AND DECAY HEATS) OF WASTE TYPES UNDER CONSIDERATION	19
4.2.1. Reference Reactor.....	19
4.2.2. Monteburns Code	19
4.2.3. Waste Types under Consideration.....	22
4.2.4. About Burnup.....	22

4.2.5. Calculations and Results	23
4.2.5.1. Decay Heat Profiles	23
4.2.5.2. Decay Heat Rate Equations for the Waste Types under Consideration	31
5. REFERENCE REPOSITORY CONCEPT	33
5.1. WASTE PACKAGES	33
5.1.1. SF (SUOX and SMOX) Disposal Canisters	34
5.1.2. VHLW Disposal Canisters.....	35
5.2. BUFFER MATERIAL	35
5.3. BACKFILL MATERIAL.....	35
5.4. GEOLOGY	36
6. THERMAL ANALYSIS.....	37
6.1. ANSYS	37
6.1.1. The Finite Element Method.....	37
6.1.2. ANSYS Analysis Procedure.....	39
6.2. ANSYS MODEL OF THE SYSTEM.....	44
6.2.1. Thermal Model.....	44
6.2.2. Finite Element Model	44
6.3. RESULTS.....	48
6.3.1. Minimum Distance between SUOX Loaded Canisters.....	48
6.3.2. Minimum Distance between HLW Loaded Canisters.....	50
6.3.3. Minimum Distance between SMOX _{SRNU} Loaded Canisters.....	51
6.3.4. Minimum Distance between SMOX _{SRDU} Loaded Canisters.....	52
6.3.5. Minimum Distance between SMOX _{CCPu} Loaded Canisters.....	54
6.3.6. Minimum Distance between SMOX _{CCEU} Loaded Canisters.....	55
6.3.7. Minimum Distance between SMOX _{PC} Loaded Canisters	57
6.3.8. Minimum Distance between SRC-MOX _{SRNU} Loaded Canisters	58

7. DISPOSAL DENSITY CALCULATIONS.....	60
7.1. DISPOSAL AREA CALCULATIONS	60
7.1.1. Disposal Area Needed per Unit Mass of Each Waste Type.....	60
7.1.2. Total Disposal Area Needed for Each Fuel Cycle.....	62
7.2. COMPARISON OF FUEL CYCLES	65
8. RADIOTOXICITY CALCULATIONS	69
8.1. RADIOTOXICITY CALCULATIONS FOR WASTES	70
8.2. COMPARISON OF FUEL CYCLES	74
9. CONCLUSION	77
APPENDIX I: SRcU COMPOSITIONS AND DECAY HEATS	78
APPENDIX II: DECAY HEAT CURVE FITS FOR WASTE TYPES UNDER CONSIDERATION	82
APPENDIX III: THERMAL ANALYSES AND DISPOSAL DENSITY CALCULATIONS FOR 100 YEARS COOLING TIME	106
APPENDIX IV: RESULTS OF THERMAL ANALYSIS FOR VHLW DISPOSAL CANISTER LOADED WITH % 15 WASTE AND 3 VHLW CYLINDERS	108
APPENDIX V: SENSITIVITY ANALYSIS FOR ROCK THERMAL PROPERTIES	111
APPENDIX VI: RESULTS OF THERMAL ANALYSIS FOR 100 °C TEMPERATURE LIMIT	112

LIST OF FIGURES

	<u>Page</u>
Figure 2.1. Generalized nuclear fuel cycle	5
Figure 2.2. Schematic representation of a multi-barrier concept in geological disposal [1]	8
Figure 4.1. OT cycle	14
Figure 4.2. SR cycle	16
Figure 4.3. CC cycle	17
Figure 4.4. PC cycle	18
Figure 4.5. SRNU-RcMOX cycle	18
Figure 4.6. Computational flow diagram	20
Figure 4.7. Interaction of MONTEBURNS with MCNP and ORIGEN2 [34]	22
Figure 4.8. Decay heat profiles of SUOX burned to 33000, 40000 and 50000 MWd/tU	23
Figure 4.9. Decay heat outputs for HLWs per equivalent ton of reprocessed heavy metal	25
Figure 4.10. Decay heat profiles of SMOX _{SRNU} burned to 33000, 40000 and 50000 MWd/tHM	26
Figure 4.11. Decay heat profiles of SMOX _{SRDU} burned to 33000, 40000 and 50000 MWd/tHM	27
Figure 4.12. Decay heat profiles of SMOX _{CCPu} burned to 33000, 40000 and 50000 MWd/tHM	28
Figure 4.13. Decay heat profiles of SMOX _{CCEU} burned to 33000, 40000 and 50000 MWd/tHM	29
Figure 4.14. Decay heat profiles of SMOX _{PC} burned to 33000, 40000 and 50000 MWd/tHM	29
Figure 4.15. Decay heat profiles of SRC-MOX _{SRNU} burned to 33000, 40000 and 50000 MWd/tHM	30
Figure 5.1. UK HLW/SF repository concept [33].....	33
Figure 5.2. SF disposal canister [33]	34
Figure 5.3. VHLW disposal canister [33]	35

Figure 6.1. One dimensional linear element [44]	38
Figure 6.2. (a) Free meshing, (b) Mapped meshing [46]	42
Figure 6.3. Solid model of repository created using ANSYS	45
Figure 6.4. SOLID87 element geometry [46].....	46
Figure 6.5. 3-D meshed model of repository	46
Figure 6.6. Temperature as a function of time on the canister surface and at the interface between bentonite and rock, spacing 3.90 m, SUOX with 33000 MWd/tHM burnup	49
Figure 6.7. Temperature as a function of time on the canister surface and at the interface between bentonite and rock, spacing 5.54 m, SUOX with 40000 MWd/tHM burnup	49
Figure 6.8. Temperature as a function of time on the canister surface and at the interface between bentonite and rock, spacing 10.00 m, SUOX with 50000 MWd/tHM burnup	49
Figure 6.9. Temperature as a function of time on the canister surface and at the interface between bentonite and rock, spacing 4.00 m, HLW from reprocessing of 33000 MWd/tHM burnup SUOX	50
Figure 6.10. Temperature as a function of time on the canister surface and at the interface between bentonite and rock, spacing 3.90 m, HLW from reprocessing of 40000 MWd/tHM burnup SUOX	50
Figure 6.11. Temperature as a function of time on the canister surface and at the interface between bentonite and rock, spacing 3.90 m, HLW from reprocessing of 50000 MWd/tHM burnup SUOX	51
Figure 6.12. Temperature as a function of time on the canister surface and at the interface between bentonite and rock, spacing 3.00 m, SMOX _{SRNU} with 33000 MWd/tHM burnup	51
Figure 6.13. Temperature as a function of time on the canister surface and at the interface between bentonite and rock, spacing 4.80 m, SMOX _{SRNU} with 40000 MWd/tHM burnup	52
Figure 6.14. Temperature as a function of time on the canister surface and at the interface between bentonite and rock, spacing 13.00 m, SMOX _{SRNU} with 50000 MWd/tHM burnup	52

Figure 6.15. Temperature as a function of time on the canister surface and at the interface between bentonite and rock, spacing 3.42 m, SMOX _{SRDU} with 33000 MWd/tHM burnup	53
Figure 6.16. Temperature as a function of time on the canister surface and at the interface between bentonite and rock, spacing 5.54 m, SMOX _{SRDU} with 40000 MWd/tHM burnup	53
Figure 6.17. Temperature as a function of time on the canister surface and at the interface between bentonite and rock, spacing 18.80 m, SMOX _{SRDU} with 50000 MWd/tHM burnup	53
Figure 6.18. Temperature as a function of time on the canister surface and at the interface between bentonite and rock, spacing 3.10 m, SMOX _{CCPU} with 33000 MWd/tHM burnup	54
Figure 6.19. Temperature as a function of time on the canister surface and at the interface between bentonite and rock, spacing 5.00 m, SMOX _{CCPU} with 40000 MWd/tHM burnup	54
Figure 6.20. Temperature as a function of time on the canister surface and at the interface between bentonite and rock, spacing 16.00 m, SMOX _{CCPU} with 50000 MWd/tHM burnup	55
Figure 6.21. Temperature as a function of time on the canister surface and at the interface between bentonite and rock, spacing 5.80 m, SMOX _{CCEU} with 33000 MWd/tHM burnup	56
Figure 6.22. Temperature as a function of time on the canister surface and at the interface between bentonite and rock, spacing 9.50 m, SMOX _{CCEU} with 40000 MWd/tHM burnup	56
Figure 6.23. Temperature as a function of time on the canister surface and at the interface between bentonite and rock, SMOX _{CCEU} with 50000 MWd/tHM burnup	56
Figure 6.24. Temperature as a function of time on the canister surface and at the interface between bentonite and rock, spacing 3.10 m, SMOX _{PC} with 33000 MWd/tHM burnup	57
Figure 6.25. Temperature as a function of time on the canister surface and at the interface between bentonite and rock, spacing 4.94 m, SMOX _{PC} with 40000 MWd/tHM burnup	57
Figure 6.26. Temperature as a function of time on the canister surface and at the interface between bentonite and rock, spacing 13.70 m, SMOX _{PC} with 50000 MWd/tHM burnup	58

Figure 6.27. Temperature as a function of time on the canister surface and at the interface between bentonite and rock, spacing 12.60 m, SRc-MOX _{SRNU} with 33000 MWd/tHM burnup	59
Figure 6.28. Temperature as a function of time on the canister surface and at the interface between bentonite and rock, SRc-MOX _{SRNU} with 40000 MWd/tHM burnup	59
Figure 6.29. Temperature as a function of time on the canister surface and at the interface between bentonite and rock, SRc-MOX _{SRNU} with 50000 MWd/tU burnup	59
Figure 8.1. Radioactivities of wastes for 33000 MWd/tHM burnup	71
Figure 8.2. Radioactivities of wastes for 40000 MWd/tHM burnup	71
Figure 8.3. Radioactivities of wastes for 50000 MWd/tHM burnup	72
Figure 8.4. Ingestion radiotoxicities of wastes for 33000 MWd/tHM burnup	72
Figure 8.5. Ingestion radiotoxicities of wastes for 40000 MWd/tHM burnup	73
Figure 8.6. Ingestion radiotoxicities of wastes for 50000 MWd/tHM burnup	73
Figure A.I.1. Decay heat profiles of SRcU burned to 33000, 40000 and 50000 MWd/tHM	78
Figure A.I.2. (a) Exponential fit of decay heat of SRcU with 33000 MWd/tHM, (b) Values of coefficients in Put's Formula.....	79
Figure A.I.3. (a) Exponential fit of decay heat of SRcU with 40000 MWd/tHM, (b) Values of coefficients in Put's Formula.....	80
Figure A.I.4. (a) Exponential fit of decay heat of SRcU with 50000 MWd/tHM, (b) Values of coefficients in Put's Formula.....	81
Figure A.II.1. (a) Exponential fit of decay heat of SUOX with 33000 MWd/tHM, (b) Values of coefficients in Put's Formula.....	82
Figure A.II.2. (a) Exponential fit of decay heat of SUOX with 40000 MWd/tHM, (b) Values of coefficients in Put's Formula.....	83
Figure A.II.3. (a) Exponential fit of decay heat of SUOX with 50000 MWd/tHM, (b) Values of coefficients in Put's Formula.....	84
Figure A.II.4. (a) Exponential fit of decay heat of HLW with 33000 MWd/tHM, (b) Values of coefficients in Put's Formula.....	85

Figure A.II.5. (a) Exponential fit of decay heat of HLW with 40000 MWd/tHM, (b) Values of coefficients in Put's Formula.....	86
Figure A.II.6. (a) Exponential fit of decay heat of HLW with 50000 MWd/tHM, (b) Values of coefficients in Put's Formula.....	87
Figure A.II.7. (a) Exponential fit of decay heat of $SMOX_{SRNU}$ with 33000 MWd/tHM, (b) Values of coefficients in Put's Formula	88
Figure A.II.8. (a) Exponential fit of decay heat of $SMOX_{SRNU}$ with 40000 MWd/tHM, (b) Values of coefficients in Put's Formula	89
Figure A.II.9. (a) Exponential fit of decay heat of $SMOX_{SRNU}$ with 50000 MWd/tHM, (b) Values of coefficients in Put's Formula	90
Figure A.II.10. (a) Exponential fit of decay heat of $SMOX_{SRDU}$ with 33000 MWd/tHM, (b) Values of coefficients in Put's Formula	91
Figure A.II.11. (a) Exponential fit of decay heat of $SMOX_{SRDU}$ with 40000 MWd/tHM, (b) Values of coefficients in Put's Formula	92
Figure A.II.12. (a) Exponential fit of decay heat of $SMOX_{SRDU}$ with 50000 MWd/tHM, (b) Values of coefficients in Put's Formula	93
Figure A.II.13. (a) Exponential fit of decay heat of $SMOX_{CCPu}$ with 33000 MWd/tHM, (b) Values of coefficients in Put's Formula	94
Figure A.II.14. (a) Exponential fit of decay heat of $SMOX_{CCPu}$ with 40000 MWd/tHM, (b) Values of coefficients in Put's Formula	95
Figure A.II.15. (a) Exponential fit of decay heat of $SMOX_{CCPu}$ with 50000 MWd/tHM, (b) Values of coefficients in Put's Formula	96
Figure A.II.16. (a) Exponential fit of decay heat of $SMOX_{CCEU}$ with 33000 MWd/tHM, (b) Values of coefficients in Put's Formula	97
Figure A.II.17. (a) Exponential fit of decay heat of $SMOX_{CCEU}$ with 40000 MWd/tHM, (b) Values of coefficients in Put's Formula	98
Figure A.II.18. (a) Exponential fit of decay heat of $SMOX_{CCEU}$ with 50000 MWd/tHM, (b) Values of coefficients in Put's Formula	99
Figure A.II.19. (a) Exponential fit of decay heat of $SMOX_{PC}$ with 33000 MWd/tHM, (b) Values of coefficients in Put's Formula	100
Figure A.II.20. (a) Exponential fit of decay heat of $SMOX_{PC}$ with 40000 MWd/tHM, (b) Values of coefficients in Put's Formula	101

Figure A.II.21. (a) Exponential fit of decay heat of SMOX_{PC} with 50000 MWd/tHM, (b) Values of coefficients in Put's Formula	102
Figure A.II.22. (a) Exponential fit of decay heat of $\text{SRC-MOX}_{\text{SRNU}}$ with 33000 MWd/tHM, (b) Values of coefficients in Put's Formula	103
Figure A.II.23. (a) Exponential fit of decay heat of $\text{SRC-MOX}_{\text{SRNU}}$ with 40000 MWd/tHM, (b) Values of coefficients in Put's Formula	104
Figure A.II.24. (a) Exponential fit of decay heat of $\text{SRC-MOX}_{\text{SRNU}}$ with 50000 MWd/tHM, (b) Values of coefficients in Put's Formula	105
Figure A.IV.1. Temperature as a function of time on the canister surface and at the interface between bentonite and rock, spacing 10 m, % 15 w/o HLW in glass frit from reprocessing of 33000 MWd/tHM burnup SUOX.....	108
Figure A.IV.2. Temperature as a function of time on the canister surface and at the interface between bentonite and rock, spacing 10 m, % 15 w/o HLW in glass frit from reprocessing of 40000 MWd/tHM burnup SUOX.....	108
Figure A.IV.3. Temperature as a function of time on the canister surface and at the interface between bentonite and rock, spacing 10 m, % 15 w/o HLW in glass frit from reprocessing of 50000 MWd/tHM burnup SUOX.....	109
Figure A.IV.4. Temperature as a function of time on the canister surface and at the interface between bentonite and rock, spacing 7 m, 3 VHLW cylinders in disposal canister, 33000 MWd/tHM burnup.....	109
Figure A.IV.5. Temperature as a function of time on the canister surface and at the interface between bentonite and rock, spacing 6.7 m, 3 VHLW cylinders in disposal canister, 40000 MWd/tHM burnup.....	110
Figure A.IV.6. Temperature as a function of time on the canister surface and at the interface between bentonite and rock, spacing 6.7 m, 3 VHLW cylinders in disposal canister, 50000 MWd/tHM burnup.....	110

LIST OF TABLES

	<u>Page</u>
Table 4.1. Review of fuel cycle scenarios and resultant waste types	22
Table 4.2. Isotopic compositions of U and Pu in 5 year cooled SUOX for 33000, 40000 and 50000 MWd/tU burnups.....	24
Table 4.3. Values of the coefficients in Put's formula for the waste types under consideration	32
Table 6.1. Thermal properties of materials used in the thermal model of repository [47, 48]	47
Table 7.1. Minimum distance between canisters and disposal area needed per ton of each waste type	61
Table 7.2. Amount of wastes generated in each fuel cycle per ton of fresh U fuel loaded into the reactor.....	63
Table 7.3. Total disposal area needed in each fuel cycle.....	64
Table 7.4. Energy produced in each fuel cycle per ton of fresh U fuel loaded into the reactor	67
Table 7.5. Results of disposal density calculations for fuel cycles.....	68
Table 8.1. Decay times for waste types.....	75
Table 8.2. Average decay times for fuel cycles	76
Table A.III.1. Minimum distance between canisters and disposal area needed per ton of each waste type (100 years cooling time)	106
Table A.III.2. Results of disposal density calculations for fuel cycles (100 years cooling).....	107
Table A.V.1. Disposal area needed per ton of waste (sensitivity analysis).....	111
Table A.V.2. Disposal densities for OT and SRNU fuel cycles (sensitivity analysis)	111
Table A.VI.1. Minimum distance between canisters and disposal area needed per ton of each waste type (100 °C thermal constraint).....	112
Table A.VI.2. Results for fuel cycles (100 °C thermal constraint)	112

LIST OF ACRONYMS

SF	Spent Fuel
FPS	Fission Products
OT	Once-Through
HLW	High Level Waste
PWR	Pressurized Water Reactor
LWR	Light Water Reactor
w/o	Weight Percent
U	Uranium
Pu	Plutonium
PUREX	Plutonium Uranium Reduction and Extraction
MOX	Mixed Oxide Fuel
REDOX	Reduction and Oxidation
BUTEX	Butoxy-diethyl-ether
TBP	Tributyl Phosphate
VHLW	Vitrified High Level Waste
SR	Standard Reprocessing Cycle
SUOX	Spent Uranium Oxide
RU	Recovered Uranium
NU	Natural Uranium
DU	Depleted Uranium
CC	Complete Co-processing Cycle
SRNU	Standard Reprocessing Cycle with Natural Uranium Fertile Makeup Material
SRDU	Standard Reprocessing Cycle with Depleted Uranium Fertile Makeup Material
RcU	Recycled Uranium

SRcU	Spent Recycled Uranium
SMOX	Spent Mixed Oxide Fuel
SMOX _{SRNU}	Spent Mixed Oxide Fuel Generated from Standard Reprocessing Cycle with Natural Uranium Fertile Makeup Material
SMOX _{SRDU}	Spent Mixed Oxide Fuel Generated from Standard Reprocessing Cycle with Depleted Uranium Fertile Makeup Material
EU	Enriched Uranium
CCEU	Complete Co-processing Cycle with Enriched Uranium Fissile Makeup
CCPu	Complete Co-processing Cycle with Plutonium Fissile Makeup
SMOX _{CCEU}	Spent Mixed Oxide Fuel Generated from Complete Co-processing Cycle with Enriched Uranium Fissile Makeup
SMOX _{CCPu}	Spent Mixed Oxide Fuel Generated from Complete Co-processing Cycle with Plutonium Fissile Makeup
PC	Partial Co-processing
SMOX _{PC}	Spent Mixed Oxide Fuel Generated from Partial Co-processing
SRNU-RcMOX	Closed Cycle with Spent Mixed Oxide Fuel Standard Reprocessing and Recycling
RcMOX _{SRNU}	Recycled Mixed Oxide Fuel
SRc-MOX _{SRNU}	Spent Recycled Mixed Oxide Fuel
HM	Heavy Metal
DAAF	Disposal-Area Advantage Factor
SKB	Swedish Nuclear Fuel and Waste Company
FEM	Finite Element Method
CAD	Computer-Aided Drawing
DOF	Degree of Freedom

1. INTRODUCTION

The nuclear fuel cycle includes manufacturing of fresh fuel, irradiation of the fuel in a reactor and management of spent fuel (SF). All activities taking place before irradiation in a reactor form the “front-end” of the fuel cycle. The “back-end” of the fuel cycle, which covers all SF management activities, starts with the discharge of SF from the reactor.

SF discharged from a reactor contains fissile isotopes, fertile isotopes, fission products (FPs) and several actinides. SF can be disposed of directly or reprocessed in order to recover valuable materials in it. If SF is not reprocessed, the nuclear fuel cycle is called “once-through cycle” (OT) or open cycle. In OT cycle, after necessary storage periods, SF is planned to be directly disposed of in a permanent disposal facility. If SF is reprocessed, the nuclear fuel cycle is named “closed cycle”. By reprocessing, fissile and fertile isotopes are separated from FPs and other actinides and barren materials are put into a proper form to be disposed of as high-level waste (HLW).

SF discharged from a typical Pressurized Water Reactor (PWR) contains roughly 95 weight percent (w/o) uranium (U) and 1 w/o plutonium (Pu); the remainder consists of FPs and other actinides. By the standard methods of reprocessing, U and Pu contained in SF can be recovered as pure and separate streams. Alternative schemes referred to as “co-processing” can also be devised to recover U and Pu in SF as a mixture. Reprocessing scheme selected in the back end of the fuel cycle changes the isotopic composition of recovered materials and the type and amount of waste that needs disposal.

The permanent disposal method widely accepted for SF/HLW is the geological disposal. In geological disposal, canisters containing SF/HLW are simply placed into boreholes in a geological formation deep underground, specifically selected for final disposal of nuclear wastes. The design of the geological repository depends on density of waste disposal. Waste disposal density is the amount of waste that can be safely emplaced per unit area of the geological repository and strongly depends on the characteristics (amount, isotopic composition, decay heat profile etc.) of the nuclear waste.

In the present study, back end fuel cycle options for PWR are discussed in terms of effects on HLW management and, more specifically, on geological disposal. OT and alternative closed nuclear fuel cycles for a typical PWR are compared with respect to disposal densities in a permanent geological repository and radiological toxicities of wastes generated.

This study is completed in three steps. In the first step, fuel cycle scenarios used in the evaluations are developed by using different back end fuel cycle options for fuel removed from the reference reactor. Resulting waste forms arising from considered fuel cycles are identified and volumes and compositions of them are estimated.

In the second step, disposal areas needed per unit mass of waste types under consideration are determined using the results of the first step and performing the thermal analysis. Thermal analysis is performed for a reference repository concept by using finite element method.

In the third step, by connecting the disposal areas to the amounts of wastes to be disposed of and the electricity generated in each fuel cycle, the fuel cycles under consideration are compared. First, total amounts of waste types produced and total disposal areas required per unit mass of fresh fuel loaded into the reactor in each fuel cycle are calculated. Then, results are converted to “total electrical energy (MWe-yr) produced per unit waste disposal area (m^2)”, which is taken as the conclusive parameter to compare the fuel cycles under consideration with regard to waste disposal density. At the end of the third step, effects of the fuel cycle options on waste management are discussed from a radiological perspective.

This thesis is structured in the following manner:

In second chapter a general nuclear fuel cycle is introduced. A review of previous studies on back end nuclear fuel cycle and geological disposal is presented in the third chapter. The fourth chapter includes description of nuclear fuel cycle scenarios considered in the study and determination of characteristics of waste forms generated in these fuel cycles. The reference geological repository concept is described in the fifth chapter. The thermal analysis, which is the basis of disposal density calculations, forms the subject of the sixth chapter. Waste

disposal density calculations and comparison of fuel cycles are presented in the seventh chapter. Eighth chapter of the thesis includes the comparison of radiological toxicities of fuel cycles. Conclusions and recommendations for future work are given in the final chapter, the ninth. Supporting information can be found in the appendices.

2. THE NUCLEAR FUEL CYCLE

This introductory chapter covers a general overview of nuclear fuel cycle. The nuclear fuel cycle starts with exploring and mining of the uranium and ends with permanent disposal of nuclear wastes. The cycle consists of “front-end” processes that occur before fuel sent to reactor and “back-end” steps that take place after SF is discharged from reactor. The processes included in the back-end categorize the fuel cycle either as “open” or “closed”. When the SF is reprocessed and recovered materials are recycled, the cycle becomes “closed”. If SF is not reprocessed, the cycle is “open”. Figure 2.1 exhibits a general flow diagram of the nuclear fuel cycle.

2.1. FRONT END OF THE NUCLEAR FUEL CYCLE

The front-end of the nuclear fuel cycle involves uranium ore mining and milling, conversion, enrichment and fuel fabrication steps.

2.1.1. Uranium Mining and Milling

Uranium is the primary fuel for conventional nuclear power plants. It is a naturally occurring element and widely distributed in the earth’s crust. Naturally occurring uranium consists of about 99.3% U-238, 0.71% U-235 and trace amount of U-234. U-235 is the fissile isotope of uranium which can be used as nuclear fuel, but its concentration has to be increased with enrichment process.

Uranium ore can be mined by surface (open-cut) and underground mining techniques. After mining, grinding and chemical leaching processes are applied in order to obtain uranium concentrate (U_3O_8). Uranium concentrate is a powder form material which can be used in the next steps of the nuclear fuel cycle.

2.1.2. Conversion

Before the enrichment, uranium concentrate (U_3O_8) needs to be converted to uranium hexafluoride (UF_6) in gaseous form. The conversion process consists of removing impurities and combining the purified uranium with fluorine to create the UF_6 gaseous.

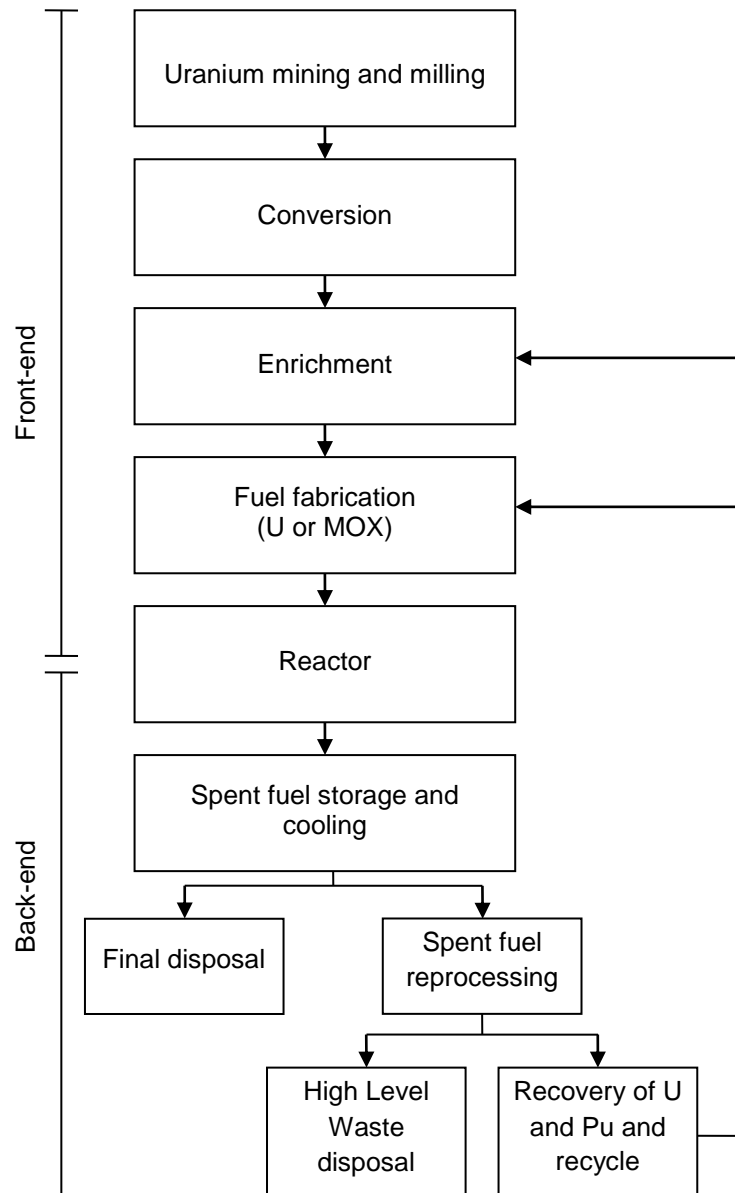


Figure 2.1. Generalized nuclear fuel cycle

2.1.3. Enrichment

Since natural uranium contains only about 0.71 percent of the U-235 isotope and nuclear reactor (Light Water Reactor) fuel has to have higher percentages of U-235, an enrichment step is necessary. Enrichment is done by an isotope separation technique based on the mass difference between U-235 and U-238 isotopes. Gaseous diffusion and gas centrifuge are the only methods commercially used to enrich U.

2.1.4. Fabrication

Fabrication is the final step of the front-end of the nuclear fuel cycle. After the enrichment, UF_6 is sent to a fuel fabrication plant where it is converted to uranium dioxide and manufactured into fuel pellets. These pellets are loaded into cylindrical metal tubes and fuel rods are produced. Then, the rods are put together to form a fuel assembly which is ready for use in the nuclear reactor.

2.2. BACK END OF THE NUCLEAR FUEL CYCLE

Back-end of the nuclear fuel cycle starts with the discharge of SF from the reactor. The back-end fuel cycle processes differ depending on the SF management strategy. There are two SF management options: Direct disposal and reprocessing. In the direct disposal option, SF is sent to permanent disposal after an interim storage period. In the reprocessing option, SF is reprocessed after a sufficient cooling period to recover usable isotopes in it. The recovered materials are then recycled in the reactors. The waste materials are put into a proper form to be disposed of as HLW. HLW is sent to permanent disposal after a storage period if cooling is necessary.

2.2.1. Spent Fuel Storage and Cooling

SF discharged from reactor is highly radioactive and generates significant amount of heat. It has to be shielded and cooled before the further steps of back-end fuel cycle. After removal from the reactor, SF must be stored in water-filled pools at the reactor facility. This initial cooling period lasts at least 150 days and reduces both radioactivity and decay heat of SF to a level that is safe to transport. If pool capacity is enough, SF is normally stored in the cooling pool before being sent for reprocessing or permanent disposal. When there is no room in the pool, the oldest SF is transferred from the pools on site to interim storage facilities and stored there until it is reprocessed or permanently disposed of. Wet storage in pools and dry cask storage are the most widely used interim storage methods.

2.2.2. Reprocessing of Spent Fuel

SF discharged from a reactor contains fissile isotopes (U-235, Pu-239) and fertile isotopes (U-238), highly radioactive FPs and several actinides. SF can be reprocessed to recover valuable materials (fissile and fertile isotopes) contained in

it. Recovered fissile and fertile isotopes can be converted to fuel and recycled in the reactors.

Several chemical processes exist to perform reprocessing. All current commercial reprocessing plants use the PUREX (Plutonium Uranium Reduction and Extraction) solvent extraction method. U and Pu can be recovered separately or as a solution of U+Pu, depending on the reprocessing scheme applied.

In the standard purex, U and Pu are recovered in highly pure forms. U and Pu are first separated from FP's and other actinides, and then from each other. The recovered U can be re-enriched, re-fabricated and re-fed into a nuclear reactor. The Pu product is mixed with natural U or depleted U in order to produce mixed oxide (MOX) fuel with an appropriate fissile content and reintroduced to the reactor.

In complete co-processing, U and Pu are not separated from each other throughout the entire process. The only product of complete co-processing is a mixed U+Pu solution with a fissile content of approximately that of the SF solution. This solution is blended with a fissile makeup material for producing MOX with a proper fissile content.

In partial co-processing, one pure U product stream and one mixed uranium-plutonium (U+Pu) product stream are produced. Mixed uranium-plutonium stream has about the necessary fissile content that MOX fuel must have, so only small adjustments are required.

2.2.3. Permanent Disposal

Permanent disposal is the emplacement of radioactive wastes in an appropriate facility without the intention of retrieval. In the direct disposal option, SF itself is considered as high level waste because of its high level of radioactivity and sent to permanent disposal after an interim storage period. In the reprocessing option, the waste materials remaining after recovery of U and Pu are put into a proper form to be disposed of as HLW. HLW is sent to permanent disposal after a cooling period.

The final (permanent) disposal method widely accepted for SF/HLW is the geological disposal. In geological disposal, canisters containing SF/HLW are simply placed into boreholes in a geological formation deep underground,

specifically selected for final disposal. The geological formation should be stable and deep enough to avoid surface events and to prevent accidental or intentional access to wastes in the long run. Crystalline rock (granite, welded tuff and basalt), salt and clay are the most suitable formations for geological disposal.

There are many different geological disposal concepts depending on the geological setting, engineered components and waste emplacement mode adopted. But, all of the concepts are based on the multi-barrier system that ensures the long term safety of the waste. In the multi-barrier system, the solid waste material, the waste containers, the engineered components of the repository and the surrounding geological environment work in concert to isolate the radioactive and toxic components. A schematic representation of a multi-barrier concept is provided in Figure 2.2 [1]. The principle applied in the multiple-barrier concept is: the canister isolates, the buffer seals and the rock protects [2]. Type of radioactive waste (SF/HLW) and geological environment of the repository determine the design of the multi-barrier system. Canisters and buffer materials are selected by considering these two factors.

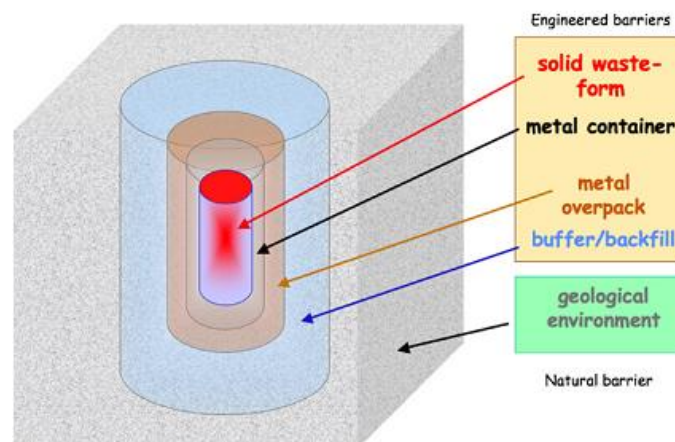


Figure 2.2. Schematic representation of a multi-barrier concept in geological disposal [1]

3. LITERATURE REVIEW

The nuclear power plants have been operating for over half a century. SF/HLW containing radioactive materials has since then been generated by reactors. Because of the radioactive materials in it, SF/HLW potentially hazardous for thousands of years, and it must be managed for very long-term. The management of the SF/HLW from the time it is discharged from the reactor until to disposal forms the back-end of the nuclear fuel cycle. Back-end fuel cycle options and permanent disposal solutions are important for the sustainability of nuclear industry. This chapter is a summarization of relevant findings from review of literature pertaining to back-end nuclear fuel cycles for PWR reactors and permanent waste disposal.

For the back-end of nuclear fuel cycle, two different options have been proposed: OT and closed cycle with standard reprocessing. Reprocessing of SF from light water reactors is commercially available today. The first reprocessing operations were set up for the extraction of Pu for the military purposes and carried out with a bismuth phosphate process. Many methods for Pu separation were considered, but solvent extraction was selected as the most suitable reprocessing method [3]. The first solvent extraction method used for large scale separation of U and Pu from SF was the REDOX (Reduction and Oxidation) process. The process was developed at Argonne National Laboratory, and installed by the General Electric Company at Hanford plant in 1951 [4]. A slightly different process, called BUTEX (Butoxy-diethyl-ether) was developed by a group of British chemists and adopted for large scale separation of U and Pu from SF. Because of the chemical engineering type problems in both REDOX and BUTEX, PUREX method was developed [3]. PUREX process involves dissolving the fuel elements in a nitric acid and solvent extraction of plutonium and uranium with tributyl phosphate (TBP) in hydrocarbon diluents. First, SF is chopped into small pieces and dissolved in nitric acid. Then, the nitric acid solution, which contains U and Pu, is subjected to a solvent extraction process using TBP. U and Pu are selectively taken up in the TBP phase and separated from the FPs and minor actinides. The U and Pu are then separated in multi-stage extraction cycles and purified [4]. PUREX was first developed by Knolls Atomic Power Laboratory at Oak Ridge National Laboratory

in 1952. Large reprocessing plant based on the PUREX process started operating in 1954 at Savannah River. Since the opening of the first PUREX plant at Savannah River in 1954, considerable amount of experience has been gained in PUREX reprocessing technology and PUREX is still being used in all commercial reprocessing plants currently operating [5].

During the past 70 years, various PUREX flowsheets and alternative reprocessing options have been proposed in order to reduce the volume and radiotoxicity of the waste sent for final disposal. PUREX with additional separations, PUREX with different solvents, COEX and UREX technologies are the most discussed proposals. The COEX process is a simplification of PUREX and separates U and Pu together. Zabunoğlu and Ozdemir [6] constructed the flowsheet of COEX. In UREX, pure stream of U is separated. UREX basically uses the same process as PUREX with addition of acetohydroxamic acid which reduces the extractability of plutonium and neptunium [7].

Recent studies are focussed on comparison of these alternative reprocessing schemes. In a study performed by Eccles [8] application of separation technologies, in particular solvent extraction and ion exchange in the uranium nuclear fuel cycle is discussed. Chandler [9] compared the reprocessing methods for LWR fuel over several attributes such as complexity, safety, wastes, and proliferation risks and provided a decision analysis methodology for reprocessing issue. It was concluded in this study that COEX is the first choice when proliferation is desired while the PUREX is the first choice when it is desired to separate Pu and have high decontamination factor. When no preferences are stated the technology chosen is COEX.

Reprocessing scheme selected in the back-end of the fuel cycle changes the isotopic composition of recovered materials and the type and amount of waste that needs disposal. There is considerable amount of study on determination of isotopic composition of fuels produced by standard reprocessing and of these spent fuels after irradiation. However, there is no study on neutronic characteristics of wastes generated from fuel cycles closed with other reprocessing methods such as COEX and UREX. In this thesis, amounts and

isotopic compositions of wastes from fuel cycles with alternative reprocessing schemes are evaluated as the first step of study.

The widely accepted permanent solution for disposing of SF/HLW is deep geological disposal facilities. Geological disposal at a depth of some hundreds of metres in a carefully engineered repository was first formally advanced as an appropriate, safe solution to radioactive management in 1950s, in the United States [10]. Currently, there are no active deep geological repositories. However, various geological disposal projects are under way in many countries, notably U.S.A., Sweden, and Finland. Although final designs for geological disposal repositories are not complete, reference designs exist, and considerable number of research has been performed concerning particular aspects of the geological disposal.

A wide range of geological disposal concepts have been proposed according to different host rocks and underground design. Three main repository designs that have been identified for the disposal of high level radioactive waste in geological formation are in-floor disposal, in-room disposal [11, 12] and disposal in very deep drill holes [13, 14]. The in-floor type disposal concept comprises the construction of tunnels at an appropriate depth (200-1000 m). Boreholes are then drilled at suitable intervals into the tunnel floor [15, 16, 17]. HLW containers are placed in the boreholes and backfilled. In-room disposal is similar to in-floor disposal. However, there is no borehole in the in-room disposal concept, and, HLW is placed inside the tunnels [18, 19].

In-floor disposal method has several advantages over the in-room disposal method. The major advantages are flexibility in the arrangement of waste units in the rock mass in the vertical and horizontal directions and ease of operation as waste units are shielded in the borehole. The disadvantage of in-floor disposal is the specialised plant would be required to drill holes within the limited tunnel space [20].

The concept of disposal in very deep drill holes, radioactive wastes are placed in the great depths of up to 4-6 km so that the possibility of migration of radionuclides to the biosphere by circulating groundwater can be greatly reduced. Disposal in very deep drill holes is not suitable for all waste forms due to the existing high

ambient temperature at that depth. That is especially the case for borosilicate-containing waste forms [20].

Swedish reference repository concept KBS-3 developed by SKB (Swedish Nuclear Fuel and Waste Company) for SF in Sweden is the widely accepted in floor type repository concept. The method is based on the encapsulation of SF in copper canisters that are embedded in bentonite clay about 500 m down in crystalline bedrock. Today, geological disposal plans of several countries (such as Finland and UK) are based on the KBS-3 concept.

The disposal concept KBS-3 was first described in a safety report published in 1983. Since then, extensive research and development work has been performed and these studies have been generated considerable amount of literature.

Research and development work covers a wide range of issues affecting the geological repository concept, such as mining techniques, underground repository design, stability of the disposal tunnels, chemical interactions, and etc. Since the geochemical interaction between waste form and medium and thermal effects of waste emplacement on repository components are the major factors affecting the development of repository design, researches have been focussed on these issues.

Studies on repository geochemistry include geochemical processes in bentonite, the chemical behaviour of the radionuclides and other contaminants (dissolution-precipitation; sorption-desorption) under different geochemical conditions etc [21-29].

Tarandi's work [30] is the basic reference for thermal modeling related to a geological repository. In the study, depth of the repository is 500 m, space between the tunnels varies between 25-60 m, and spacing between boreholes varies between 4.3-8 meters. Boreholes contain 4.7 m high disposal canisters. The initial loading per canister is 850 W and thermal loading decreases exponentially with time. In the study, the heat transfer mechanism is assumed to be pure conduction and one-dimensional model (from ground level down to a depth of 4000 m) is used to describe the temperature profile along a vertical axis through the repository centre.

Thunvik and Braester [31] performed the thermal analysis for the repository with the same geometry of Tarandi's study. They changed the tunnel spacing (20-30 m) and borehole spacing (3-6.2 m). The initial heat load per canister is 1066 W instead of 850 W, in accordance with the SKB-91 disposal canister specifications. In the study, the calculation method is based on a finite element solution of the heat conduction equation. On the whole, this work is consistent with Tarandi's work, but makes use of a more recent canister specification and of a higher computing capacity.

Ageskog and Jansson [32] made finite element analyses of heat transfer in the repository and determined temperature distribution in buffer and rock regions. In this study, the modeled geometry is much more detailed than in the studies described above; canister, buffer, backfill and rock are described in detail.

KBS-3 repository concept was proposed for disposal of spent fuel, originally. But, this disposal concept has been adopted by the UK for high level waste and spent fuel. In the technical report prepared by UK Nirex Ltd., an outline design for reference HLW/SF concept for UK has been developed [33]. This report includes calculations of peak canister temperature performed for a set of assumed reference repository conditions such as heat output, canister spacing etc.

In this study, for KBS-3 repository concept thermal analysis will be performed for canisters loaded with spent fuel, high level waste and spent MOX and results will be used to determine disposal densities of wastes for fuel cycles.

4. NUCLEAR FUEL CYCLE: ALTERNATIVES AND GENERATED WASTE FORMS

This chapter describes the nuclear fuel cycle models that are compared with regard to geological waste disposal densities. Fuel cycle scenarios are developed by using different back end fuel cycle options for fuel removed from a reference PWR reactor.

4.1. NUCLEAR FUEL CYCLE ALTERNATIVES

4.1.1. Once-through Cycle

In the once-through fuel cycle (OT cycle), spent fuel is disposed of directly as waste after being removed from the reactor. Figure 4.1 shows the OT cycle for PWR.

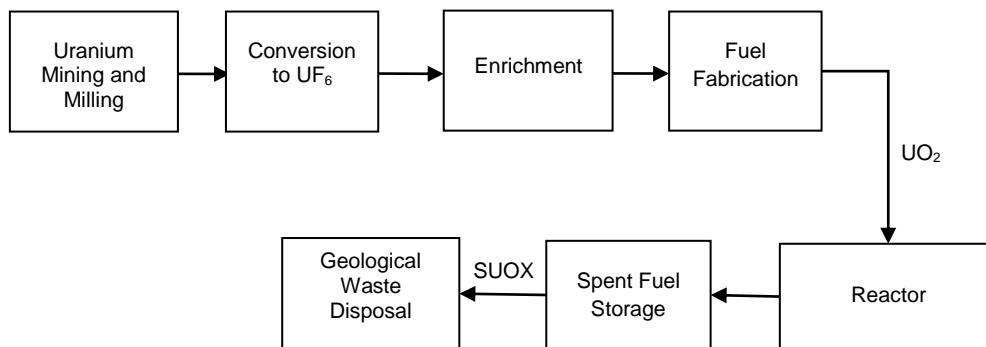


Figure 4.1. OT cycle

In the OT cycle, that is sent to the final disposal is SF rods in canisters, denoted in this context as SUOX (Spent Uranium OXide).

4.1.2. Closed Cycle

Spent fuel removed from the reactor still contains substantial fissionable materials such as U and Pu. U and Pu isotopes can be recovered from spent fuel by reprocessing so that they can be recycled as mixed oxide fuel (MOX). By recycling U and Pu in SF, up to 40 % reduction in fresh fuel requirements can be achieved. During reprocessing, FPs and other actinides are obtained as a separate, barren stream and defined as HLW. After vitrification, vitrified HLW (VHLW) is planned to be disposed of in a permanent disposal facility (waste repository). Such a cycle in which U and Pu in SF are recovered and recycled is called as “Closed Cycle”.

Besides the VHLW, during the disassembling and chop-leach processes of the reprocessing some other radioactive materials (cladding hulls, other fuel assembly structural materials, etc.) are generated. Although these materials are generated in significant amounts, they are usually classified as Intermediate Level Waste, because they vary, to a considerable extent, in radioactivity level and chemical composition from the constituents of spent fuel and are not taken into account in this study.

4.1.2.1. Standard Reprocessing Cycle

In the standard reprocessing cycle (SR), U and Pu in spent fuel are first separated from FPs and other actinides, and then separated from each other. The recovered uranium (RU) can be returned to the conversion plant for conversion to UF_6 and subsequent re-enrichment. The recovered Pu is blended with a fertile material in order to produce MOX with an appropriate fissile content. Natural uranium (NU) and depleted uranium (DU) can be used as fertile makeup materials. SR cycles are then denoted as SRNU (NU is used as fertile makeup material) and SRDU (DU is used as fertile makeup material). Figure 4.2 shows the SR cycle.

In case of SR, during reprocessing, the HLW solution containing FPs and other actinides is obtained; it is then glassified to form VHLW. VHLW is one of the waste forms to be considered in SR. In addition, recycle U (RcU) and MOX, after being re-irradiated in the reactor, come out as spent RcU (SRcU) and spent MOX (SMOX). Since multiple recycling is not considered, SRcU and SMOX are categorized as waste and sent to the final disposal.

SMOXs generated from SRDU and SRNU cycles are denoted as $SMOX_{SRDU}$ and $SMOX_{SRNU}$ respectively. Then, in SRDU and SRNU cycles, the waste types to be sent to repository are VHLW, SRcU, $SMOX_{SRDU}$ (for SRDU cycle) and $SMOX_{SRNU}$ (for SRNU cycle).

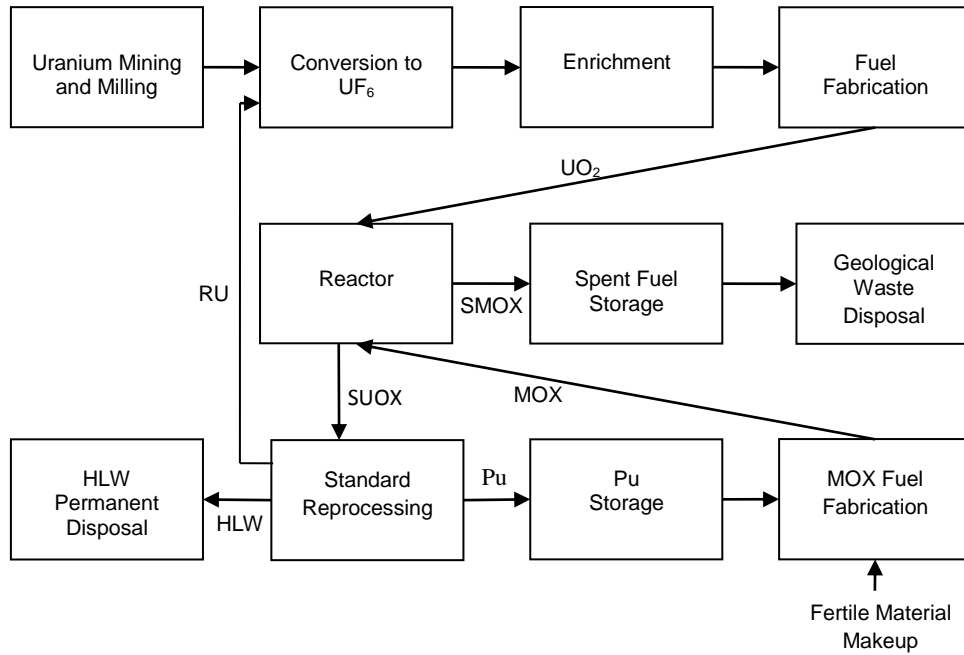


Figure 4.2. SR cycle

4.1.2.2. Complete Co-processing Cycle

In the complete co-processing (CC) cycle, U and Pu in spent fuel are separated from waste together. The product of complete co-processing is a mixed U and Pu solution. This solution is blended with a fissile makeup material for producing MOX with a proper fissile content. Enriched uranium (EU) and Pu from a standard reprocessing plant can be used as fissile makeup materials. CC cycles are then denoted as CCEU (EU is used as fissile makeup material) and CCPu (Pu from standard reprocessing is used as fissile makeup material). Produced MOX is re-irradiated in the reactor and then come out as spent MOX (SMOX). SMOXs generated from CCEU and CCPu cycles are denoted as $SMOX_{CCEU}$ and $SMOX_{CCPu}$ respectively. Figure 4.3 shows the CC cycle.

In the CC cycle, the waste types to be sent to repository are VHLW from complete co-processing of SUOX, $SMOX_{CCEU}$ (for CCEU case) and $SMOX_{CCPu}$ (for CCPu case).

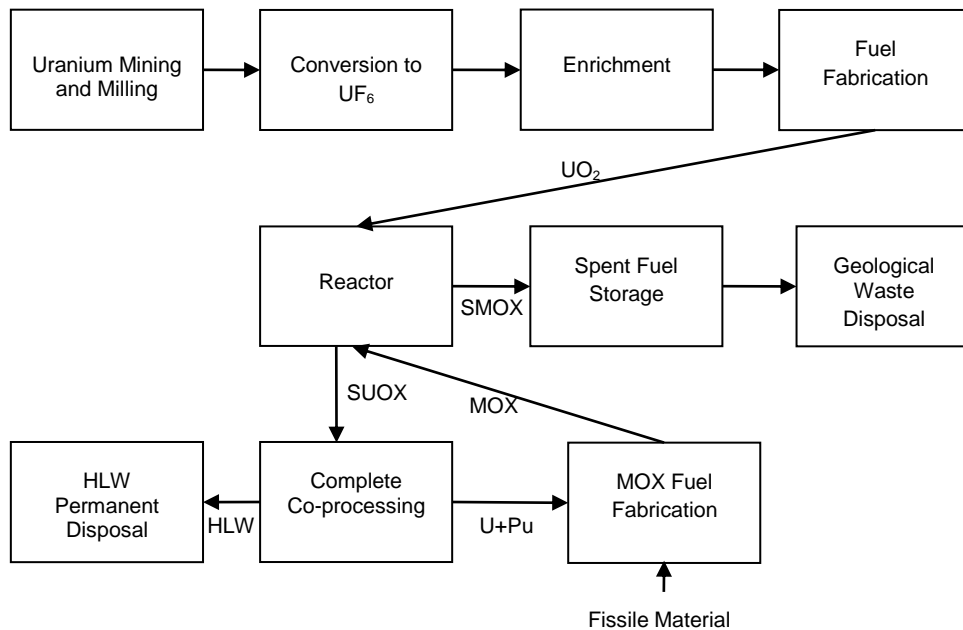


Figure 4.3. CC cycle

4.1.2.3. Partial Co-processing Cycle

In the partial co-processing (PC) cycle, the resultant products are one pure U stream and one mixed U+Pu solution. U+Pu mixture has an appropriate fissile isotope fraction to directly produce MOX fuel. There is no need to blending and fissile make up material. Produced MOX is re-irradiated in the reactor and then come out as spent MOX (SMOX_{PC}). The U product of partial co-processing is processed separately. The RU can be re-enriched and recycled (RcU) in the reactor. Figure 4.4 shows the PC cycle.

In the PC cycle, the waste types to be sent to repository are VHLW from partial co-processing of SUOX, SRcU and SMOX_{PC}.

4.1.2.4. Closed Cycle with Spent MOX: Standard Reprocessing and Recycling

In the closed cycle with spent MOX standard reprocessing and recycling (SRNU-RcMOX), after spent fuel is reprocessed to recover U and Pu in it, the recovered U is recycled and the recovered Pu is blended with NU to produce MOX fuel, then MOX fuel is irradiated in the reactor. After irradiation, spent MOX (SMOX_{SRNU}) is reprocessed to recover plutonium. This Pu is used to produce new MOX fuel and this MOX fuel is also sent to reactor. After irradiation, the spent MOX fuel (SRc-MOX_{SRNU}) is disposed of directly. Figure 4.5 shows the SRNU-RcMOX cycle.

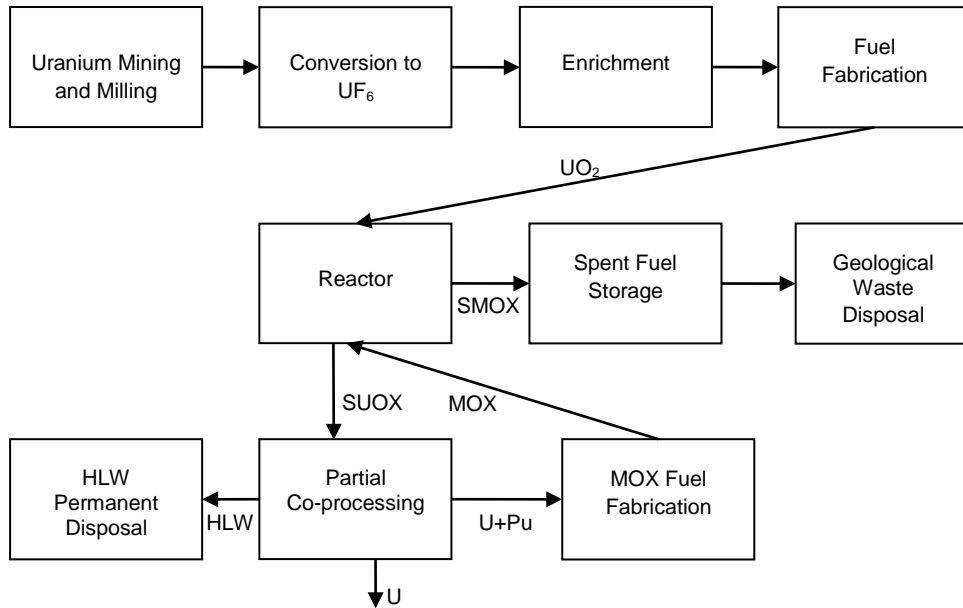


Figure 4.4. PC cycle

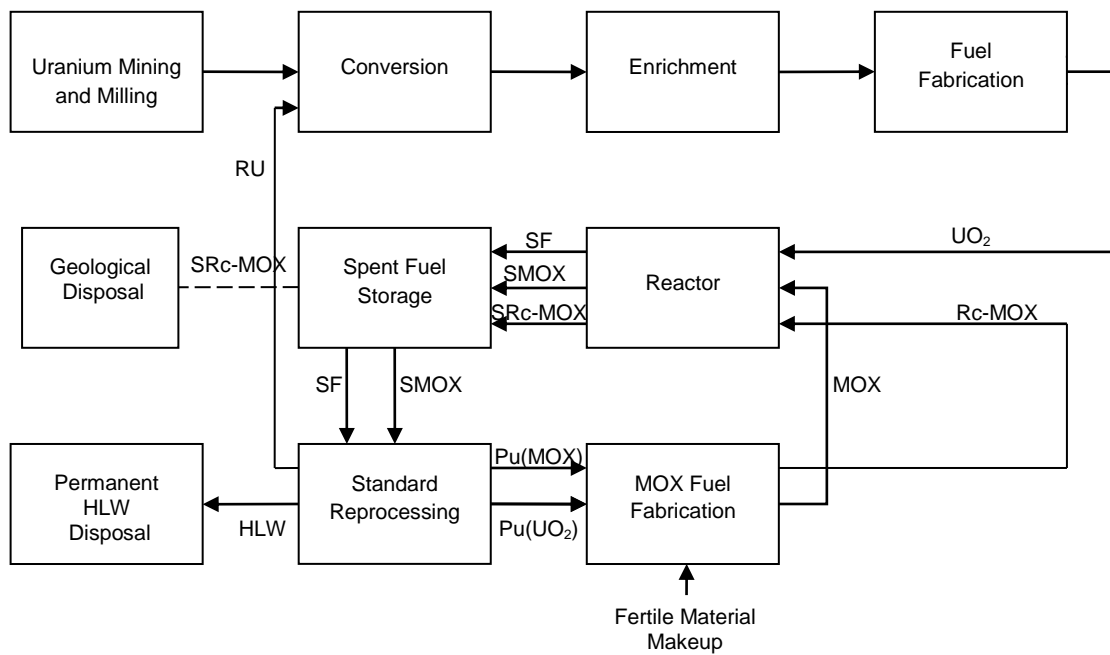


Figure 4.5. SRNU-RcMOX cycle

In the SRNU-RcMOX cycle, VHLWs arising from reprocessing of SUOX and SMOX, SRcU and SRc-MOX_{SRNU} are the waste types will be sent to geological repository.

4.2. DETERMINATION OF CHARACTERISTICS (COMPOSITIONS AND DECAY HEATS) OF WASTE TYPES UNDER CONSIDERATION

Heat dissipation from a radioactive waste is one of the most important factors in geological repository design (waste disposal density) and it depends on the waste type and composition. Waste composition is a function of initial enrichment and burnup of the fuel, average reactor power, reprocessing sheet and off-reactor cooling time of waste.

Waste disposal density calculations for fuel cycles under consideration have two major parts: (1) determination of compositions and decay heat profiles of wastes generated from fuel cycle and (2) determination of disposal area (or density) through thermal analysis using the results of first step as input. The computational flow chart is given in Figure 4.6.

Isotopic compositions and decay heat profiles of waste forms arising from fuel cycles under consideration are evaluated for a reference PWR by using MONTEBURNS code. Results are obtained for selected burnups in order to observe the effect of burnup on waste disposal density. In the heat-source-term calculations for all the waste types, a total storage period of 50 years between discharge from reactor and final disposal is assumed.

4.2.1. Reference Reactor

A 1000-MWe PWR loaded with 3.3 w/o enriched UO_2 fuel, with a discharge burnup of 33000 MWd/tU and with an irradiation time of 1000 days is taken as the reference. SF discharged in the reference case consists of about 95.5 w/o U, 1 w/o Pu, 3.5 w/o FPs and other actinides. The U in SF contains around 0.85 w/o U-235. About 70 w/o of Pu in SF is composed of fissile isotopes (~59 w/o Pu-239 and ~11 w/o Pu-241).

4.2.2. Monteburns Code

MONTEBURNS is a fully automated tool that links the Monte Carlo transport code MCNP with the radioactive decay and burnup code ORIGEN2. MONTEBURNS produces a large number of criticality and burnup results based on various material feed/removal specifications, power(s), and time intervals. The program processes input from the user that specifies the system geometry, initial material compositions, feed/removal specifications, and other code-specific parameters.

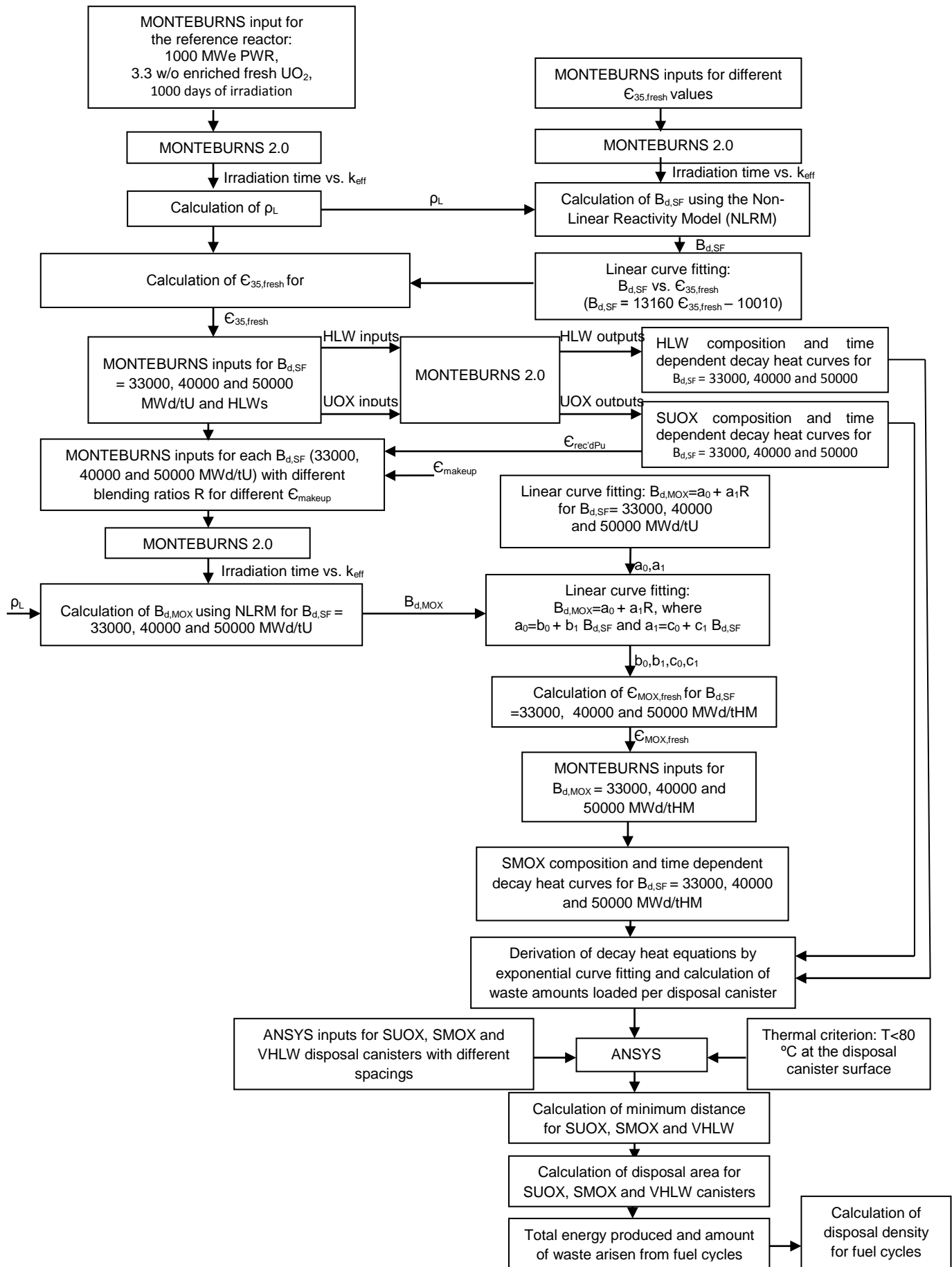


Figure 4.6. Computational flow diagram

Various results from MCNP, ORIGEN2, and other calculations are then output successively as the code runs. The principle function of MONTEBURNS is to transfer one-group cross section and flux values from MCNP to ORIGEN2, and then transfer the resulting material compositions (after irradiation and/or decay) from ORIGEN2 back to MCNP in a repeated, cyclic fashion [34].

The code consists of a Perl script which executes both of these codes and links the information between them. To run MONTEBURNS, an MCNP input deck and MONTEBURNS input file are required with the option of an additional material feed file [35].

The primary way in which MCNP and ORIGEN2 interact through MONTEBURNS is that MCNP provides one-group microscopic cross-sections and fluxes to ORIGEN2 for burnup calculations. After ORIGEN2 and MCNP have been run, results for each burn step are written into output files, and the isotopic compositions obtained from ORIGEN2 are used to generate a new MCNP input file for the next burn step. This MCNP input file contains the adjusted composition and density of each material being analyzed. To increase the accuracy of the burnup calculation, a “predictor” step is used in which ORIGEN2 is run halfway through the designated burn step. One-group cross-sections are then calculated at the midpoint of the burn step by MCNP. This assumes that the isotopics of the system at the midpoint are a reasonable approximation of the isotopics over the entire burn step (actually it is only important that the neutron flux energy spectrum be representative of the entire burn step) [34]. This assumption is valid and helps to increase the accuracy of the results under the restriction that burn steps are not too long (generally less than 2500 MWd/tHM) [35].

MONTEBURNS prints out a neutron flux spectrum and the grams of a number of isotopes present for each predictor and each outer burn step in an output file. After the predictor step is executed, then ORIGEN2 is re-executed with the new one-group cross-sections [34]. Figure 4.7 shows the interaction of MONTEBURNS with MCNP and ORIGEN2.

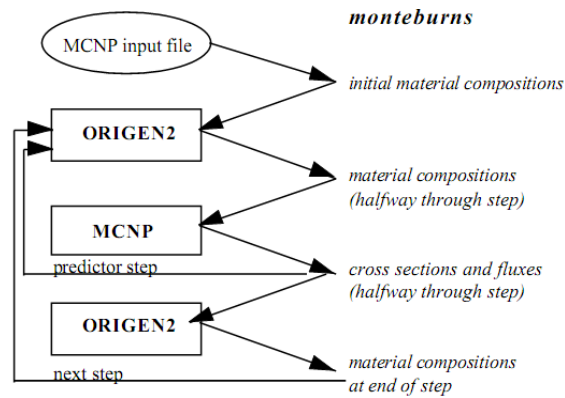


Figure 4.7. Interaction of MONTEBURNS with MCNP and ORIGEN2 [34]

4.2.3. Waste Types under Consideration

Review of fuel cycle scenarios and resultant waste types used in waste disposal density analysis is given in Table 4.1.

Table 4.1. Review of fuel cycle scenarios and resultant waste types

Cycle	Waste Type
OT	SUOX
SRNU	VHLW _{UOX} , SMOX _{SRNU}
SRDU	VHLW _{UOX} , SMOX _{SRDU}
CCEU	VHLW _{UOX} , SMOX _{CCEU}
CCPu	VHLW _{UOX} , SMOX _{CCPu}
PC	VHLW _{UOX} , SMOX _{PC}
SRNU-RcMOX	VHLW _{UOX} , VHLW _{SMOX} , SRC-MOX _{SRNU}

4.2.4. About Burnup

Since composition and decay heat of any waste type are dependent on burnup, to observe the effect of burnup on waste disposal, computations are performed for a few selected burnup values: 33000 (the reference), 40000 and 50000 MWd/tHM (Heavy Metal). Note that in case of OT cycle, there is only one burnup (discharge burnup of SF) value affecting the waste composition and decay heat. In case of closed cycle (SRNU, SRDU, CCEU, CCPu, PC or SRNU-RcMOX), not only burnup of SFs, but also burnup of recycle fuels (SRcU, SMOX or SRcMOX) affect the waste contents and decay heats. To simplify the analysis in closed cycle cases, it is assumed that burnup of SF and burnup of recycle fuels are the same. So, when the specified burnup is, for instance, 40000 MWd/tHM, what is meant is both the burnup of SF from which U, Pu and VHLW are extracted and the burnup to which RcU and MOX are burned are 40000 MWd/tHM.

4.2.5. Calculations and Results

Isotopic compositions and decay heat profiles of SUOX, SMOXs from each fuel cycle and VHLWs from reprocessing of SUOX and SMOX are evaluated for selected burnups using MONTEBURNS. Then, the corresponding expressions for decay heat profiles are derived.

4.2.5.1. Decay Heat Profiles

SUOX:

In the reference case, 3.3 w/o enrichment is required to reach 33000 MWd/tU. Enrichment of fresh U fuels for reaching 40000 and 50000 MWd/tU are calculated as 3.80 and 4.56 w/o from [36]. With these fresh U values as input, isotopic compositions and decay heat profiles are obtained from MONTEBURNS. Decay heat profiles of SUOX burned to 33000, 40000 and 50000 MWd/tU are shown in Figure 4.8. Decay heat profiles shown in Figure 4.8 are used as heat source terms in the thermal model for SUOX disposal. Note that the same computational parameters and the leakage reactivity as in [36] are used in all runs of MONTEBURNS for the results to be consistent and comparable.

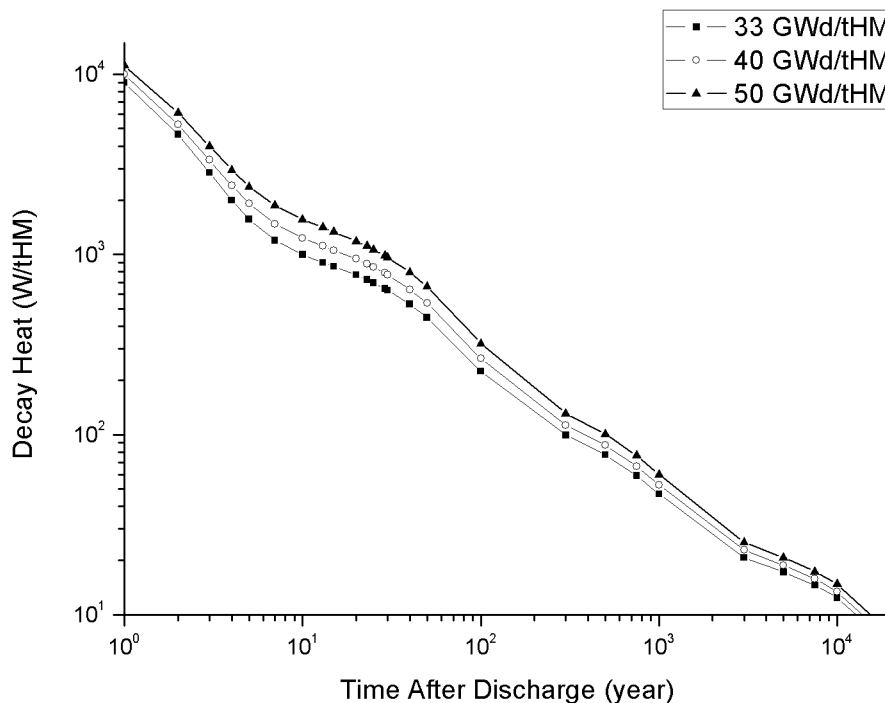


Figure 4.8. Decay heat profiles of SUOX burned to 33000, 40000 and 50000 MWd/tU

VHLW:

In the closed cycle, it is assumed that SUOX is cooled for 5 years before reprocessing. Compositions of 5-year cooled SUOX for 33000, 40000 and 50000 MWd/tU are given in Table 4.2. After removing 99.9% of Pu and U from SUOX, the remaining part, consisting of fission FPs and other actinides, is defined as HLW. The HLW is blended into glass frit to obtain VHLW containing 10 w/o HLW. The decay heat profiles of HLWs from reprocessing of SUOX fuels burned to 33000, 40000 and 50000 MWd/tU are determined by MONTEBURNS. The decay heat outputs for HLWs per equivalent ton of reprocessed heavy metal, which are to be used as heat source terms in the thermal model, are given in Figure 4.9.

Table 4.2. Isotopic compositions of U and Pu in 5 year cooled SUOX for 33000, 40000 and 50000 MWd/tU burnups

	Discharge Burnup of SF (MWd/tU)		
	33000	40000	50000
U-234	1.52460E+02	1.67141E+02	1.85210E+02
U-235	8.19894E+03	8.27800E+03	8.26670E+03
U-236	4.04300E+03	4.90130E+03	6.15485E+03
U-238	9.45250E+05	9.36215E+05	9.23793E+05
Total U	9.57644E+05	9.49562E+05	9.38399E+05
Pu-238	1.19709E+02	1.72788E+02	2.64263E+02
Pu-239	4.67543E+03	4.89000E+03	5.09328E+03
Pu-240	2.15702E+03	2.39418E+03	2.66522E+03
Pu-241	7.53264E+02	8.60550E+02	9.89294E+02
Pu-242	3.90749E+02	5.01423E+02	6.60659E+02
Total Pu	8.09617E+03	8.81895E+03	9.67272E+03
FP's and other actinides	3.42598E+04	4.16191E+04	5.19283E+04
Fissile U (w/o in U)	0.8562	0.8718	0.8809
Fissile Pu (w/o in Pu)	67.05	65.21	62.88
Fissile U+Pu (w/o in U+Pu)	1.4111	1.4638	1.5135

Quantities are in gram per ton of SUOX.

Composition and decay heat of VHLW from reprocessing of SMOX in the SRNU-RcMOX cycle is also obtained. It is found that decay heat profile of VHLW from SMOX is almost the same as of VHLW from SUOX. Since, VHLW from SUOX characteristics are used in disposal density calculations.

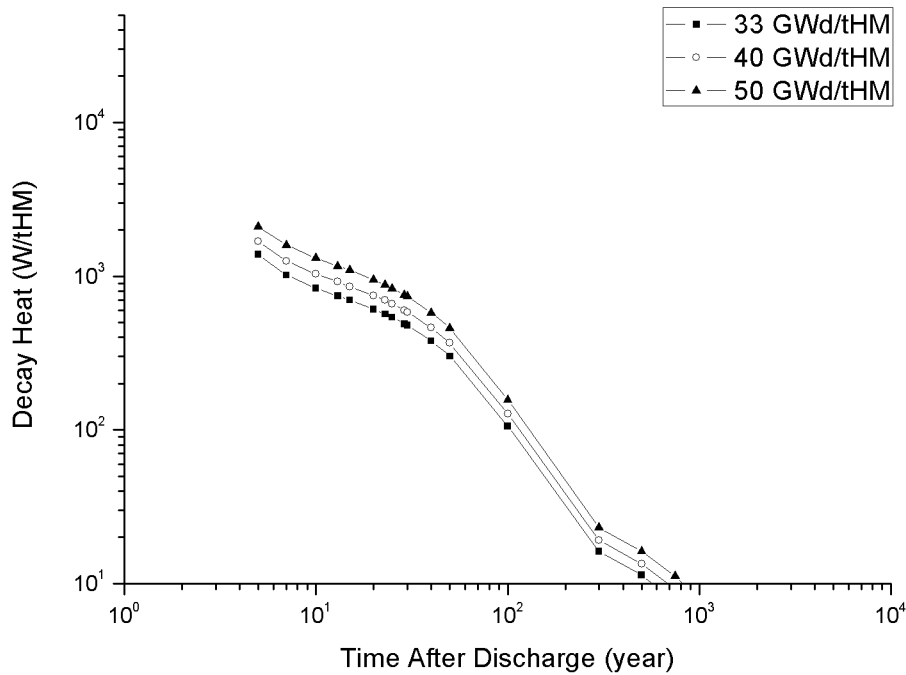


Figure 4.9. Decay heat outputs for HLWs per equivalent ton of reprocessed heavy metal

SMOX_{SRNU}:

Isotopic compositions of Pu in SF burned to 33000, 40000 and 50000 MWd/tU are given in Table 4.2. Pu in SF, after being separated in reprocessing, is blended with natural U to produce MOX_{SRNU} fuel. Total fissile contents of fresh MOX_{SRNU} fuels required to reach 33000, 40000 and 50000 MWd/tHM are calculated as 4.064, 4.852 and 6.045 w/o, respectively [36]. Using fresh MOX_{SRNU} compositions as input to MONTEBURNS, decay heat profiles and compositions of SMOX_{SRNU} are obtained and results are shown in Figure 4.10. Decay heat profiles of SMOX_{SRNU} are to be used as heat source terms in the thermal model for SMOX_{SRNU} disposal.

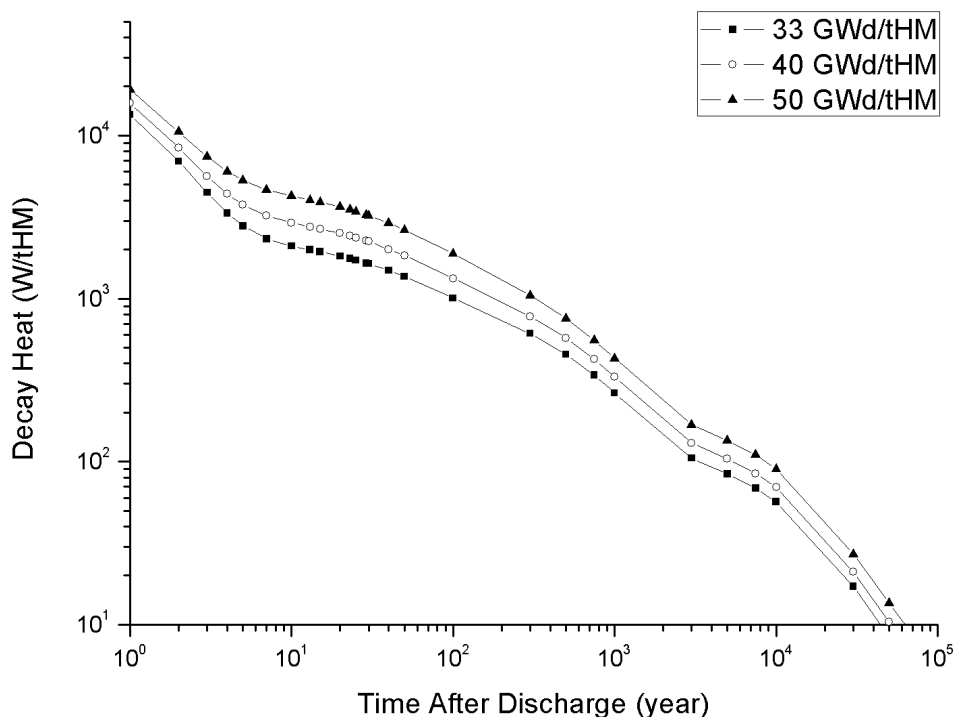


Figure 4.10. Decay heat profiles of $\text{SMOX}_{\text{SRDU}}$ burned to 33000, 40000 and 50000 MWd/tHM

SMOX_{SRDU}:

Recovered Pu in SFs with compositions given in Table 4.2. is blended with 0.3 w/o depleted U to produce MOX_{SRDU} fuel. Total fissile contents of fresh MOX_{SRDU} fuels required to reach 33000, 40000 and 50000 MWd/tHM are calculated as 4.087, 4.892 and 6.078 w/o, respectively [36]. Using fresh MOX_{SRDU} compositions as input to MONTEBURNS, decay heat profiles and compositions of $\text{SMOX}_{\text{SRDU}}$ are obtained. Decay heat profiles of $\text{SMOX}_{\text{SRDU}}$ burned to 33000, 40000 and 50000 MWd/tHM are given in Figure 4.11.

SMOX_{CCPu}:

Isotopic compositions of U+Pu mixture recovered from SF burned to 33000, 40000 and 50000 MWd/tU are given in Table 4.2. The mixed U+Pu product is blended with 70 wt% fissile Pu (probably from a standard reprocessing plant) in order to produce MOX_{CCPu} fuel with proper fissile content. Fresh MOX_{CCPu} compositions are determined by using the computational method given in [36].

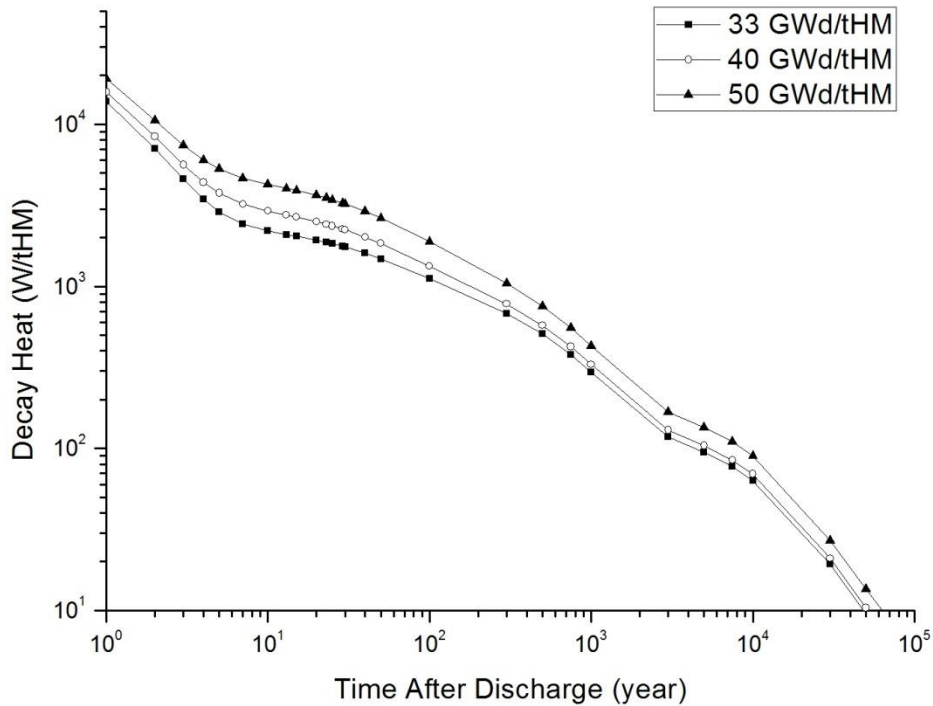


Figure 4.11. Decay heat profiles of SMOX_{SRDU} burned to 33000, 40000 and 50000 MWd/tHM

Total fissile contents of fresh MOX_{CCPu} fuels required to reach 33000, 40000 and 50000 MWd/tHM are calculated as 4.270, 5.112 and 6.427 w/o respectively. With these fresh MOX_{CCPu} values as input, isotopic compositions and decay heat profiles of SMOX_{CCPu} are obtained from MONTEBURNS. Decay heat profiles of SMOX_{CCPu} burned to 33000, 40000 and 50000 MWd/tHM are shown in Figure 4.12.

SMOX_{CCEU}:

Fresh MOX_{CCEU} compositions are determined by using the computational method given in [36]. U+Pu mixture is blended with 10 wt% enriched U and MOX_{CCEU} fuel is produced. The fresh MOX_{CCEU} enrichments needed for 33000, 40000 and 50000 MWd/tHM burnup values are calculated as 3.493, 4.029 and 4.815 w/o, respectively. Using fresh MOC_{CCEU} enrichments as input to the MONTEBURNS, decay heat profiles of SMOX_{CCEU} are determined for 33000, 40000 and 50000

MWd/tHM discharge burnup. Decay heat profiles of $\text{SMOX}_{\text{CCEU}}$ burned to 33000, 40000 and 50000 MWd/tHM are shown in Figure 4.13.

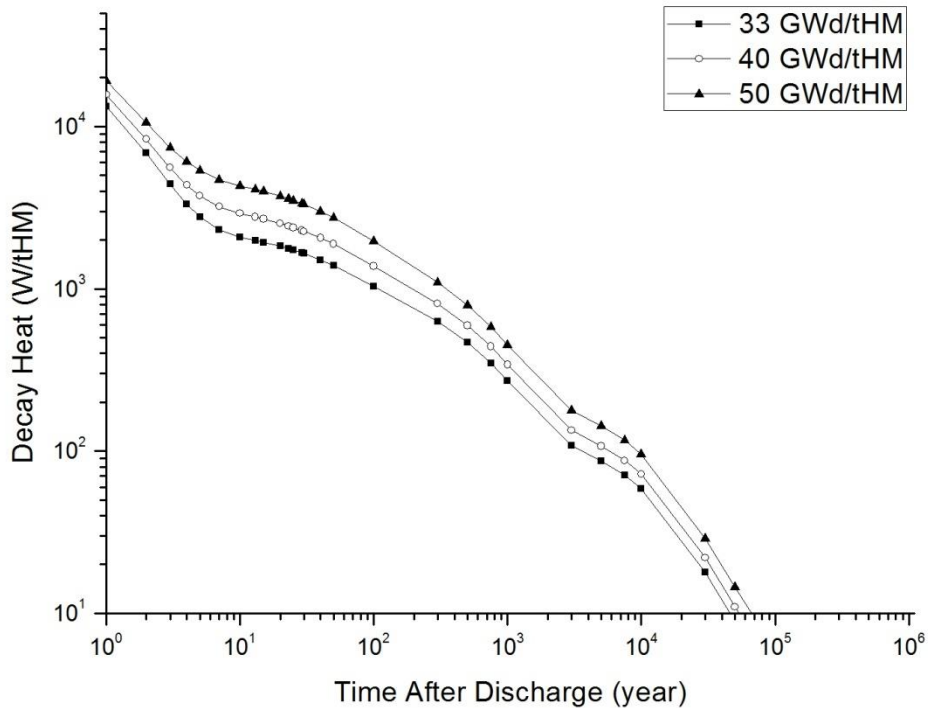


Figure 4.12. Decay heat profiles of $\text{SMOX}_{\text{CCPu}}$ burned to 33000, 40000 and 50000 MWd/tHM

SMOX_{PC}:

U+Pu mixtures with isotopic compositions given in Table 4.2 are used to produce SMOX_{PC} fuels with appropriate enrichments to reach 33000, 40000 and 50000 MWd/tHM burnup. Total fissile contents of fresh MOX_{PC} fuels required to reach 33000, 40000 and 50000 MWd/tHM are calculated as 4.287, 5.049 and 6.327 w/o, respectively. Using these fresh MOX_{PC} values as input, isotopic compositions and decay heat profiles for SMOX_{PC} are obtained from MONTEBURNS. Decay heat profiles of SMOX_{PC} burned to 33000, 40000 and 50000 MWd/tHM are shown in Figure 4.14.

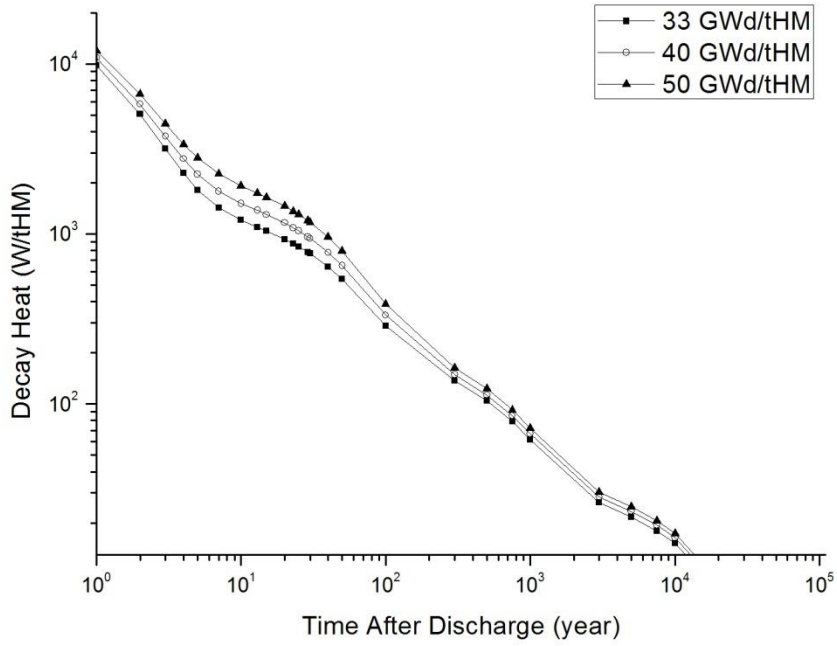


Figure 4.13. Decay heat profiles of SMOX_{CCEU} burned to 33000, 40000 and 50000 MWd/tHM

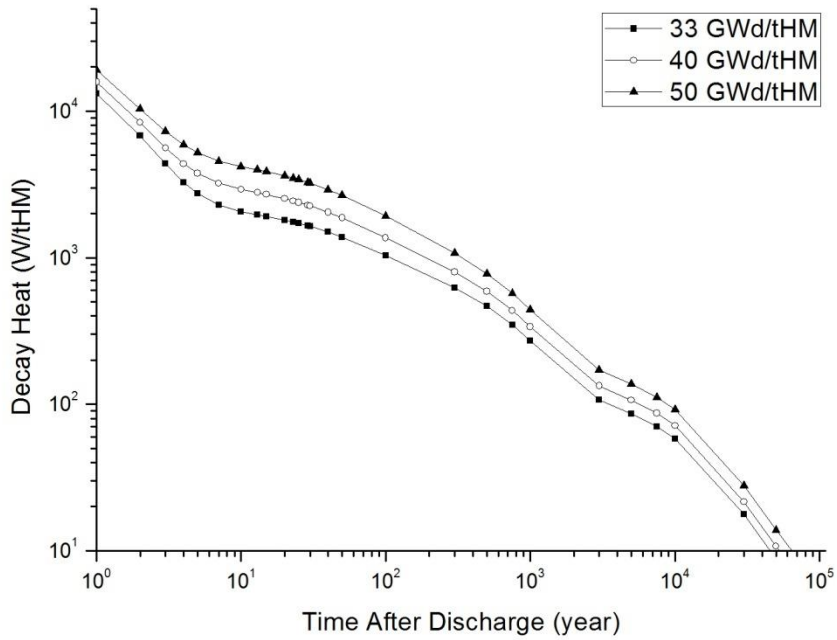


Figure 4.14. Decay heat profiles of SMOX_{PC} burned to 33000, 40000 and 50000 MWd/tHM

SRc-MOX_{SRNU}:

SMOX_{SRNU} fuels burned to 33000, 40000 and 50000 MWd/tHM are reprocessed in order to recover Pu and recovered Pu is blended with natural U to produce Rc-MOX_{SRNU} fuel. Total fissile contents of fresh Rc-MOX_{SRNU} fuels required to reach 33000, 40000 and 50000 MWd/tHM are calculated as 5.349, 6.402 and 7.797 w/o, respectively. These Rc-MOX_{SRNU} fuels are also sent to reference reactor and resultant SRc-MOX_{SRNU} radioactive decay characteristics are evaluated with MONTEBURNS code. Decay heat profiles of SRc-MOX_{SRNU} burned to 33000, 40000 and 50000 MWd/tHM are shown in Figure 4.15. Decay heat profiles of SRc-MOX_{SRNU} are to be used as heat source terms in the thermal model for SRc-MOX_{SRNU} disposal.

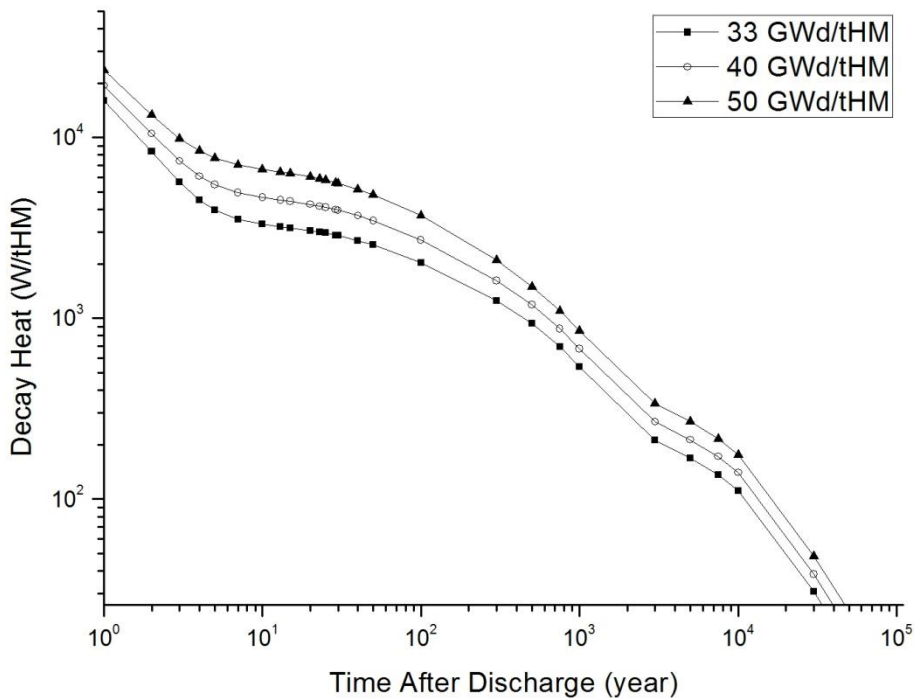


Figure 4.15. Decay heat profiles of SRc-MOX_{SRNU} burned to 33000, 40000 and 50000 MWd/tHM

SRcU:

For 33000, 40000 and 50000 MWd/tHM, the enrichments of RcU required are calculated from the expression in [37] as 3.520, 4.130 and 5.020 w/o respectively and with them used as input to MONTEBURNS, SRcU compositions and decay

heats are obtained. It is found that decay heat profiles of SRcU are almost the same as those of SUOX; so, it is proper to assume SRcU is simply SUOX with the same burnup. SRcU decay heat profiles are given in Appendix I.

4.2.5.2. Decay Heat Rate Equations for the Waste Types under Consideration

In order to obtain heat generation rate equations which are to be used as the heat source terms in thermal analyses, time dependent decay heat curves are fitted to a sum of four exponential terms. Eqn. 4.1 (Put's formula) given below provides an adequate fit for the heat release rates of the three waste types:

$$Q(t) = \sum_i A_i e^{-b_i t} \quad (Q \text{ in W/tHM}) \quad (\text{Eqn. 4.1})$$

where t is defined as the time (in year) elapsed since the production of the waste form [38]. A set of values of the coefficients A_i and b_i was derived by Put for vitrified waste arising from the reprocessing of spent fuel with a burnup of 33000 MWd/tHM [38]. Put's formula is used to provide an adequate fit for the other waste types. Values of the coefficients to be used in Put's formula are given in Table 4.3. Fits are given in Appendix II.

Table 4.3. Values of the coefficients in Put's formula for the waste types under consideration

Waste Type	Burnup	A ₁	A ₂	A ₃	A ₄	b ₁	b ₂	b ₃	b ₄
SUOX	33000	990.18	120.73	14.27	11.60	0.02325	0.00166	0.00013	3.1375E-5
	40000	1219.81	138.18	15.76	13.02	0.02324	0.00167	0.00014	3.2642E-5
	50000	1535.27	157.30	48.54	27.20	0.02411	0.00152	0.00869	5.5445E-5
HLW	33000	3553.84	924.75	178.55	25.85	0.46464	0.02405	0.13193	0.00166
	40000	3047.97	1115.03	157.39	30.14	0.39371	0.02386	0.08421	0.00154
	50000	4507.80	1415.02	285.93	37.13	0.43267	0.02409	0.09953	0.00159
SMOX _{SRNU}	33000	1131.78	703.28	390.09	116.68	0.02503	0.00152	0.00692	6.7581E-5
	40000	1495.36	865.25	552.25	138.58	0.02745	0.00155	0.00788	6.9608E-5
	50000	2100.53	1058.92	660.44	177.22	0.02728	0.00159	0.00765	8.0955E-5
SMOX _{SRDU}	33000	1093.46	778.85	415.86	130.62	0.02393	0.00151	0.00662	6.7187E-5
	40000	1566.19	963.95	672.92	158.44	0.02479	0.00151	0.00682	6.7771E-5
	50000	2193.85	1290.69	1251.59	217.53	0.02814	0.00160	0.00794	8.1000E-5
SMOX _{CCPU}	33000	1056.08	737.68	367.05	128.57	0.02377	0.00158	0.00725	7.9308E-5
	40000	1492.74	950.21	678.93	160.73	0.0268	0.00160	0.00795	8.0658E-5
	50000	2206.31	1259.51	1248.25	214.13	0.0288	0.00160	0.00810	8.1097E-3
SMOX _{CCEU}	33000	1083.29	170.74	104.18	31.72	0.02570	0.00162	0.0112	7.281E-5
	40000	1381.87	187.58	154.98	34.46	0.02652	0.00164	0.0119	7.431E-5
	50000	1781.36	200.75	266.16	37.15	0.02789	0.00163	0.0126	7.392E-5
SMOX _{PC}	33000	1101.46	731.03	324.28	129.06	0.02241	0.00157	0.0065	7.841E-5
	40000	1529.51	962.43	755.41	161.82	0.02964	0.00161	0.0086	8.120E-5
	50000	2223.53	909.71	718.16	151.05	0.0284	0.0016	0.0081	8.217E-5
SRC-MOX _{SRNU}	33000	1476.82	1098.37	749.91	257.08	0.00159	0.0205	0.0071	8.474E-5
	40000	1863.09	1462.83	1445.83	323.97	0.00159	0.0240	0.0072	8.437E-5
	50000	2321.53	2183.31	2444.18	407.82	0.00159	0.0255	0.0076	8.473E-5

5. REFERENCE REPOSITORY CONCEPT

The UK HLW/SF repository [33] based on the KBS-3 concept developed by SKB (Swedish Nuclear Fuel and Waste Company) for SF in Sweden, is taken as the reference repository. In the reference disposal concept, SF (SUOX and SMOX) or VHLW is placed into copper canisters with a cast iron insert. Two different copper canisters are used for SF and VHLW. The canisters are surrounded by bentonite buffer and placed vertically into holes excavated along parallel tunnels at a depth of 500 m in granite rock. The depths of deposition holes for SF and VHLW canisters are 7.55 and 6.25 meters, respectively and the diameter of each hole is 1.75 meters. Disposal tunnel diameter is 5.5 meters. The distance between the disposal tunnels is 40 meters [33]. Figure 5.1 shows the UK HLW/SF repository concept.

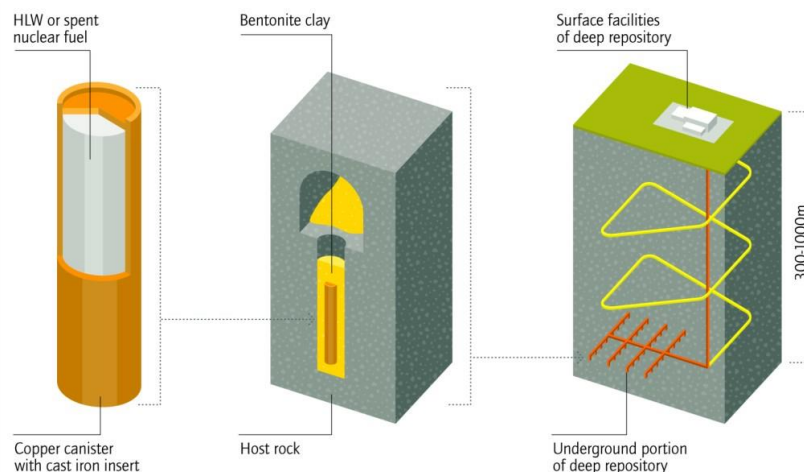


Figure 5.1. UK HLW/SF repository concept [33]

5.1. WASTE PACKAGES

In the reference repository, radioactive waste is packaged within a nodular cast iron insert and placed into a copper shell to create the disposal canister. The disposal canister shells would be fabricated from oxygen-free, phosphorous doped (OFP) copper with a wall thickness of 50 mm [39]. Under suitable geochemical conditions, the corrosion of copper is extremely slow, and the copper canister is expected to maintain its integrity, despite corrosion, for an extremely long time [33]. While the copper shell provides the necessary corrosion barrier for the system, the cast iron insert of the canister bears the load and provides the

mechanical strength needed. Cast iron insert also provides radiation shielding and keeps the fuel assemblies in a fixed configuration.

Cast iron insert would be made with appropriately sized openings to accept SF assemblies and VHLW. After loading the waste, disposal canister inner casting would be fitted with a bolted lid, the air would be evacuated and replaced with inert gas, and the canister would then be sealed. Subsequently, the lid would be placed on the copper outer shell and electron-beam welded to the body. The electron-beam weld would constitute the permanent containment seal of the disposal canister [33].

5.1.1. SF (SUOX and SMOX) Disposal Canisters

In the SUOX disposal case, four SUOX assemblies would be packaged within a copper canister. In the SMOX/SRc-MOX disposal case, one SMOX or SRcMOX assembly would be placed into disposal canister. Each SF assembly has a square cross-section 0.214 m by 0.214 m and 4.1 m long. SF disposal canister is 4.5 m long and 0.9 m in diameter [33]. SF disposal canister is illustrated in Figure 5.2.

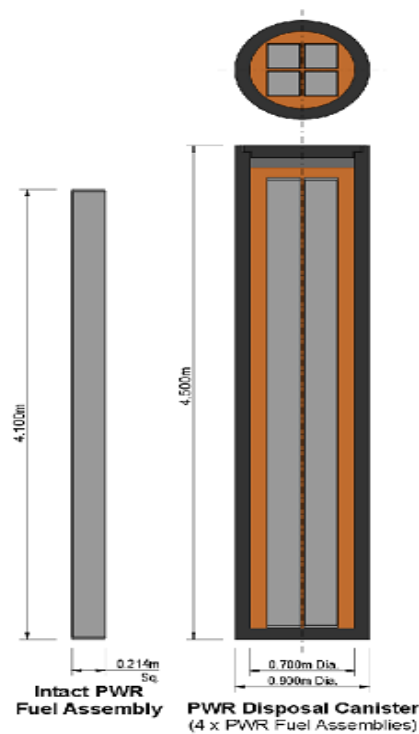


Figure 5.2. SF disposal canister [33]

5.1.2. VHLW Disposal Canisters

A VHLW canister is 3.2 m long and 0.9 m in diameter and contains two stainless steel cylinders loaded with VHLW. Each stainless steel cylinder is 0.43 m in diameter and 1.34 m long. It is assumed that each VHLW cylinder is loaded with 150 liters VHLW bearing 10 w/o waste. VHLW disposal canisters are illustrated in Figure 5.3.

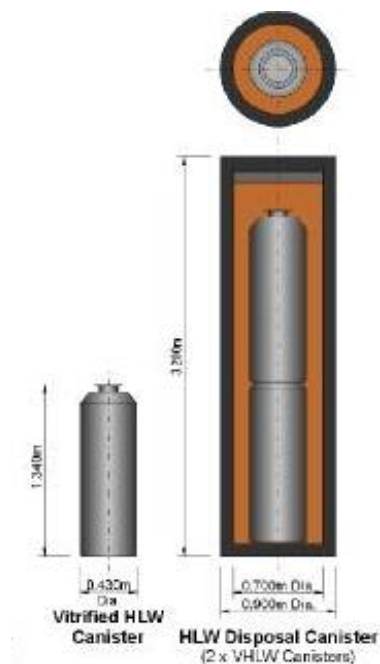


Figure 5.3. VHLW disposal canister [33]

5.2. BUFFER MATERIAL

After emplacement in to deposition hole, the disposal canister is surrounded by a buffer layer. The disposal canister would be buffered with bentonite blocks and rings. Bentonite buffer protects the disposal canister against small movements in the rock, absorbs water while swelling and prevents direct contact with the groundwater. It also contains any radionuclides that eventually escape from the canister.

5.3. BACKFILL MATERIAL

Following the deposition of disposal canisters in all the deposition holes within a deposition tunnel, the deposition tunnel would be backfilled and sealed. Backfilling is used to stabilize the access openings, to limit associated rock damage and to restrict inadvertent intrusion. It may also provide a degree of chemical buffering. In most cases, backfill and seals made of buffer are used to seal the disposal cells

and to facilitate waste isolation and repository closure [40]. In the reference repository, backfilling of the deposition tunnels would involve the introduction of a mixture of crushed rock and bentonite in a ratio of 70 %:30 % [33].

5.4. GEOLOGY

The host rock and the geological environment of the repository provide stable mechanical, chemical and hydrologic conditions around the engineered barriers and isolates the radionuclides from the biosphere for very long times. Mainly clay rock, salt rock and crystalline rock (granite, welded tuff and basalt) are being considered as possible host rocks. In the reference repository concept, the host rock formation in which the repository would be constructed is selected as granite. Due to its high solidity and cavity stability the crystalline provides favourable features for the construction of a repository. Also its very low solution behaviour and low temperature sensitivity are favourable for disposal.

In contrast to the clay and salt host rocks, crystalline rocks are generally more strongly jointed and thus provide numerous natural pathways for gases and solutions. Therefore the safe enclosure of the emplaced waste against inflowing groundwater needs to be ensured by additional barriers on a bentonite basis or on a concrete basis [41].

6. THERMAL ANALYSIS

Once disposal canisters are placed into deposition holes, temperatures of the repository components increase due to the heat generation in disposal canisters. Temperature affects many processes occurring in the repository, thus, during the repository design, it is necessary to determine an appropriate density of emplacement of heat-generating wastes and investigate the resultant time-dependent temperature distributions. In this study, thermal analysis is performed with ANSYS finite element code to calculate the time-dependent temperature distribution in the reference repository. Results of the analysis are used to determine the minimum distance between deposition holes by ensuring that thermal criteria limiting the canister surface temperature is satisfied.

6.1. ANSYS

ANSYS is finite element analysis software that can be used in modeling problems in wide range of engineering fields such as structural, thermal, mechanical, fluid dynamics, electrical. This section describes briefly the finite element method which is the basis of ANSYS code and general features of the ANSYS computer program.

6.1.1. The Finite Element Method

Physical phenomena and engineering problems are generally described in terms of differential and integral equations. However, in general, these equations have complex domains and can not be solved by analytical methods. The finite element method (FEM) is a numerical procedure that can be used to find approximate solutions of equations that describe the engineering problems with complex domain.

In a continuum (a body of matter or simply a region of space in which a particular phenomenon is occurring) problem of any dimension the field variable (e.g., displacement, stress, temperature, pressure or velocity) possesses infinitely many values because it is a function of each geometric point in the body or solution region [42]. As a result, continuum problem has an infinite number of unknowns. In the FEM, the problem is reduced to one with a finite number of unknowns by breaking down the solution region into sub-regions called as finite elements and approximating the variation of the field variable within each element by a simple,

known function (called as approximation or interpolation function). Finite elements are considered to be interconnected at specified points called as nodes and approximating functions are defined in terms of the values of the field variable at nodes. When finite element equations for the whole continuum are written, the new unknowns will be the nodal values of the field variable. By solving the finite element equations, the nodal values of the field variable will be known and once these are known, the approximation functions define the field variable throughout the entire geometry [43].

Since the approximation function describes the behaviour of field variable in each element and approximates the solution, it is important to select an appropriate approximation function in finite element analysis. Approximation function should satisfy certain convergence requirements and its solution must be simple from the computational point. Polynomials are the most widely used approximating functions. It is easy to perform differentiation and integration with polynomials; hence it is easier to formulate and computerize the finite element equations with polynomial functions. Besides, accuracy of the solution can be improved by simply increasing the order of the polynomial [43].

Since the accuracy of the solution in finite element analysis depends on the size, number and shape of the elements (triangular, quadrilaterals etc.), it is also important to make discretization of the domain carefully. The size, number and shape of the elements should be chosen such that the domain is simulated as closely as possible without increasing the computational effort needed for the solution [43].

To understand how FEM works, a typical linear element with end nodes i and j is considered. Figure 6.1 shows a one dimensional linear element.

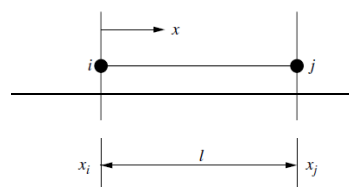


Figure 6.1. One dimensional linear element [44]

The temperature variation in that element can be represented by the following linear function [44].

$$T = \alpha_1 + \alpha_2 x \quad (\text{Eqn. 6.1})$$

Since there are two constants in the linear function, two nodes are required to determine the values of these constants. Substituting the values at nodes i and j into Eqn. 6.1 provides:

$$T_i = \alpha_1 + \alpha_2 x_i \quad (\text{Eqn. 6.2})$$

$$T_j = \alpha_1 + \alpha_2 x_j \quad (\text{Eqn. 6.3})$$

Solving these equations for α_1 and α_2 gives:

$$\alpha_1 = \frac{T_i x_j - T_j x_i}{x_j - x_i} \quad (\text{Eqn. 6.4})$$

$$\alpha_2 = \frac{T_j - T_i}{x_j - x_i} \quad (\text{Eqn. 6.5})$$

Substituting α_1 and α_2 values into Eqn. 6.1 provides:

$$T = T_i \left[\frac{x_j - x}{x_j - x_i} \right] + T_j \left[\frac{x - x_i}{x_j - x_i} \right] = N_i T_i + N_j T_j \quad (\text{Eqn. 6.6})$$

N_i and N_j are interpolation functions. By using Eqn. 6.6 temperature T can be calculated at any point within the element. For the system with many elements, this process is applied to each element and finite element equations are obtained. Then, finite element equations are assembled to obtain global equations for the entire system. These equations can be written in the matrix form:

$$[K]\{T\} = \{f\} \quad (\text{Eqn. 6.7})$$

where, $[K]$ is the global system matrix, $\{T\}$ is the vector of nodal unknowns and $\{f\}$ is the vector of loads of the system. Solution of this system of equations gives the nodal values for the unknown variable.

6.1.2. ANSYS Analysis Procedure

There are three main steps in a typical ANSYS analysis:

- Model generation

- Solution
- Review results

ANSYS program has processors (preprocessor, solution, postprocessor, etc.) that are used to perform each of these steps. In particular, model generation is done in the preprocessor and application of loads and the solution is performed in the solution processor, finally, the results are viewed in the general post processor and time history postprocessor for steady-state and transient problems, respectively [45].

6.1.2.1. Model Generation

In this stage, finite element model of the problem is created. Model generation step involves creation of geometry of the model, definition of element type, materials and material properties, and meshing the geometry with elements.

Geometry can be either created within the ANSYS program or imported from a Computer-Aided Drawing (CAD) software. There are two methods used to create the finite element model in the ANSYS program: solid modeling and direct generation. In the solid modeling method, geometry of the model is described by utilising geometric primitives and Boolean operations and then, solid model automatically meshed by using specified nodes and elements. By contrast, direct generation is a manual method of finite element modeling in which node coordinate data, connectivity of elements and load data must be prepared manually. It is convenient for simple models but can be too time consuming and may become tedious for complex models requiring large number of nodes. Since solid modeling is much more versatile and powerful than direct generation, it is the most commonly used method. In this study, the solid modeling method is used.

Before meshing the solid model, appropriate element attributes (element type, real constants, material properties, element coordinate system etc.) should be defined. The ANSYS element library contains nearly 200 element types. These elements are classified according to different criteria such as dimensionality (e.g., line, solid, shell, plane), analysis discipline (e.g., structural, thermal, magnetic, electric, fluid, or coupled-field) and material behaviour. BEAM, CPT, INFIN, MATRIX, PLANE, SHELL, SURF, CIRCU, FLUID, INTER, MESH, PRETS, SOLID, TARGE, COMBIN, FOLLW, LINK, MPC, REINF, SOLSH, TRANS, CONTAC, HF, MASS,

PIPE, ROM and SOURC are the element groups available in ANSYS. Each element type is identified by a name consisting of a group label and a unique identifying number. (BEAM3, PLANE42, SOLID96 etc.)

Element real constants are properties that depend on the element type, such as cross-sectional properties of a beam element. For example, real constants for BEAM3, the 2-D beam element, are area (AREA), moment of inertia (IZZ), height (HEIGHT), shear deflection constant (SHEARZ), initial strain (ISTRN), and added mass per unit length (ADDMAS). Not all element types require real constants, and different elements of the same type may have different real constant values.

Materials and material properties should be specified for each element type. ANSYS has a built-in global database of approximately 675 predefined materials along with their properties and default values for each property. To define a material in the model, user can copy materials from this database and use the default properties or define new materials by editing their properties.

The quality of the mesh influences the accuracy and convergence of the solution. It is important to determine shape, size and number of elements appropriate to obtain accurate simulation results. Depending on the nature of the problem and the computer capacity, the user can control the size and number of elements by using meshing controls. There are two meshing methods in ANSYS: free (unstructured) meshing and mapped (structured) mesh. Free mesh has no element shape restrictions and does not follow a specific pattern while mapped mesh restricts element shapes and needs to a regular pattern. Free meshing can be used to mesh regular or irregular surfaces and volumes, whereas mapped meshing can be used to mesh regular surfaces and volumes [46]. Figure 6.2 shows free and mapped meshes.

6.1.2.2. Solution

In the solution step, analysis type and options are defined, boundary conditions are specified and the solution for the finite element model that is generated within the first step is performed. These tasks are performed by using SOLUTION processor. System loads can also applied in model generation step by using the PREP7 preprocessor.

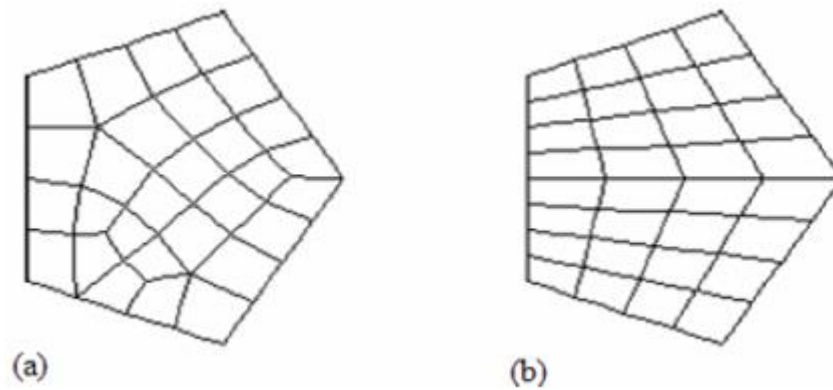


Figure 6.2. (a) Free meshing, (b) Mapped meshing [46]

In this step, analysis type and analysis options are defined first. Analysis types are generic and independent of discipline. Seven analysis types are available in ANSYS: static (or steady state), modal, harmonic, transient (time-dependent), spectrum, Eigen buckling and substructuring. Not all analysis types are valid for all disciplines. For example, as performing thermal analysis, steady state, transient and substructuring analysis types can be chosen only. The analysis type is selected according to loading conditions and the results of interest. Analysis options allows user to customize the analysis type by choosing the method of solution and related details.

Once analysis type and options are specified, loads have to be applied as the next step. In ANSYS terminology, the term 'load' includes boundary conditions (constraints, supports or boundary field specifications) and other loads applied internally or externally. There are six load groups in ANSYS: Degree-of-freedom (DOF) constraints, forces, surface loads, body loads, inertia loads, and coupled-field loads [46].

- A DOF constraint fixes a degree of freedom to a known value. (Displacements in a structural analysis, prescribed temperatures in a thermal analysis, etc.)
- A force is a concentrated load applied at a node in the model. (Moments in a structural analysis, heat flow rates in a thermal analysis, current segments in a magnetic analysis, etc.)

- A surface load is a distributed load applied over a surface. (Pressures in a structural analysis, convections in a thermal analysis, etc.)
- A body load is a volumetric or field load. (Fluences in a structural analysis, heat generation rates in a thermal analysis, etc.)
- Inertia loads are used mainly in structural analysis and assignable to the inertia (mass matrix) of a body, such as gravitational acceleration and angular velocity.
- Coupled-field loads involve applying results from one analysis as loads in another analysis.

Load step and substep are two important load-related terms in ANSYS program. A load step is a set of loads for which the solution is obtained. In a structural analysis, for example, wind loads may be applied in one load step and gravity in a second load step. Load steps are also useful in dividing a transient load history curve into several segments.

Substeps are points within a load step at which solutions are calculated. They are mainly used for accuracy and convergence purposes in transient and nonlinear analyses. Substeps are also known as time steps which are taken over a period of time.

Loads can be applied on the model in a variety of ways in the ANSYS program. Also, by using load step options such as number of substeps, time at the end of load step and output controls, user can control how the loads are used during solution.

Once the loads of the system have been defined, solution calculations are initiated by using solver. When this command is issued, the ANSYS program calculates the results for model and loading information generated by user. The ANSYS solver writes the results of analysis to the results file and also to the database during solution. The solution phase calculates two types of results data:

- Primary data consist of the degree-of-freedom solution calculated at each node: displacements in a structural analysis, temperatures in a thermal analysis, magnetic potentials in a magnetic analysis, and so on. These are also known as nodal solution data.

- Derived data are those results calculated from the primary data, such as stresses and strains in a structural analysis, thermal gradients and fluxes in a thermal analysis, magnetic fluxes in a magnetic analysis, and etc.

6.1.2.3. Reviewing the Results

After obtaining the solution, results of the analysis are viewed in postprocessors. Results can be reviewed by using either general postprocessor or time history postprocessor. General postprocessor allows user to review the results over the entire model at specific load steps and substeps (or at specific time-points or frequencies). Time history postprocessor allows user to review the variation of a particular result item at specific points in the model with respect to time, frequency, or some other result item.

6.2. ANSYS MODEL OF THE SYSTEM

6.2.1. Thermal Model

Once SF/HLW disposal canisters are disposed in the repository, a transient heat diffusion phenomenon gives rise because of the heat generated in disposal canisters. After backfilling the repository tunnels, radiation and convection will be negligible. The heat transfer in the repository is mainly by conduction and represented with the following three dimensional heat conduction equation:

$$\frac{\partial}{\partial t}(\rho c_p T) = \frac{\partial}{\partial x} \left[k \frac{\partial T}{\partial x} \right] + \frac{\partial}{\partial y} \left[k \frac{\partial T}{\partial y} \right] + \frac{\partial}{\partial z} \left[k \frac{\partial T}{\partial z} \right] + q(t) \quad (\text{Eqn. 6.8})$$

where c_p is the specific heat coefficient [J/(kg.°C)], k is the thermal conductivity coefficient [W/(m.°C)], ρ is the density [kg/m³] and q is the heat generation rate [J/(m³.s)].

6.2.2. Finite Element Model

ANSYS finite element code is used to develop a 3-D thermal model of the repository. It is assumed that the repository contains infinite number of disposal tunnels filled with infinite number of disposal canisters with the same thermal output.

Due to the geometrical and loading symmetry of the repository, thermal model is simplified to one quarter of a deposition hole with three symmetry surfaces. One-quarter model includes nuclear waste (a canister containing 4 assemblies of

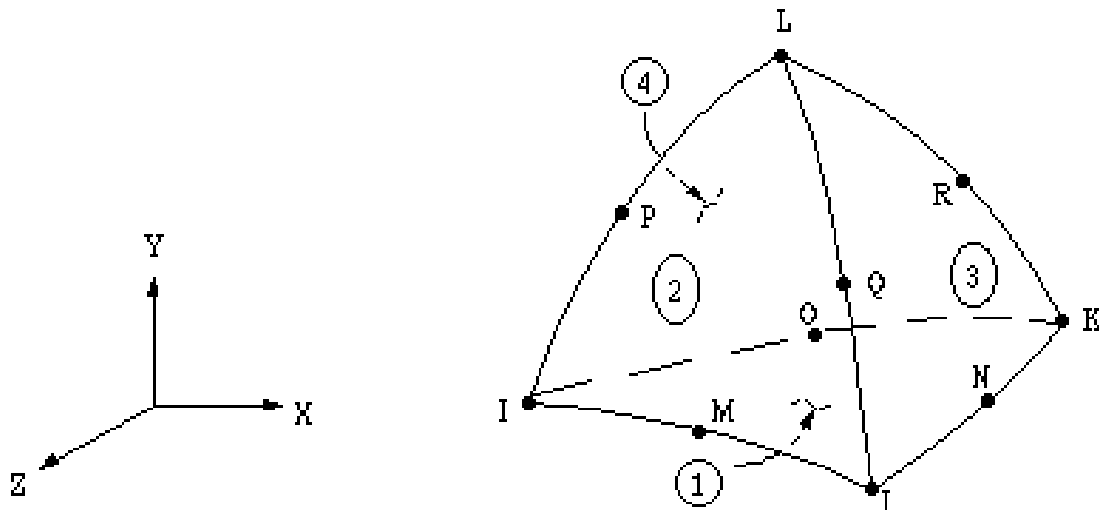


Figure 6.4. SOLID87 element geometry [46]

Mesh sizes used for discretization of waste, cast iron insert, copper canister, bentonite buffer, tunnel and host rock regions are 0.1, 0.1, 0.05, 0.2, 0.3 and 0.5 meters respectively. The influence of mesh size on analysis results is also checked. Since there is no significant effect of mesh size variation on results, element sizes are selected by taking into account the computational time and the memory available in the computer used.

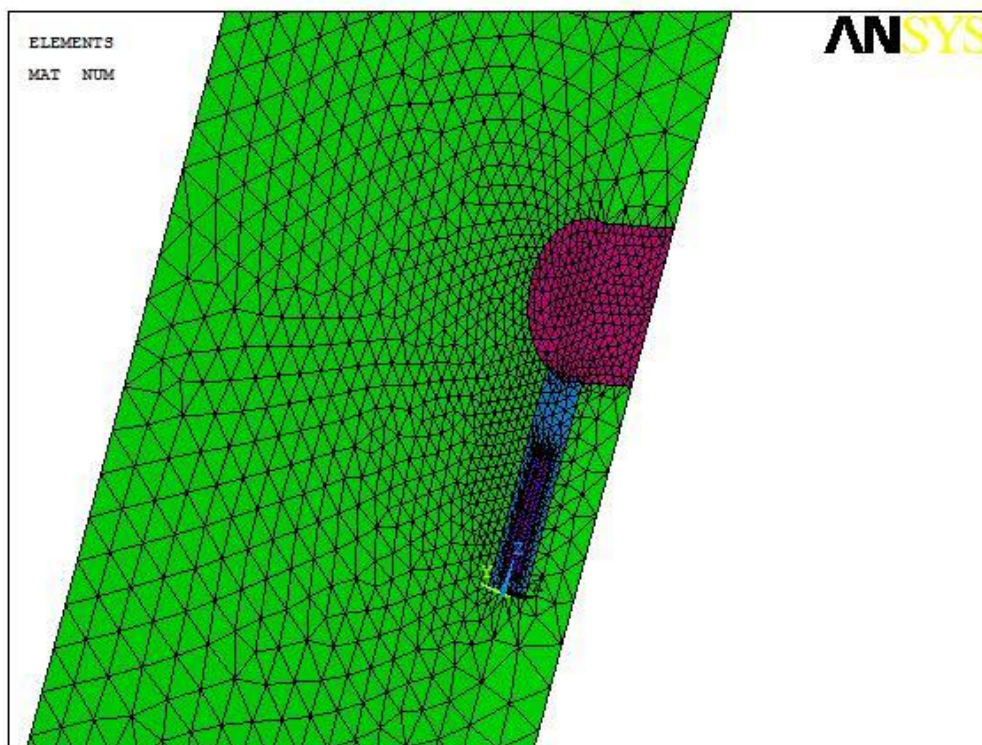


Figure 6.5. 3-D meshed model of repository

Transient thermal analysis in ANSYS requires density, thermal conductivity and specific heat values of materials as input. Thermal properties of the materials of interest are given in Table 6.1. All thermal properties are assumed as isotropic.

Constant temperature boundary conditions are applied at the top and bottom boundaries of the model. While setting the constant temperature boundary conditions, it is assumed that the ground surface temperature of the repository is 15 °C and the geothermal gradient is 30 °C/km. All symmetric boundaries are assumed to be adiabatic.

The heat-source term is applied as volumetric heat generation in the waste region of the model. Time-dependent volumetric heat generation rate for SF/HLW waste is derived from decay heat profile obtained in Chapter 5 by considering the amount of waste loaded per canister.

Table 6.1. Thermal properties of materials used in the thermal model of repository [47, 48]

Material	Properties	Values
Spent fuel/HLW	Density (kg/m ³)	2000/2750
	Thermal Conductivity (W/m.°C)	0.135/1.355
	Specific Heat (J/kg.°C)	2640/1089
Cast Iron Insert	Density (kg/m ³)	7200
	Thermal Conductivity (W/m.°C)	52
	Specific Heat (J/kg.°C)	504
Copper Canister	Density (kg/m ³)	8900
	Thermal Conductivity (W/m.°C)	386
	Specific Heat (J/kg.°C)	383
Bentonite	Density (kg/m ³)	1970
	Thermal Conductivity (W/m.°C)	1
	Specific Heat (J/kg.°C)	1380
Backfill Material	Density (kg/m ³)	2270
	Thermal Conductivity (W/m.°C)	2.0
	Specific Heat (J/kg.°C)	1190
Rock	Density (kg/m ³)	2650
	Thermal Conductivity (W/m.°C)	3.2
	Specific Heat (J/kg.°C)	815

In the source term calculations, it is assumed that the wastes are disposed after a total storage period of 50 years (before and after reprocessing).

After meshing the model and applying the boundary conditions, transient thermal analysis is performed to obtain temperature distribution around a disposal canister over a period of 20 years after deposition.

6.3. RESULTS

Thermal analyses are performed for various spacing values and the minimum distance between boreholes for each waste type is determined with reference to the thermal constraint. The thermal constraint is that the temperature at the canister surface must not exceed 100 °C. Most countries engaged in repository design exercises have opted for 100 °C or less for the maximum buffer temperature, because bentonite will remain chemically intact for more than one million years as long as the temperature does not exceed 100 °C [47]. In this study, the temperature limit is reduced to 80 °C, in order to include a margin of 10 °C to cover for natural deviations in environmental parameters and in fuel data and another 10 °C to cover the risk of occurrence of an air gap between the canister and the buffer [49].

Computations are performed for a few selected burnup values: 33000 (the reference), 40000 and 50000 MWd/tHM in order to observe the effect of burnup on waste disposal. Minimum distance between canisters and maximum canister surface temperature for each waste type is given below.

6.3.1. Minimum Distance between SUOX Loaded Canisters

For SUOXs with 33000, 40000 and 50000 MWd/tHM, minimum canister spacings are 3.90, 5.54 and 10.00 meter respectively. Time-dependent temperatures on the canister surface and at the interface between bentonite and rock for SUOXs with 33000, 40000 and 50000 MWd/tHM placed at the minimum distances are shown in Figures 6.6, 6.7 and 6.8 respectively. For each burnup value, maximum temperature on the canister surface is 79.75, 79.48 and 79.70 °C and is reached at 11.5, 9.5 and 7.0 years after disposal.

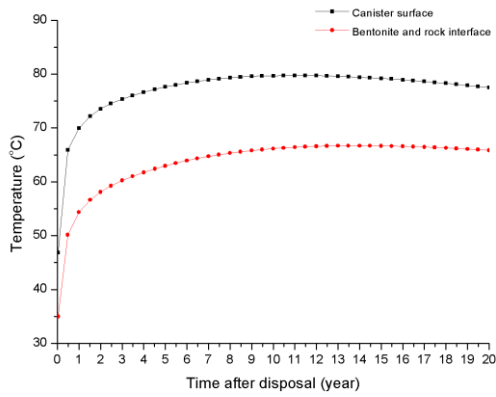


Figure 6.6. Temperature as a function of time on the canister surface and at the interface between bentonite and rock, spacing 3.90 m, SUOX with 33000 MWd/tHM burnup

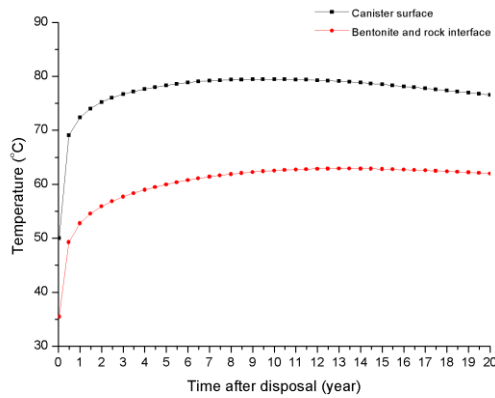


Figure 6.7. Temperature as a function of time on the canister surface and at the interface between bentonite and rock, spacing 5.54 m, SUOX with 40000 MWd/tHM burnup

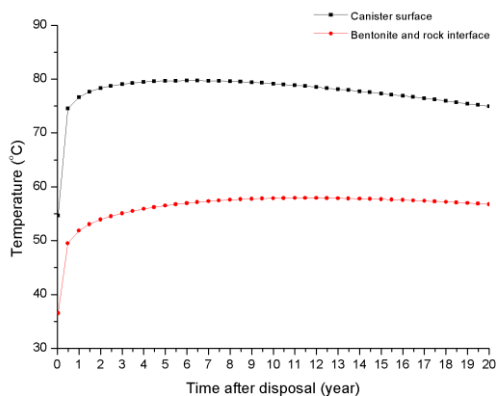


Figure 6.8. Temperature as a function of time on the canister surface and at the interface between bentonite and rock, spacing 10.00 m, SUOX with 50000 MWd/tHM burnup

6.3.2. Minimum Distance between HLW Loaded Canisters

For VHLWs from reprocessing of 33000, 40000 and 50000 MWd/tHM burnup SUOXs, minimum canister spacings are 4.00, 3.90 and 3.90 meter respectively. Time-dependent temperatures on the canister surface and at the interface between bentonite and rock for VHLWs with 33000, 40000 and 50000 MWd/tHM placed at the minimum distances are shown in Figures 6.9 through 6.11. For each burnup value, maximum temperature on the canister surface is 79.70, 79.77 and 79.82 °C and is reached at 8.5, 7.5 and 7.0 years after disposal.

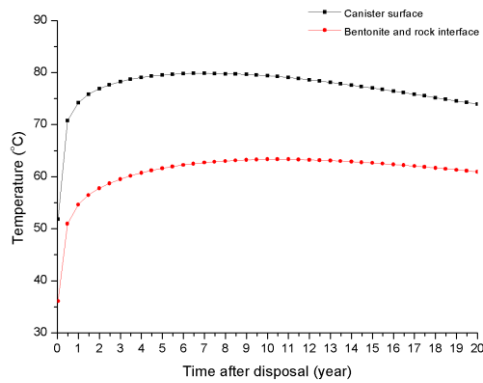


Figure 6.9. Temperature as a function of time on the canister surface and at the interface between bentonite and rock, spacing 4.00 m, HLW from reprocessing of 33000 MWd/tHM burnup SUOX

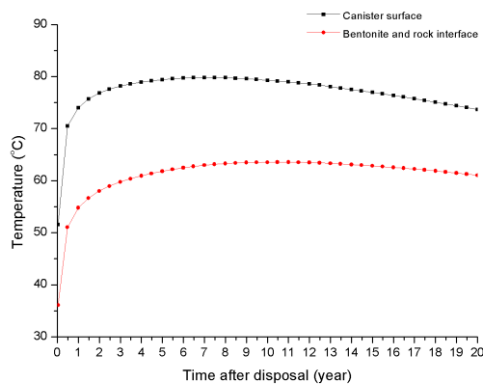


Figure 6.10. Temperature as a function of time on the canister surface and at the interface between bentonite and rock, spacing 3.90 m, HLW from reprocessing of 40000 MWd/tHM burnup SUOX

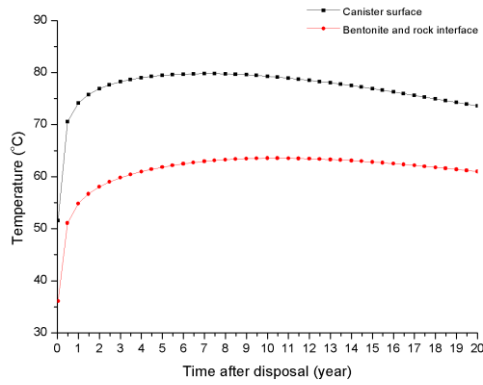


Figure 6.11. Temperature as a function of time on the canister surface and at the interface between bentonite and rock, spacing 3.90 m, HLW from reprocessing of 50000 MWd/tHM burnup SUOX

6.3.3. Minimum Distance between SMOX_{SRNU} Loaded Canisters

Minimum distance between SMOX_{SRNU} canisters for 33000, 40000 and 50000 MWd/tHM burnup values are 3.00, 4.80 and 13.00 meter respectively. Figures 6.12, 6.13 and 6.14 show the time dependent temperatures on the canister surface and at the rock-bentonite interface for minimum canister spacings. Maximum temperature on the canister surface is 79.92, 79.85 and 79.95 °C and is reached at 16.5, 16.5 and 13.5 years after disposal, for 33000, 40000 and 50000 MWd/tHM respectively.

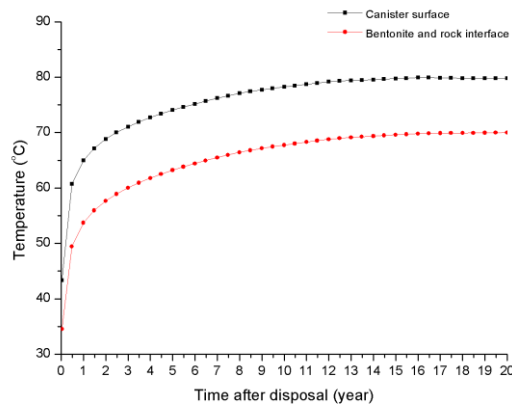


Figure 6.12. Temperature as a function of time on the canister surface and at the interface between bentonite and rock, spacing 3.00 m, SMOX_{SRNU} with 33000 MWd/tHM burnup

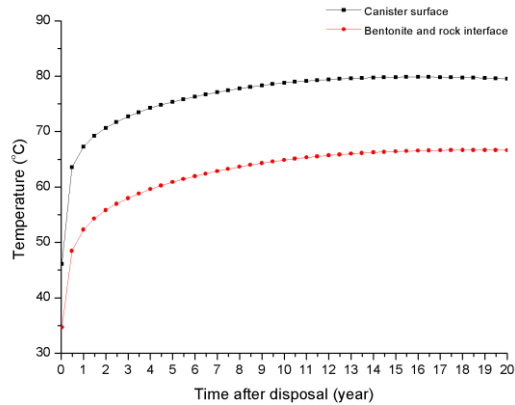


Figure 6.13. Temperature as a function of time on the canister surface and at the interface between bentonite and rock, spacing 4.80 m, SMOX_{SRNU} with 40000 MWd/tHM burnup

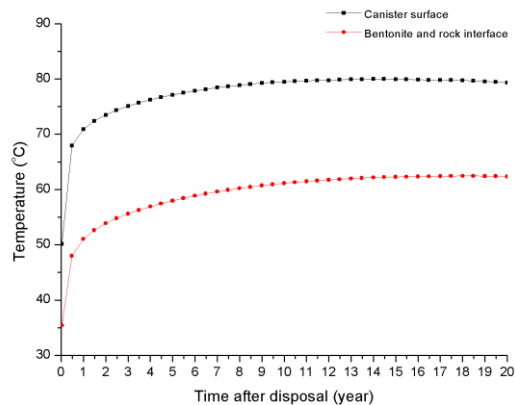


Figure 6.14. Temperature as a function of time on the canister surface and at the interface between bentonite and rock, spacing 13.00 m, SMOX_{SRNU} with 50000 MWd/tHM burnup

6.3.4. Minimum Distance between SMOX_{SRDU} Loaded Canisters

Minimum distance between SMOX_{SRDU} canisters for 33000, 40000 and 50000 MWd/tHM burnup values are 3.42, 5.54 and 18.80 meter respectively. Figures 6.15, 6.16 and 6.17 show time dependent temperatures on the canister surface and at the rock-bentonite interface for minimum canister spacings. Maximum temperature on the canister surface is 79.82, 79.98 and 79.97 °C and is reached at 16.5, 16.0 and 9.5 years after disposal, for 33000, 40000 and 50000 MWd/tHM respectively.

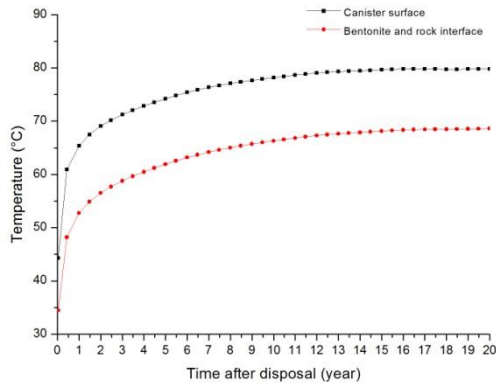


Figure 6.15. Temperature as a function of time on the canister surface and at the interface between bentonite and rock, spacing 3.42 m, SMOX_{SRDU} with 33000 MWd/tHM burnup

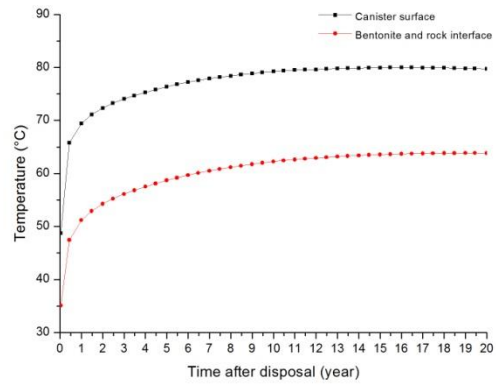


Figure 6.16. Temperature as a function of time on the canister surface and at the interface between bentonite and rock, spacing 5.54 m, SMOX_{SRDU} with 40000 MWd/tHM burnup

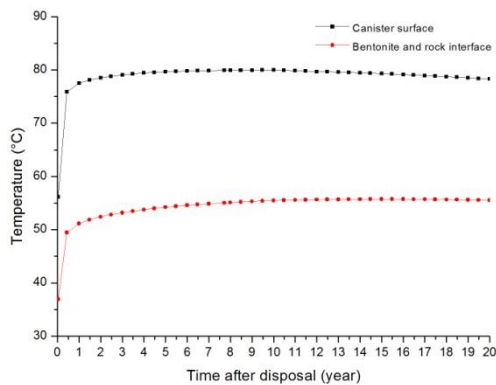


Figure 6.17. Temperature as a function of time on the canister surface and at the interface between bentonite and rock, spacing 18.80 m, SMOX_{SRDU} with 50000 MWd/tHM burnup

6.3.5. Minimum Distance between SMOX_{CCPu} Loaded Canisters

Minimum distance between SMOX_{CCPu} canisters for 33000, 40000 and 50000 MWd/tHM burnup values are 3.10, 5.00 and 16.00 meter respectively. Figures 6.18, 6.19 and 6.20 show the time dependent temperatures on the canister surface and at the rock-bentonite interface for minimum canister spacings. Maximum temperature on the canister surface is 79.70, 79.94 and 79.88 °C and is reached at 16.5, 16.0 and 10.5 years after disposal, for 33000, 40000 and 50000 MWd/tHM respectively.

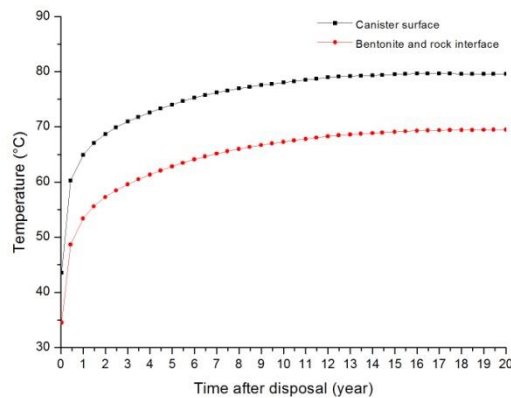


Figure 6.18. Temperature as a function of time on the canister surface and at the interface between bentonite and rock, spacing 3.10 m, SMOX_{CCPu} with 33000 MWd/tHM burnup

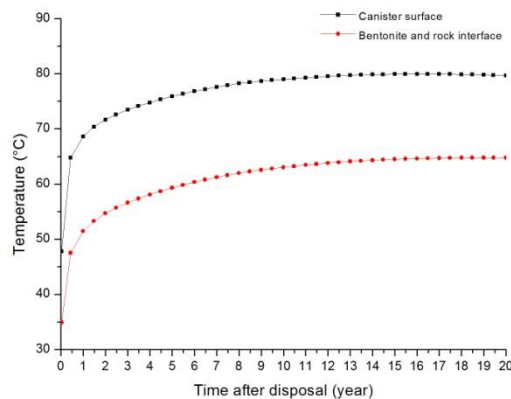


Figure 6.19. Temperature as a function of time on the canister surface and at the interface between bentonite and rock, spacing 5.00 m, SMOX_{CCPu} with 40000 MWd/tHM burnup

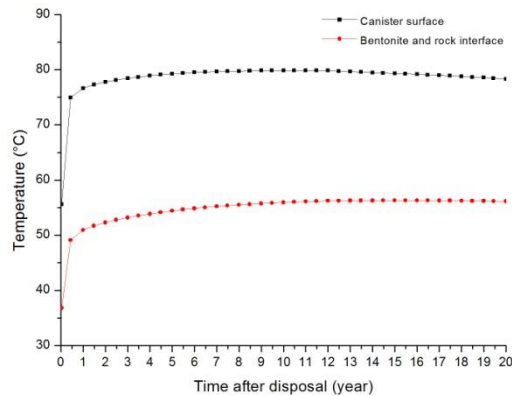


Figure 6.20. Temperature as a function of time on the canister surface and at the interface between bentonite and rock, spacing 16.00 m, SMOX_{CCPu} with 50000 MWd/tHM burnup

6.3.6. Minimum Distance between SMOX_{CCEU} Loaded Canisters

As seen in Figure 4.13, decay heat generation of SMOX_{CCEU} is much lower than other SMOX types under consideration and it is in the same order of SUOX decay heat generation. When disposal canister is loaded with one SMOX_{CCEU} assembly, the thermal limits cannot be attained. Thus, four SMOX_{CCEU} assemblies are loaded into disposal canister. Minimum distance between SMOX_{CCEU} canisters for 33000, 40000 MWd/tHM burnup values are 5.80 and 9.50 meter respectively. For 33000 and 40000 MWd/tHM, maximum temperature on the canister surface is 79.79 and 79.94 °C and is reached at 10.0 and 7.5 years after disposal, respectively. Figures 6.21 and 6.22 show the time dependent temperatures on the canister surface and at the rock-bentonite interface for minimum spacings for canisters loaded with 33000 and 40000 MWd/tHM SMOX_{CCEU} assemblies, respectively. For 50000 MWd/tHM, temperature limits are exceeded shortly after canisters are placed in to disposal hole. Time dependent temperatures on the canister surface and at the rock-bentonite interface for 50000 MWd/tHM is given in Figure 6.23.

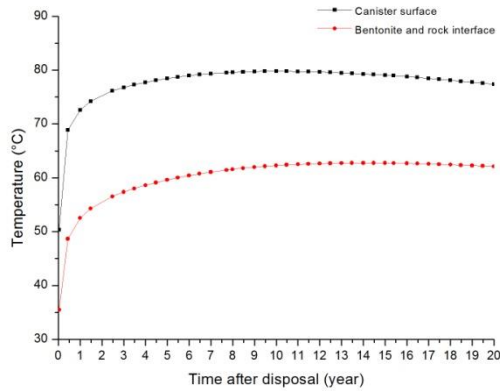


Figure 6.21. Temperature as a function of time on the canister surface and at the interface between bentonite and rock, spacing 5.80 m, SMOX_{CCEU} with 33000 MWd/tHM burnup

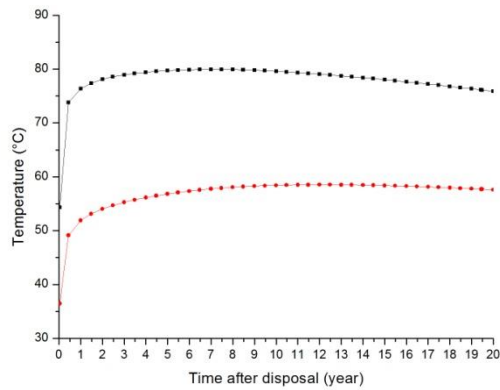


Figure 6.22. Temperature as a function of time on the canister surface and at the interface between bentonite and rock, spacing 9.50 m, SMOX_{CCEU} with 40000 MWd/tHM burnup

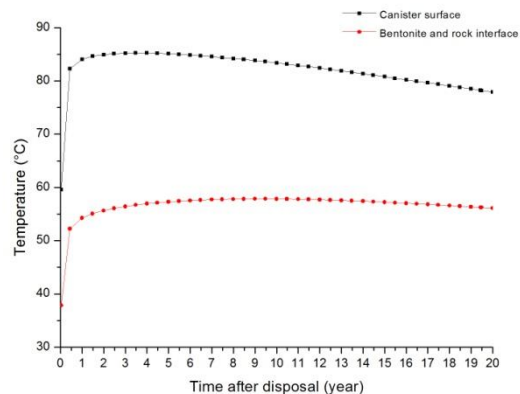


Figure 6.23. Temperature as a function of time on the canister surface and at the interface between bentonite and rock, SMOX_{CCEU} with 50000 MWd/tHM burnup

6.3.7. Minimum Distance between SMOX_{PC} Loaded Canisters

Minimum distance between SMOX_{PC} canisters for 33000, 40000 and 50000 MWd/tHM burnup values are 3.10, 4.94 and 13.70 meter respectively. Figures 6.24, 6.25 and 6.26 show the time dependent temperatures on the canister surface and at the rock-bentonite interface for minimum canister spacings. Maximum temperature on the canister surface is 79.55, 79.94 and 79.99 °C and is reached at 19.5, 16.0 and 11.0 years after disposal, for 33000, 40000 and 50000 MWd/tHM respectively.

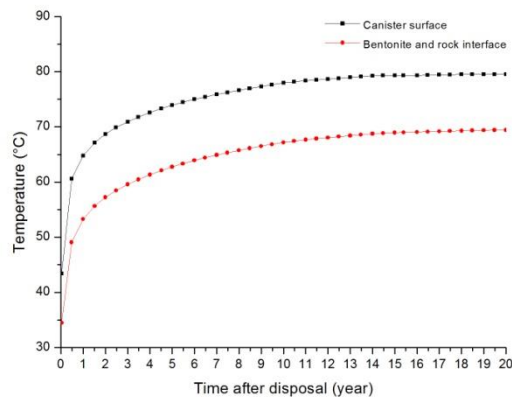


Figure 6.24. Temperature as a function of time on the canister surface and at the interface between bentonite and rock, spacing 3.10 m, SMOX_{PC} with 33000 MWd/tHM burnup

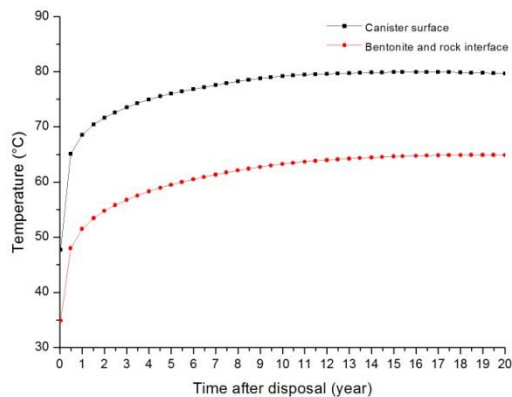


Figure 6.25. Temperature as a function of time on the canister surface and at the interface between bentonite and rock, spacing 4.94 m, SMOX_{PC} with 40000 MWd/tHM burnup

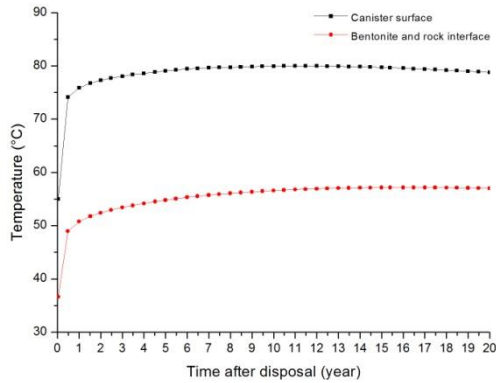


Figure 6.26. Temperature as a function of time on the canister surface and at the interface between bentonite and rock, spacing 13.70 m, SMOX_{PC} with 50000 MWd/tHM burnup

6.3.8. Minimum Distance between SRC-MOX_{SRNU} Loaded Canisters

Minimum distance between canisters loaded with 33000 MWd/tHM burnup SRC-MOX_{SRNU} assemblies is 12.60 meters. Maximum temperature on the canister surface is 79.88 °C and is reached at 14.5 years after disposal. Figure 6.27 shows time dependent temperature on the canister surface and at the rock-bentonite interface for minimum spacing for disposal canisters loaded with 33000 MWd/tHM SRC-MOX_{SRNU} assemblies. In case of loading canisters with 40000 and 50000 MWd/tHM burnup SRC-MOX_{SRNU} assemblies, temperature limits are exceeded very quickly. Figure 6.28 and 6.29 show time dependent temperatures on the canister surface and at the rock-bentonite interface for disposal canisters loaded with 40000 MWd/tHM and 50000 MWd/tHM SRC-MOX_{SRNU} assemblies, respectively.

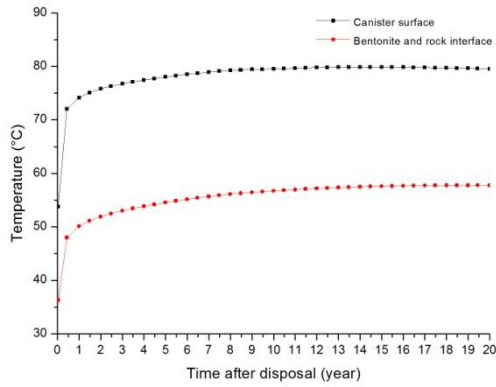


Figure 6.27. Temperature as a function of time on the canister surface and at the interface between bentonite and rock, spacing 12.60 m, SRc-MOX_{SRNU} with 33000 MWd/tHM burnup

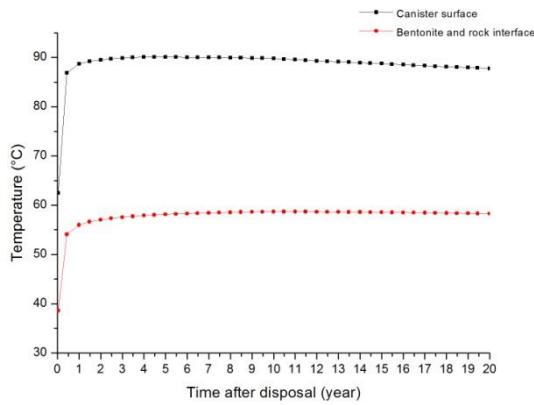


Figure 6.28. Temperature as a function of time on the canister surface and at the interface between bentonite and rock, SRc-MOX_{SRNU} with 40000 MWd/tHM burnup

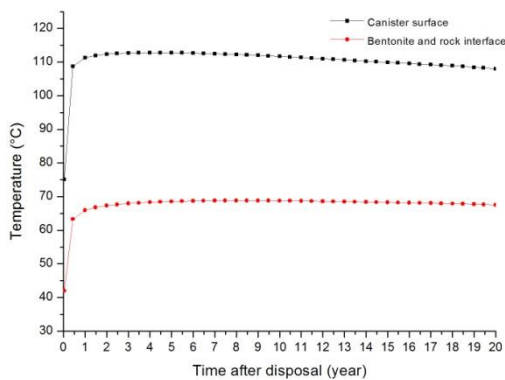


Figure 6.29. Temperature as a function of time on the canister surface and at the interface between bentonite and rock, SRc-MOX_{SRNU} with 50000 MWd/tHM burnup

7. DISPOSAL DENSITY CALCULATIONS

Disposal density of each fuel cycle is derived from net electricity produced by the fuel loaded to reactor and area needed to dispose waste arising from this fuel. First, total amounts of wastes generated and total disposal areas required per unit mass of fresh fuel loaded into the reactor in each fuel cycle are calculated. Then, results are converted to “total electrical energy (MWe-yr) produced per unit waste disposal area (m²)”, which is taken as the conclusive parameter to compare the fuel cycles under consideration with regard to waste disposal density.

7.1. DISPOSAL AREA CALCULATIONS

Total disposal area needed for each fuel cycle is determined by connecting the unit disposal area needed for each waste type to be disposed of and total amounts of those wastes generated in the cycle.

7.1.1. Disposal Area Needed per Unit Mass of Each Waste Type

Disposal area needed to safely dispose one ton of each waste type in the reference repository is calculated from the minimum distance between boreholes, distance between tunnels, and amount of waste loaded into a canister. For the waste types, disposal areas per canister are calculated first. Then, disposal areas per unit mass of wastes are obtained by considering the amount of wastes loaded to disposal canister. Results are given in Table 7.1.

As seen in Table 7.1, on the basis of per unit mass in the form ready to be buried in the repository, SRC-MOX_{SRNU} takes up the greatest disposal area for 33000 MWd/t. For 40000 and 50000 MWd/t, SMOX_{SRDU} requires the greatest disposal area. As burnup goes up, disposal area required increases significantly for SUOX and SMOX. Area needed for VHLW is not sensitive to the burnup. For 33000 and 40000 MWd/ton, SUOX needs considerably less area than VHLW, but at about 50000 MWd/ton, VHLW exhibits a small advantage.

A sensitivity analysis is also performed for evaluating the effect of variations in important parameters (such as the age of the waste at disposal, waste concentration and thermal properties of the host rock) in the disposal area required per unit mass of waste.

Table 7.1. Minimum distance between canisters and disposal area needed per ton of each waste type

Waste form	Burnup (MWd/tHM)	Canister spacing (m)	Disposal area per canister (m ² /canister)	Disposal area per ton of waste (m ² /t)
SUOX	33000	3.90	156.0	80.73
	40000	5.54	221.6	114.68
	50000	10.00	400.0	206.99
VHLW	33000	4.00	160.0	200.00
	40000	3.90	156.0	195.00
	50000	3.90	156.0	195.00
SMOX _{SRNU}	33000	3.00	120.0	248.39
	40000	4.80	192.0	397.43
	50000	13.00	520.0	1076.36
SMOX _{SRDU}	33000	3.42	136.8	283.17
	40000	5.54	221.6	458.70
	50000	18.80	752.0	1556.60
SMOX _{CCPu}	33000	3.10	124.0	256.67
	40000	5.00	200.0	413.98
	50000	16.00	640.0	1324.74
SMOX _{CCEU}	33000	5.80	232.0	120.06
	40000	9.50	380.0	196.64
	50000	-	-	-
SMOX _{PC}	33000	3.10	124.0	256.67
	40000	4.94	197.6	409.02
	50000	13.70	548.0	1134.32
SRC-MOX _{SRNU}	33000	12.60	504.0	1043.24
	40000	-	-	-
	50000	-	-	-

Cooling time affects the heat generation rate of the waste loaded in to disposal canister and hence the disposal area needed. For this reason, thermal analyses are repeated for 100 years cooling time and total disposal area needed for each fuel cycle is determined. Results of thermal analyses for 100 years cooling time and disposal area calculations are presented in Appendix III.

In order to assess the effect of concentration of waste loaded into canister on needed disposal area, alternative loading patterns are considered for disposal canisters. But, for the reference SUOX and SMOX packages, canisters and boreholes should be dimensioned in order to load more SF assemblies. However, such an investigation is out of the scope of this thesis. For the reference VHLW packages used in the study, the percentage of HLW in glass frit is 10 w/o and only

2 VHLW cylinders are put into a disposal canister. In an effort to observe what happens when more HLW is placed into a borehole, thermal analysis are repeated for waste packages containing 15 w/o HLW in glass frit and 3 VHLW cylinders. Results of thermal analysis performed for 15 w/o HLW in glass frit and 3 VHLW cylinders are presented in Appendix IV. When percentage of HLW in glass frit or number of VHLW cylinders in a disposal canister is increased, the minimum distance required between 2 boreholes also increases, and results for disposal area calculations do not change in favour of VHLW. For waste packages containing 15 w/o HLW in glass frit, temperature limits are exceeded quickly in general (depending on burnup). Similarly, for disposal canisters loaded with 3 VHLW cylinders, the thermal limits cannot be attained. In summary, trials to put a greater amount of HLW into a borehole do not yield a notable effect on the results. There can be merit in dimensioning boreholes and canisters in order to maximize the waste disposal density for VHLW. However, such an investigation for optimum design is out of the scope of this thesis.

Thermal properties of the host rock such as thermal conductivity and specific heat are the main effective factors for disposal area calculations. In order to calculate the effect of variation of host rock thermal properties, thermal analyses are repeated for conductivity and heat capacity values lower and higher than reference host rock thermal properties given in Table 6.1. Results are presented in Appendix V.

In order to assess the effect of thermal limit on needed disposal area, thermal analyses are repeated for 100 °C thermal constraint. Results of thermal analyses and disposal density calculations are given in Appendix VI.

7.1.2. Total Disposal Area Needed for Each Fuel Cycle

Disposal areas required for each fuel type is converted to total disposal areas required for fuel cycles by considering the types and amounts of wastes generated within the fuel cycles. For fuel cycles under consideration, amount of each waste type generated per ton of fresh U fuel loaded into the reactor is calculated and results are presented in Table 7.2. Total disposal areas obtained by using the waste amounts in fuel cycles are given in Table 7.3.

Table 7.2. Amount of wastes generated in each fuel cycle per ton of fresh U fuel loaded into the reactor

	OTC			SRNU			SRDU			CCPu			CCEU			PC			SRc-MOX			
	33	40	50	33	40	50	33	40	50	33	40	50	33	40	50	33	40	50	33	40	50	
Burnup GWd/tHM	Mass (t)	Mass (t)	Mass (t)	Mass (t)	Mass (t)	Mass (t)	Mass (t)	Mass (t)	Mass (t)	Mass (t)	Mass (t)	Mass (t)	Mass (t)	Mass (t)	Mass (t)	Mass (t)	Mass (t)	Mass (t)	Mass (t)	Mass (t)	Mass (t)	Mass (t)
SUOX	1	1	1	1	1	1	1	1	1	1	1	1	1	1	1	1	1	1	1	1	1	1
SMOX _{SRNU}	-	-	-	0.161	0.137	0.113	-	-	-	-	-	-	-	-	-	-	-	-	-	0.161	0.137	0.113
SMOX _{SRDU}	-	-	-	-	-	-	0.143	0.117	0.100	-	-	-	-	-	-	-	-	-	-	-	-	-
SMOX _{CCPu}	-	-	-	-	-	-	-	-	-	1.008	1.012	1.021	-	-	-	-	-	-	-	-	-	-
SMOX _{CCEU}	-	-	-	-	-	-	-	-	-	-	-	-	1.275	1.370	1.551	-	-	-	-	-	-	-
SMOX _{PC}	-	-	-	-	-	-	-	-	-	-	-	-	-	-	-	0.157	0.136	0.110	-	-	-	
SRc- MOX _{SRNU}	-	-	-	-	-	-	-	-	-	-	-	-	-	-	-	-	-	-	0.062	0.057	0.041	
SRcU	-	-	-	0.153	0.131	0.107	0.153	0.131	0.107	-	-	-	-	-	-	-	-	-	0.178	0.149	0.119	
VHLW	-	-	-	0.305	0.377	0.470	0.305	0.377	0.470	0.305	0.377	0.470	0.305	0.377	0.470	0.305	0.377	0.470	0.354	0.429	0.453	

Table 7.3. Total disposal area needed in each fuel cycle

	OTC			SRNU			SRDU			CCPu			CCEU			PC			SRc-MOX		
Burnup GWd/tHM	33	40	50	33	40	50	33	40	50	33	40	50	33	40	50	33	40	50	33	40	50
	D.A (m ²)	D.A (m ²)	D.A (m ²)	D.A (m ²)	D.A (m ²)	D.A (m ²)	D.A (m ²)	D.A (m ²)	D.A (m ²)	D.A (m ²)	D.A (m ²)	D.A (m ²)	D.A (m ²)	D.A (m ²)	D.A (m ²)	D.A (m ²)	D.A (m ²)	D.A (m ²)	D.A (m ²)	D.A (m ²)	D.A (m ²)
SUOX	80.7	114.7	207.0	-	-	-	-	-	-	-	-	-	-	-	x	-	-	-	-	x	x
SMOX _{SRNU}	-	-	-	40.0	54.5	121.6	-	-	-	-	-	-	-	-	x	-	-	-	-	x	x
SMOX _{SRDU}	-	-	-	-	-	-	40.4	53.7	155.7	-	-	-	-	-	x	-	-	-	-	x	x
SMOX _{CCPu}	-	-	-	-	-	-	-	-	-	258.7	419.0	1353.0	-	-	x	-	-	-	-	x	x
SMOX _{CCEU}	-	-	-	-	-	-	-	-	-	-	-	-	153.1	269.4	x	-	-	-	-	x	x
SMOX _{PC}	-	-	-	-	-	-	-	-	-	-	-	-	-	-	x	40.3	55.6	124.8	-	x	x
SRc- MOX _{SRNU}	-	-	-	-	-	-	-	-	-	-	-	-	-	-	x	-	-	-	64.9	x	x
SRcU	-	-	-	12.4	15.0	22.2	12.4	15.0	22.2	-	-	-	-	-	x	-	-	-	14.4	x	x
VHLW	-	-	-	61.0	73.5	79.4	61.0	73.5	79.4	61.0	73.5	79.4	61.0	73.5	x	61.0	73.5	79.4	70.8	x	x
Total area	80.7	114.7	207.0	113.3	143.0	223.1	113.8	142.2	257.2	319.7	492.5	1432.0	214.1	342.9	x	101.3	129.2	204.2	150.0	x	x

D.A: Disposal area

X: Minimum canister spacing can not be determined for SMOX and hence disposal density for fuel cycle

7.2. COMPARISON OF FUEL CYCLES

In order to compare the fuel cycles, total disposal areas required are related to the electricity generated in each fuel cycle. First, electrical energy produced in each fuel cycle per ton of fresh fuel loaded into the reactor is calculated. Then, the results for disposal areas are converted to “total electrical energy (MWe-yr) produced per unit waste disposal area (m^2)” for fuel cycles. This is taken as the conclusive parameter to compare the fuel cycles with regard to waste disposal density (area). Table 7.4 shows the electricity generated in each fuel cycle. The overall results for fuel cycles are presented in Table 7.5.

To better observe behaviour of cycles with respect to burnup and compare them, a Disposal-Area Advantage Factor (DAAF) is defined as the ratio of numerical value of MWe-yr/ m^2 in a case to that in OT cycle for the reference burnup of 33000 MWd/t, for which DAAF is taken to be unity. As can be seen in Table 7.5, as burnup goes up in all fuel cycles, electricity generated per unit disposal area goes down (or disposal area required per unit electricity produced increases). However, as burnup is increased, reduction in DAAF is more in SRDU cycle than that in other cycles; in other words, SRDU cycle is more affected by burnup.

At the reference burnup of 33000 MWd/t, OT cycle is superior to other fuel cycles; when burnup is increased to 40000 MWd/t, DAAF values become about the same for OT, SRNU, SRDU and PC cycles; and at 50000 MWd/t, SRNU cycle becomes more advantageous than other cycles. In case of closed cycles (SRNU, SRDU, CCPu, CCEU, PC, and SRc-MOX), what is to be disposed of is a combination of VHLW, SUOX (or SRcU) and SMOX instead of only SUOX in OT cycle. Based on the disposal concept and waste packages assumed in this study, per unit mass ready to be disposed of, VHLW requires considerably more disposal area than SUOX at 33000 and 40000 MWd/t; and only slightly less at 50000 MWd/t. SMOX in any case requires more disposal area than SUOX. Then, the waste types in closed cycles, in general, impose a disadvantage with respect to disposal area per unit mass. However, in case of closed cycles, the amount of electricity produced per unit mass of fresh fuel loaded into the reactor is considerably greater than that in OT cycle. Consequently, the disadvantage of closed cycles with regard to waste types is offset by the advantage with regard to amount of electricity at about 40000

MWd/t; and at higher burnups, closed cycles are better than OT cycle with respect to waste disposal density except for CCPu cycle.

Table 7.4. Energy produced in each fuel cycle per ton of fresh U fuel loaded into the reactor

Burnup GWd/tHM	OTC			SRNU			SRDU			CCPu			CCEU			PC			SRc-MOX		
	33	40	50	33	40	50	33	40	50	33	40	50	33	40	50	33	40	50	33	40	50
	E.P. (GWh e/t)	E.P. (GWh e/t)	E.P. (GWh e/t)	E.P. (GWh e/t)	E.P. (GWh e/t)	E.P. (GWh e/t)	E.P. (GWh e/t)	E.P. (GWh e/t)	E.P. (GWh e/t)	E.P. (GWh e/t)	E.P. (GWh e/t)	E.P. (GWh e/t)	E.P. (GWh e/t)	E.P. (GWh e/t)	E.P. (GWh e/t)	E.P. (GWh e/t)	E.P. (GWh e/t)	E.P. (GWh e/t)	E.P. (GWh e/t)	E.P. (GWh e/t)	E.P. (GWh e/t)
SUOX	0.258	0.312	0.390	0.258	0.312	0.390	0.258	0.312	0.390	0.258	0.312	0.390	0.258	0.312	0.258	0.258	0.312	0.390	0.258	0.312	0.390
SMOX _{SRNU}	-	-	-	0.042	0.043	0.044	-	-	-	-	-	-	-	-	-	-	-	-	0.042	0.043	0.044
SMOX _{SRDU}	-	-	-	-	-	-	0.037	0.037	0.039	-	-	-	-	-	-	-	-	-	-	-	-
SMOX _{CCPu}	-	-	-	-	-	-	-	-	-	0.260	0.316	0.398	-	-	-	-	-	-	-	-	-
SMOX _{CCEU}	-	-	-	-	-	-	-	-	-	-	-	-	0.328	0.427	0.605	-	-	-	-	-	-
SMOX _{PC}	-	-	-	-	-	-	-	-	-	-	-	-	-	-	-	0.040	0.042	0.043	-	-	-
SRc- MOX _{SRNU}	-	-	-	-	-	-	-	-	-	-	-	-	-	-	-	-	-	-	0.016	0.018	0.016
SRcU	-	-	-	0.040	0.041	0.042	0.040	0.041	0.042	-	-	-	-	-	-	-	-	-	0.046	0.046	0.460
VHLW	-	-	-	-	-	-	-	-	-	-	-	-	-	-	-	-	-	-	-	-	-

E.P.: Electricity Produced

Table 7.5. Results of disposal density calculations for fuel cycles

Burnup (MWd/tHM)	Electricity in MWe-yr produced (based on one ton of fresh fuel loaded) per unit area in m ² of disposal area required for all the SF/VHLW arising in that fuel cycle (MWe-yr/m ²)			Disposal-Area Advantage Factor (DAAF)		
	33000	40000	50000	33000	40000	50000
OT	3188.40	2720.56	1884.07	1	0.8533	0.5909
SRNU	2992.25	2765.71	2022.52	0.9385	0.8674	0.6343
SRDU	2932.55	2711.09	1750.43	0.9198	0.8503	0.5490
CCPu	1616.66	1261.79	545.68	0.5070	0.3958	0.1712
CCEU	2775.66	2134.81	-	0.8705	0.6696	-
PC	2945.02	2719.26	1999.74	0.9237	0.8529	0.6272
SRC-MOX	2413.00	-	-	0.7568	-	-

8. RADIOTOXICITY CALCULATIONS

Radiological toxicity is the other important parameter that can be used in the comparison of back-end fuel cycles with respect to geological disposal. SF discharged from a reactor contains fissile isotopes, fertile isotopes, FPs and several actinides. For this reason, SF and HLW are highly radioactive and both have high hazard potential. Because of the high hazard potential, radioactive wastes generated in fuel cycles should be managed safely before geological disposal. The long term hazard of SF and HLW is associated with actinides, particularly the Transuranics, while the short and long term risks are due to the mobility of FPs in the geosphere and the possibility of their entering the biosphere [50]. After disposal, geological repository should isolate and contain the wastes deep within the rock until the radioactivity levels decline to an insignificant level. Accordingly, providing isolation and containment of wastes over the period of high hazard potential is the key objective when designing a geological repository and it is important to reduce radiotoxicity of waste to be sent to repository. Hence, fuel cycle generating less radiotoxic waste will be more advantageous with regard to geological disposal.

The radioactivity of the waste is no direct measure of its radiotoxicity. As a measure of the radiobiological hazard, radiotoxicity of the waste may be characterised by intake of incorporating radioactivity from the waste by the human body along with inhaled air (inhalation radiotoxicity) or drinking water (ingestion radiotoxicity) [51]. Radiotoxicity for an individual radionuclide is defined as the radioactivity divided by the radioactivity concentration limit for that nuclide in 1 cm³ air (inhalation radiotoxicity) or in 1 kg of drinking water (ingestion radiotoxicity). For radioactive waste which is a mixture of radionuclides, radiotoxicity is the sum of the radiotoxicities of all nuclides present in the waste.

In a repository, ingestion radiotoxicity may be considered to be more important than inhalation radiotoxicity because the potential biological hazard to humans occurs when the radioisotope is absorbed in nearby ground water or brine and transported from the repository to potential human receptors through drinking water. Inhalation radiotoxicity is important for short-term (i.e., above-ground)

storage concerns. It may also become important in case of intrusion upon the repository site and release of radioactive elements to the air [52].

In this part of the study, effects of the radiological characteristics of the SF/HLW wastes arising from the considered fuel cycles on geological disposal are assessed. First, radiotoxicity (radioactivity and ingestion radiotoxicity) of wastes generated from each fuel cycle and disposal time of these wastes to decline to the radiotoxicity of uranium ore which is often used as a reference point are calculated. Then, fuel cycles are compared with regard to radiotoxicity by assuming all generated wastes from each fuel cycle as a mixture and by calculating the average disposal time for these mixtures to decline radiotoxicity of uranium ore.

8.1. RADIOTOXICITY CALCULATIONS FOR WASTES

For the waste types generated in the considered fuel cycles, radiotoxicity calculations are performed by using MONTEBURNS code. MONTEBURNS provides time dependent radioactivity, ingestion radiotoxicity and inhalation radiotoxicity values for wastes. Since radioactivity of any waste type is dependent on burnup, to observe the effect of burnup on waste disposal with regard to radiological toxicity, computations are performed for the same burnup values selected in the composition and decay heat profile calculations: 33000 (the reference), 40000 and 50000 MWd/tHM. Results of radiotoxicity calculations for wastes generated in considered fuel cycles are given in Figures 8.1 through 8.6. For comparison, radioactivity and ingestion radiotoxicity levels of natural uranium ore are also given in the figures.

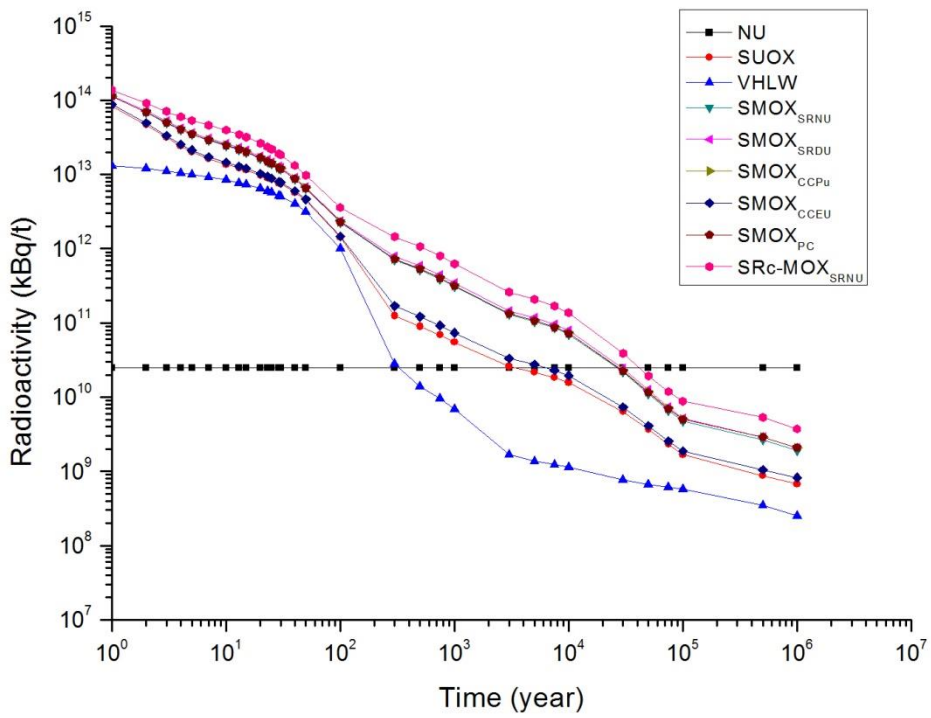


Figure 8.1. Radioactivities of wastes for 33000 MWd/tHM burnup

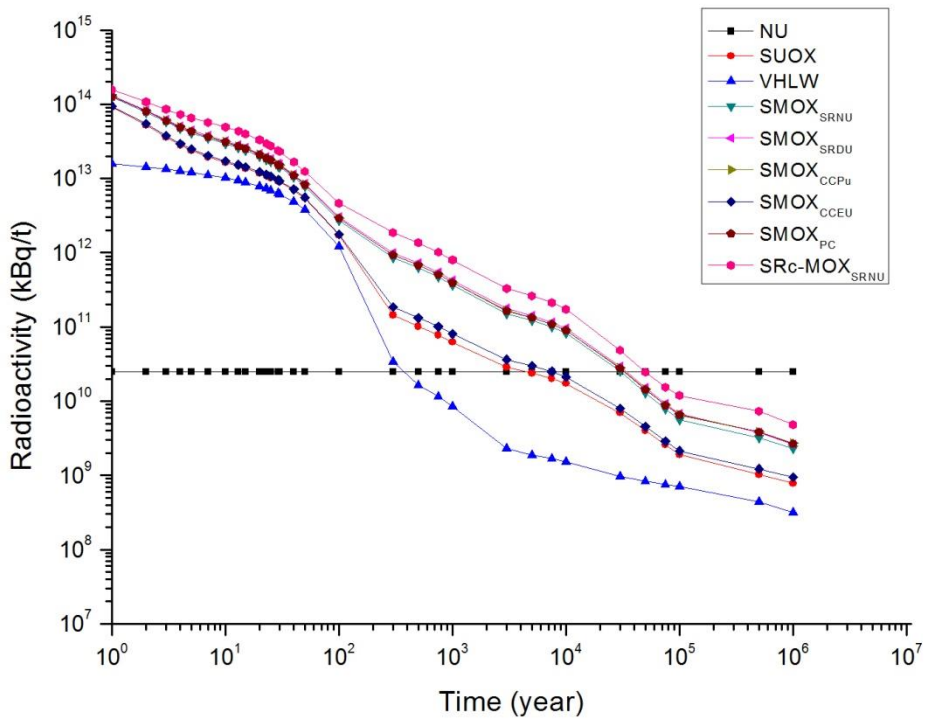


Figure 8.2. Radioactivities of wastes for 40000 MWd/tHM burnup

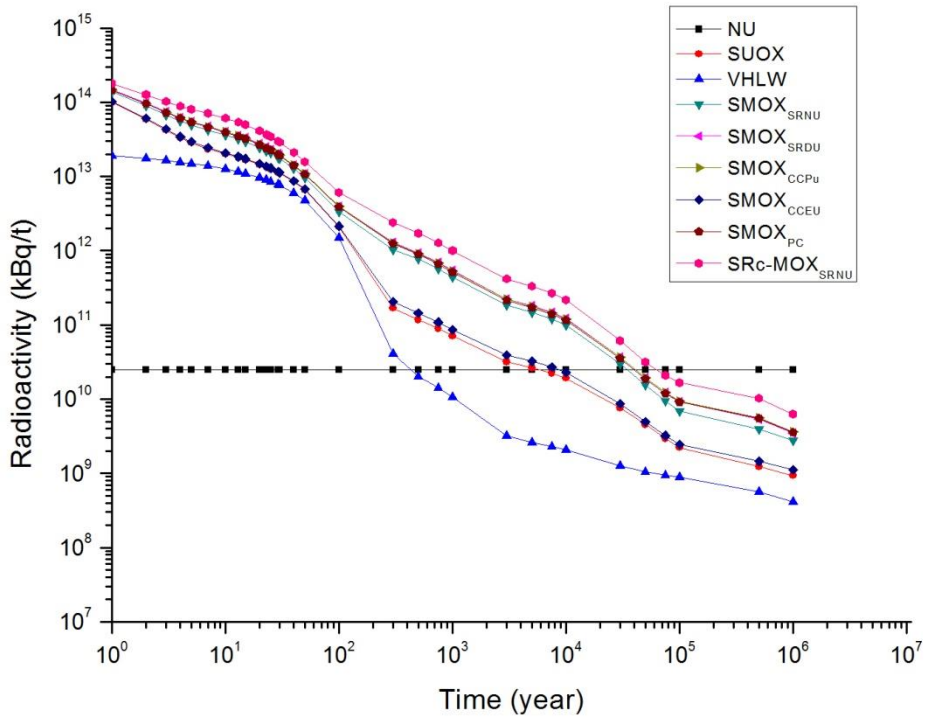


Figure 8.3. Radioactivities of wastes for 50000 MWd/tHM burnup

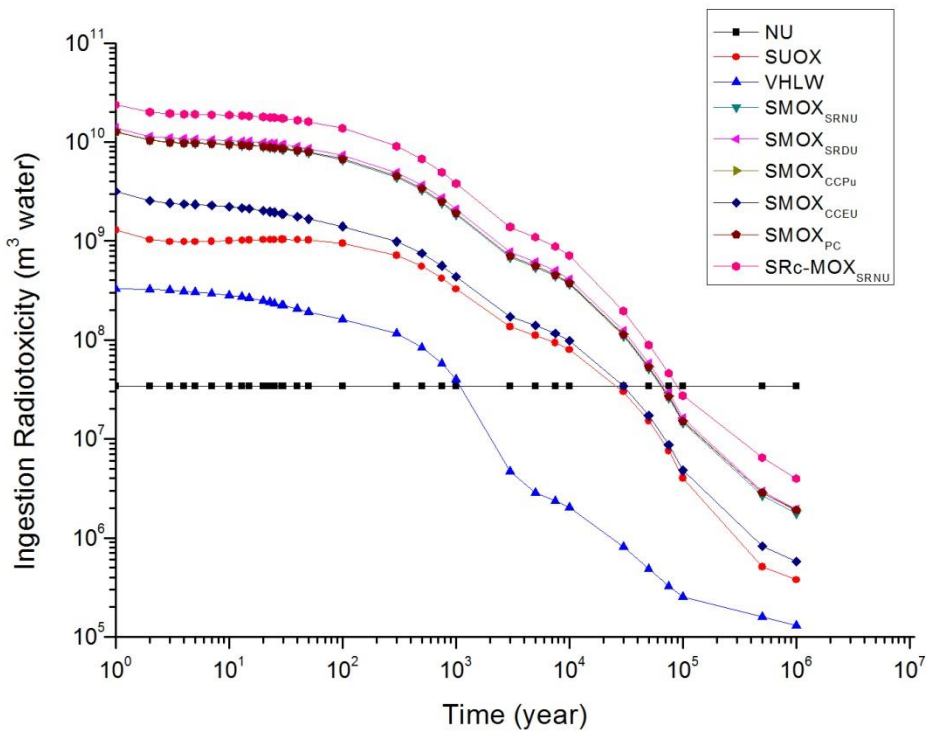


Figure 8.4. Ingestion radiotoxicities of wastes for 33000 MWd/tHM burnup

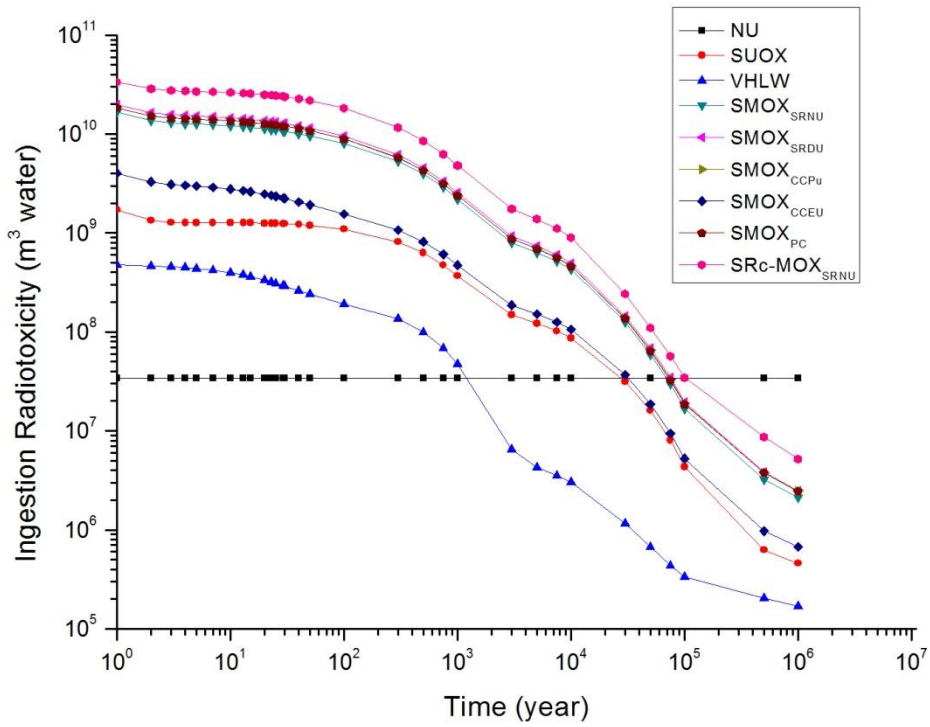


Figure 8.5. Ingestion radiotoxicities of wastes for 40000 MWd/tHM burnup

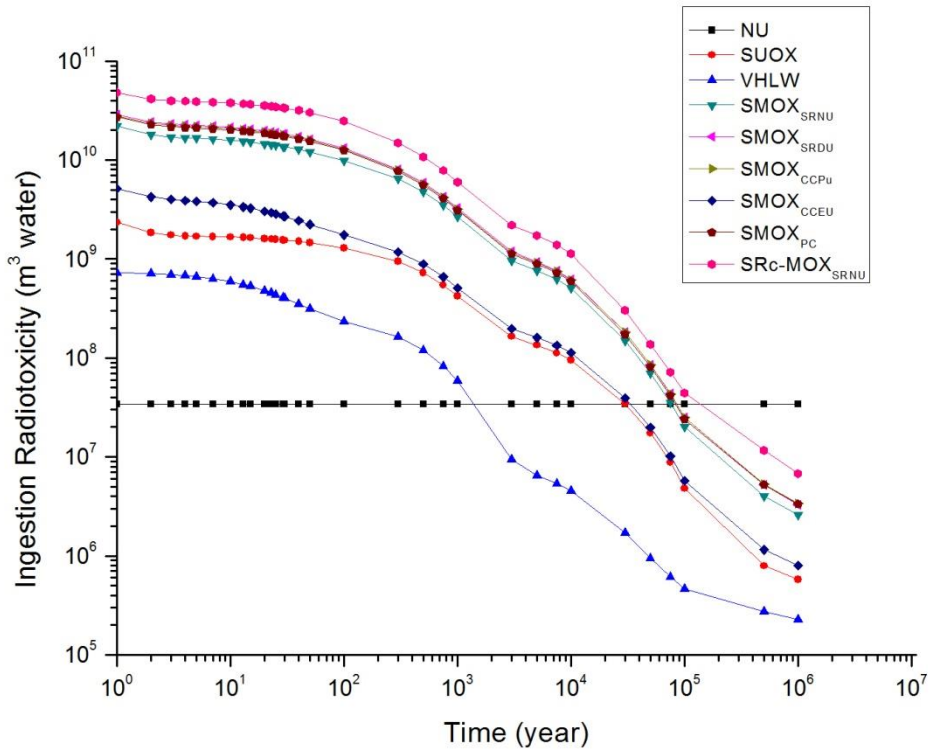


Figure 8.6. Ingestion radiotoxicities of wastes for 50000 MWd/tHM burnup

It can be seen in Figures 8.1 through 8.6 that the radioactivity and ingestion radiotoxicity of VHLW is much lower than other waste types and it decreases a great extent after 100 years of cooling time. This is mainly due to the separation of U and Pu that has a dominant impact in the long term radioactivity. Radioactivities and ingestion radiotoxicities of SUOX and SMOX_{CCEU} wastes are close to each other. SMOX_{SRNU}, SMOX_{SRDU}, SMOX_{CCPu} and SMOX_{PC} have comparable radioactivity and ingestion radiotoxicity levels.

8.2. COMPARISON OF FUEL CYCLES

In order to compare the fuel cycles with regard to radiotoxicity, the average time for each waste type to decline to the radiotoxicity level of uranium ore is determined first. As seen in Figures 8.1 through 8.6, depending on the waste type, the radioactivity and ingestion radiotoxicity of the wastes eventually decline to the levels of natural uranium over periods from a few thousands to around a hundred thousand years. Table 8.1 gives the estimated time after which the radioactivity and ingestion radiotoxicity of disposed wastes drop to the radioactivity and the radiotoxicity levels of NU.

Table 8.1. Decay times for waste types

Waste form	Burnup (MWd/tHM)	Time for 1 ton of waste to decay to NU radioactivity level (years)	Time for 1 ton of waste to decay to NU ingestion toxicity level (years)
SUOX	33000	3272	25400
	40000	4395	28422
	50000	5642	30208
VHLW	33000	335	1110
	40000	380	1195
	50000	427	1357
SMOX _{SRNU}	33000	26845	63417
	40000	30390	69567
	50000	35321	76000
SMOX _{SRDU}	33000	29445	68005
	40000	34156	75544
	50000	41033	84370
SMOX _{CCPu}	33000	27667	65167
	40000	32778	73692
	50000	40825	84230
SMOX _{CCEU}	33000	6197	29849
	40000	7556	31883
	50000	8533	33310
SMOX _{PC}	33000	27453	64667
	40000	32333	71965
	50000	38912	83340
SRC-MOX _{SRNU}	33000	41308	86736
	40000	49000	100402
	50000	62451	134162

By using the results given in Table 8.1 average decay times needed for all wastes from each fuel cycle to drop to NU radioactivity and ingestion radiotoxicity levels are calculated. In average decay time calculations for fuel cycles, the total wastes arised from each fuel cycle are considered as a mixture. Results are presented in Table 8.2.

Table 8.2. Average decay times for fuel cycles

Burnup (MWd/tHM)	Average time to decay to NU radioactivity level (years)			Average time to decay to NU ingestion toxicity level (years)		
	33000	40000	50000	33000	40000	50000
OT	3272	4395	5642	25400	28422	30208
SRNU	3930	4100	4110	11583	11533	10780
SRDU	3888	3970	4243	11345	11028	10765
CCPu	14053	16678	20893	33262	37665	43231
CCEU	3620	4368	5356	17214	18939	20788
PC	3999	4201	4245	9696	9658	9490
SRc-MOX	2512	2887	2897	7677	8192	8140

9. CONCLUSION

The purpose of this study has been to compare the once-through and alternative closed nuclear fuel cycles for a typical PWR with respect to waste disposal densities (waste disposal area required for spent fuel and high level waste) in a permanent geological repository and to radiological toxicities of wastes generated.

The study involved development of back-end fuel cycle scenarios, estimation of compositions and volumes of wastes generated from fuel cycles, thermal analyses to determine disposal areas needed per unit mass of waste types under consideration, and determination of waste disposal density for each fuel cycle. Back-end fuel cycle scenarios were developed considering different reprocessing schemes. Compositions and volumes of resultant wastes were estimated employing the MONTEBURNS code. Thermal analyses performed with the ANSYS were utilized to determine minimum distances between waste disposal canisters and disposal areas needed in a reference repository. At the end, by connecting the disposal areas to the amounts of wastes to be disposed of and the electricity generated in each fuel cycle, the fuel cycles under consideration have been compared. Effects of the fuel cycle options on waste management have also been discussed from a radiological perspective.

The results show that, at the reference burnup of 33000 MWd/t, OT cycle is superior to the other fuel cycles with regard to disposal density; when burnup is increased to around 40000 MWd/t, waste disposal density becomes about the same for OT, SRNU, SRDU and PC cycles; and at about 50000 MWd/t, SRNU cycle becomes more advantageous than the other cycles.

Note that the numerical values obtained are based on the reference disposal concept and the waste package designs selected, and these assumptions affect the results significantly in some cases. Using the methodology presented in this thesis, a recommended next step would be to compare the waste disposal densities for different disposal concepts and waste package models. Furthermore, it can be the subject of future studies to take into account any novel fuel cycle scenario and to compare it to the cycles considered here by the same approach.

APPENDIX I: SRcU COMPOSITIONS AND DECAY HEATS

For 33000, 40000 and 50000 MWd/tHM, the enrichments of R_cU required are calculated from the expression in [37] as 3.52, 4.13 and 5.02 w/o respectively and with them used as input to MONTEBURNS, SR_cU compositions and decay heats are obtained. Decay heat profiles of SR_cU burned to 33000, 40000 and 50000 MWd/tHM are shown in Figure A.I.1.

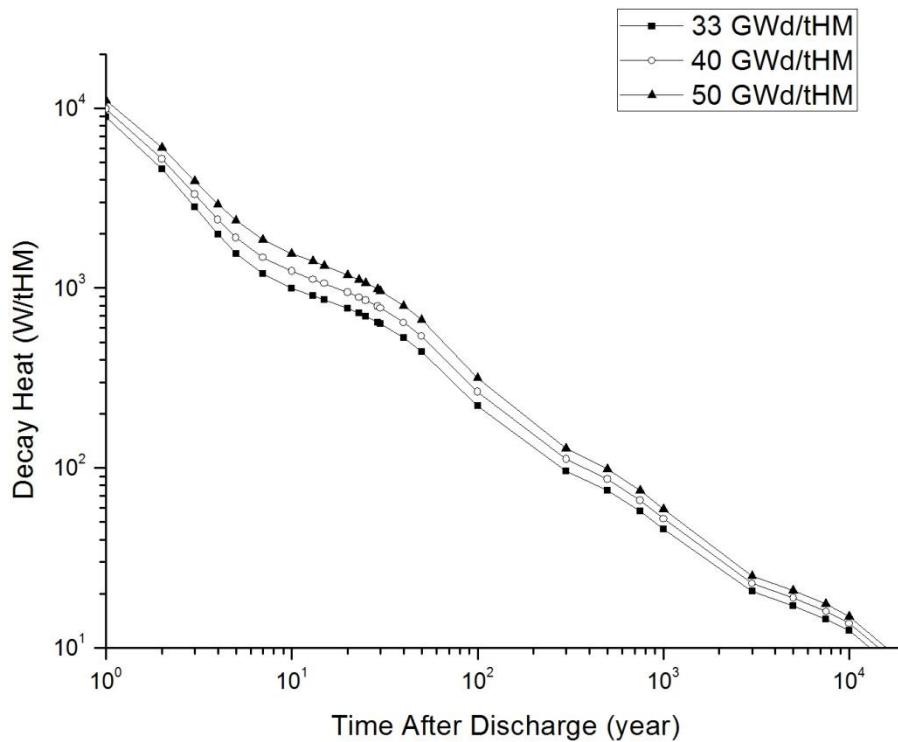
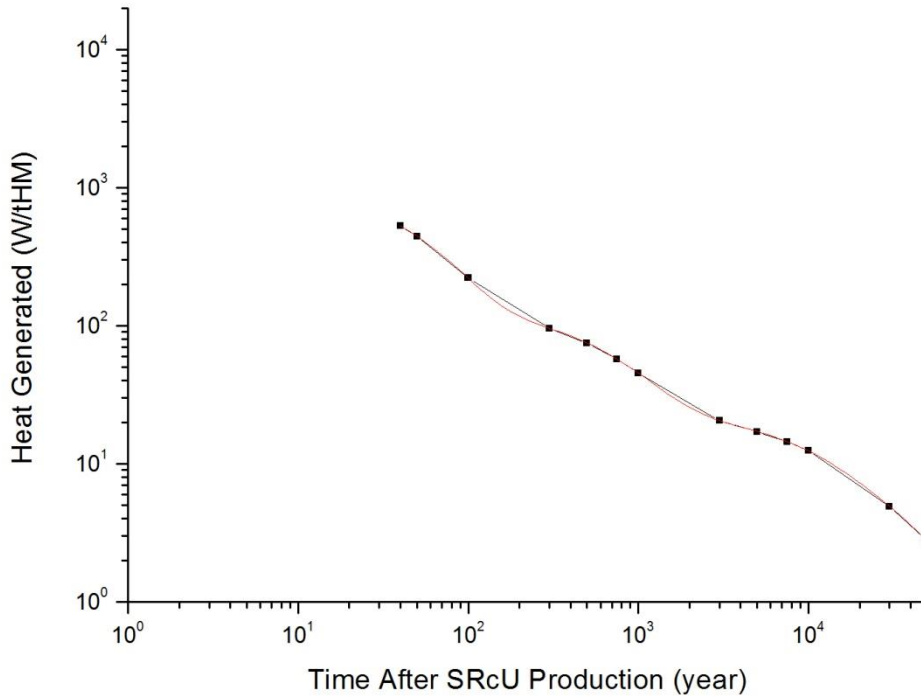


Figure A.I.1. Decay heat profiles of SR_cU burned to 33000, 40000 and 50000 MWd/tHM

Decay heat curves for SR_cUs burned to 33000, 40000 and 50000 MWd/tHM are fitted to Put's Formula in order to obtain heat generation rate equations which are to be used as the heat source terms in thermal analyses. As it can be seen from fit results for SR_cU given in Figures A.I.2, A.I.3, A.I.4 and fit results for SUOX given in Figures A.II.1, A.II.2, A.II.3 decay heat profiles of SR_cU are almost the same as those of SUOX; so, it is proper to assume SR_cU is simply SUOX with the same burnup.

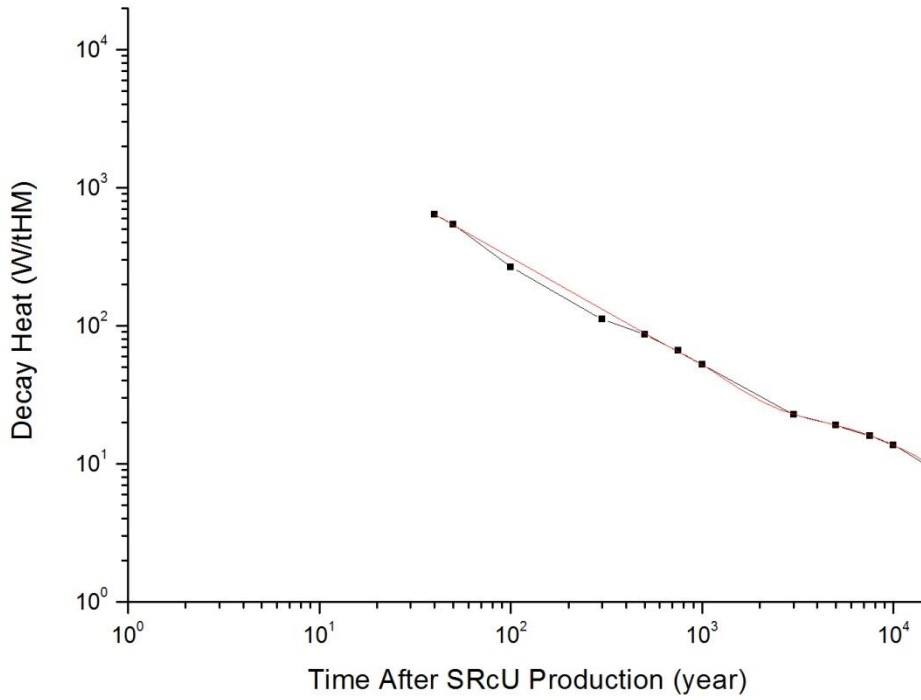


(a)

Equation	$y = A \cdot \exp(-B \cdot x) + C \cdot \exp(-D \cdot x) + E \cdot \exp(-F \cdot x) + G \cdot \exp(-H \cdot x)$		
Adj. R-Square	1		
		Value	Standard Error
B	A	993,98561	1,42815
B	B	0,02311	5,08139E-5
B	C	8,5386	3,05641
B	D	2,33939E-5	7,35042E-6
B	E	115,6756	0,56431
B	F	0,00163	1,59584E-5
B	G	16,08866	2,78136
B	H	1,05437E-4	1,82399E-5

(b)

Figure A.I.2. (a) Exponential fit of decay heat of SRcU with 33000 MWd/tHM, (b) Values of coefficients in Put's Formula

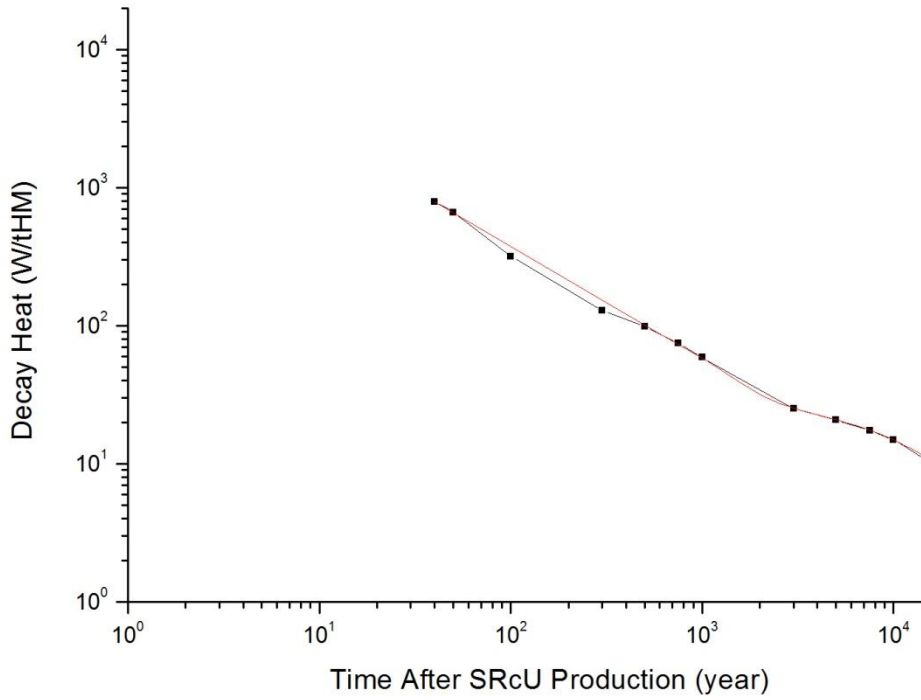


(a)

Equation	$y = A \cdot \exp(-B \cdot x) + C \cdot \exp(-D \cdot x) + E \cdot \exp(-F \cdot x) + G \cdot \exp(-H \cdot x)$		
Adj. R-Square	1		
		Value	Standard Error
B	A	1226,3382	1,33359
B	B	0,02311	3,85601E-5
B	C	9,27475	2,74868
B	D	2,32763E-5	6,14041E-6
B	E	137,11954	0,52927
B	F	0,00164	1,27102E-5
B	G	18,22754	2,49257
B	H	1,06941E-4	1,49509E-5

(b)

Figure A.I.3. (a) Exponential fit of decay heat of SRcU with 40000 MWd/tHM, (b) Values of coefficients in Put's Formula



(a)

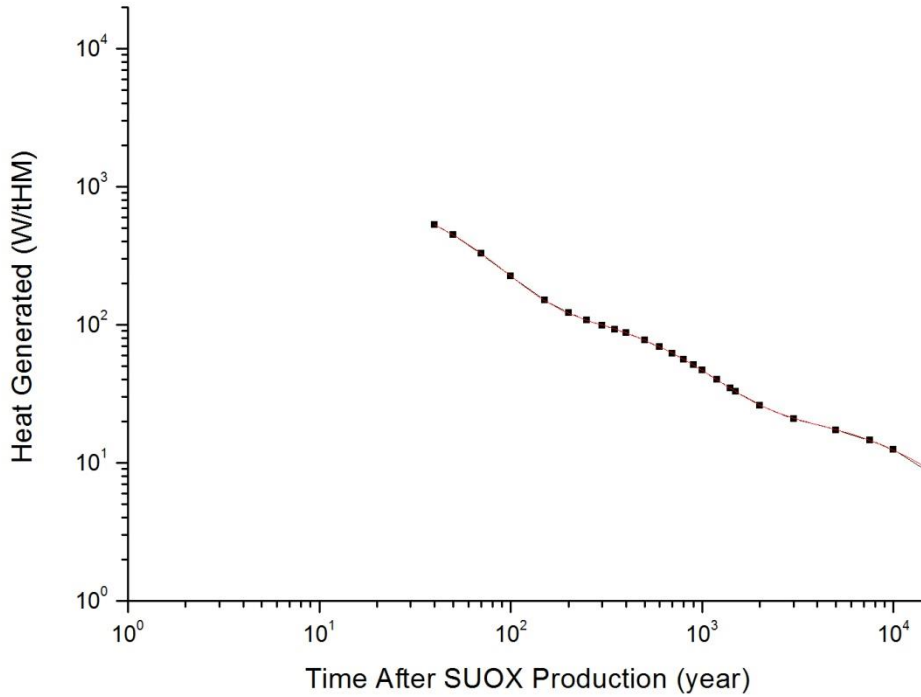
Equation	$y = A \cdot \exp(-B \cdot x) + C \cdot \exp(-D \cdot x) + E \cdot \exp(-F \cdot x) + G \cdot \exp(-H \cdot x)$		
Adj. R-Square	1		
		Value	Standard Error
B	A	1557,96333	3,76848
B	B	0,02328	8,62718E-5
B	C	160,46419	1,48573
B	D	0,00167	3,11343E-5
B	E	10,46663	7,19556
B	F	2,41346E-5	1,46352E-5
B	G	20,26469	6,47714
B	H	1,12189E-4	3,79833E-5

(b)

Figure A.I.4. (a) Exponential fit of decay heat of SRcU with 50000 MWd/tHM, (b) Values of coefficients in Put's Formula

**APPENDIX II: DECAY HEAT CURVE FITS FOR WASTE TYPES UNDER
CONSIDERATION**

SUOX:

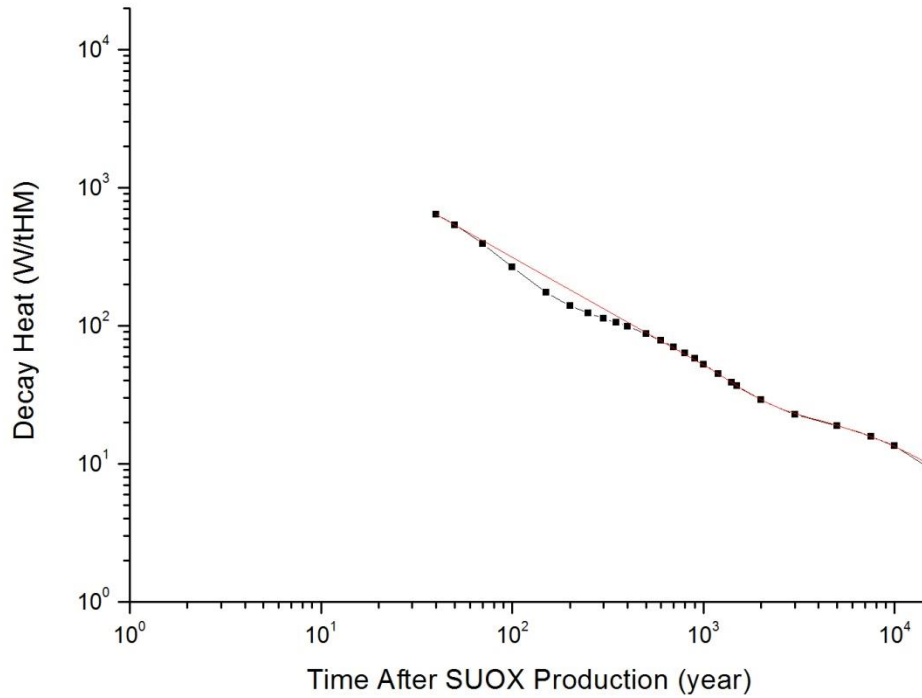


(a)

Equation	$y = A*\exp(-B*x)+C*\exp(-D*x)+E*\exp(-F*x)+G*\exp(-H*x)$		
Adj. R-Square	1		
		Value	Standard Error
B	A	990,17999	1,5906
B	B	0,02325	4,56437E-5
B	C	11,60256	3,93457
B	D	3,13746E-5	7,91485E-6
B	E	120,7312	0,4868
B	F	0,00166	1,56977E-5
B	G	14,27421	3,58238
B	H	1,31353E-4	3,30154E-5

(b)

Figure A.II.1. (a) Exponential fit of decay heat of SUOX with 33000 MWd/tHM,
(b) Values of coefficients in Put's Formula

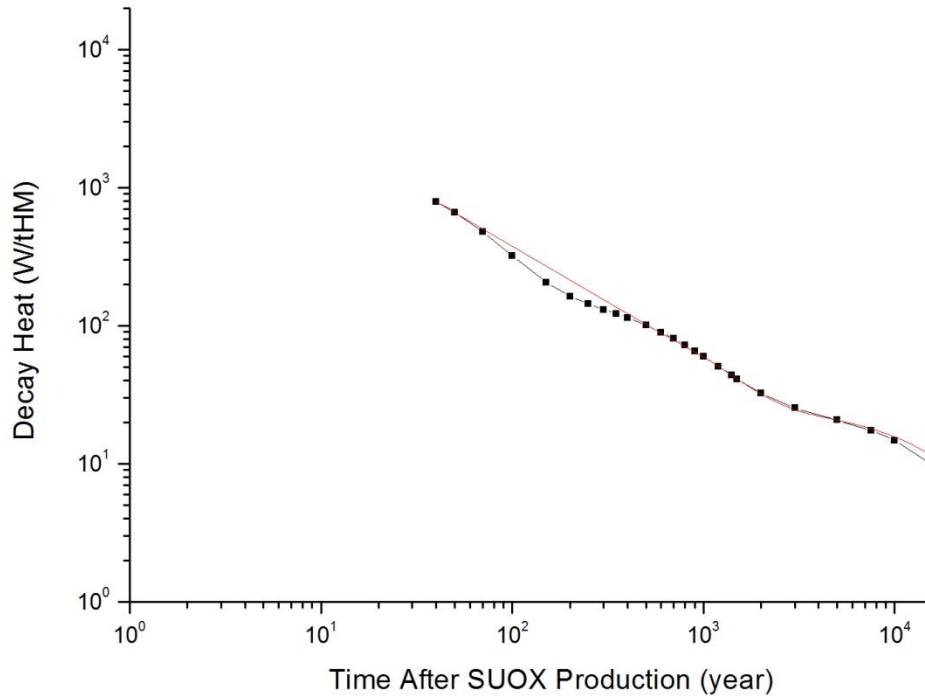


(a)

Equation	$y = A \cdot \exp(-B \cdot x) + C \cdot \exp(-D \cdot x) + E \cdot \exp(-F \cdot x) + G \cdot \exp(-H \cdot x)$		
Adj. R-Square	1		
		Value	Standard Error
B	A	1219,8048	1,89993
B	B	0,02324	4,44339E-5
B	C	13,01567	4,4881
B	D	3,26419E-5	8,30826E-6
B	E	138,78064	0,61329
B	F	0,00167	1,68501E-5
B	G	15,75659	4,02916
B	H	1,39284E-4	3,77664E-5

(b)

Figure A.II.2. (a) Exponential fit of decay heat of SUOX with 40000 MWd/tHM, (b) Values of coefficients in Put's Formula



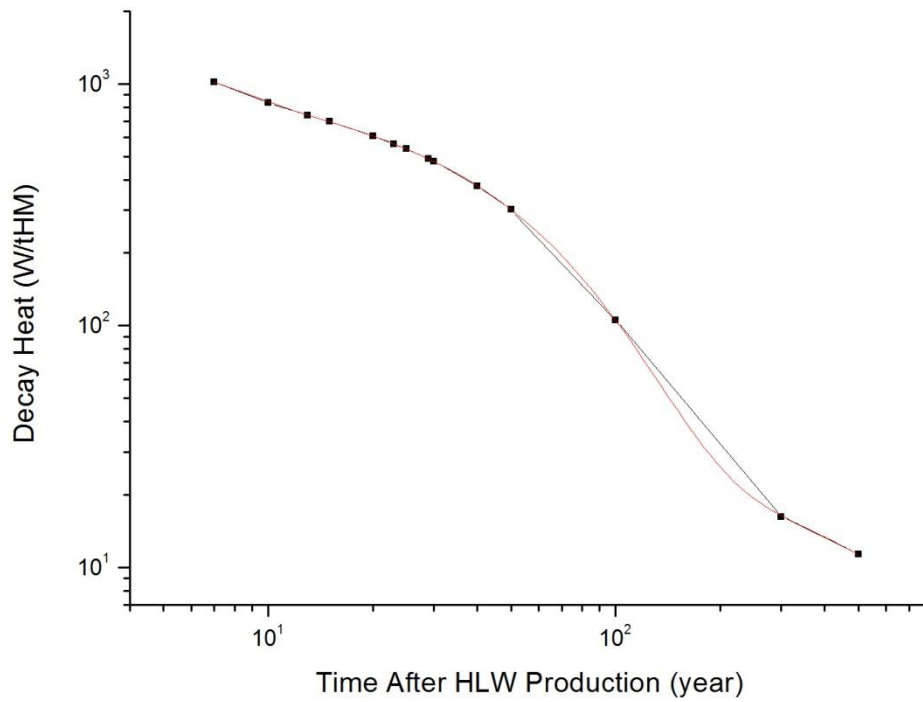
(a)

Equation	$y = A \cdot \exp(-B \cdot x) + C \cdot \exp(-D \cdot x) + E \cdot \exp(-F \cdot x) + G \cdot \exp(-H \cdot x)$		
Adj. R-Square	0,99999		
		Value	Standard Error
B	A	1535,27011	19,14335
B	B	0,02411	3,03144E-4
B	C	27,20382	0,58166
B	D	5,54445E-5	2,69466E-6
B	E	157,30349	3,28996
B	F	0,00152	3,244E-5
B	G	48,5381	21,60428
B	H	0,00869	0,00271

(b)

Figure A.II.3. (a) Exponential fit of decay heat of SUOX with 50000 MWd/tHM, (b) Values of coefficients in Put's Formula

HLW:

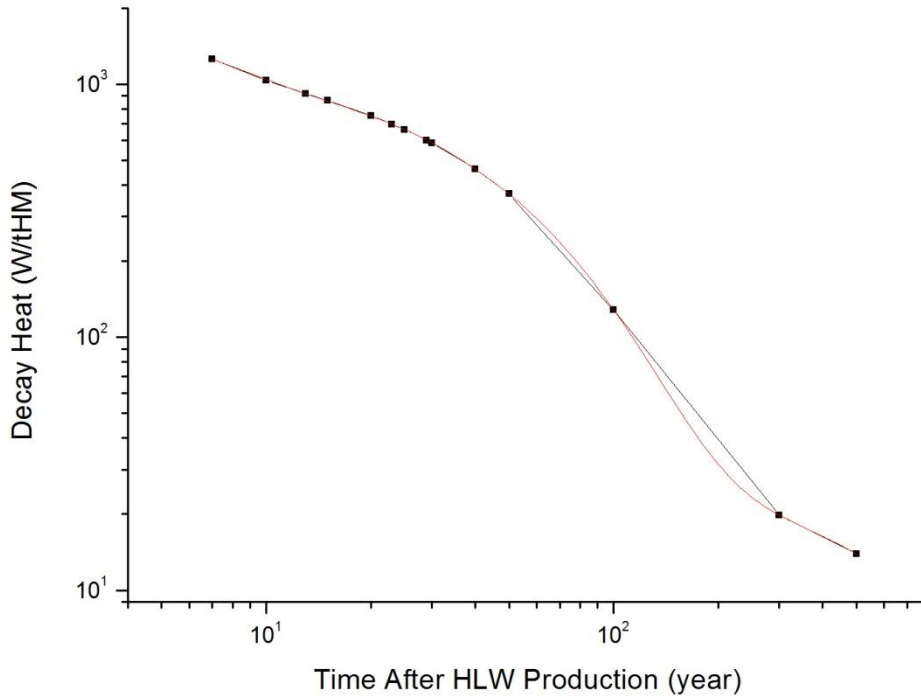


(a)

Equation	$y = A \cdot \exp(-B \cdot x) + C \cdot \exp(-D \cdot x) + E \cdot \exp(-F \cdot x) + G \cdot \exp(-H \cdot x)$		
Adj. R-Square	1		
		Value	Standard Error
B	A	3553,83792	288,1216
B	B	0,46464	0,01959
B	C	178,54834	32,14519
B	D	0,13193	0,01767
B	E	924,7459	5,29645
B	F	0,02405	1,9537E-4
B	G	25,84769	1,90312
B	H	0,00166	1,91506E-4

(b)

Figure A.II.4. (a) Exponential fit of decay heat of HLW with 33000 MWd/tHM, (b) Values of coefficients in Put's Formula

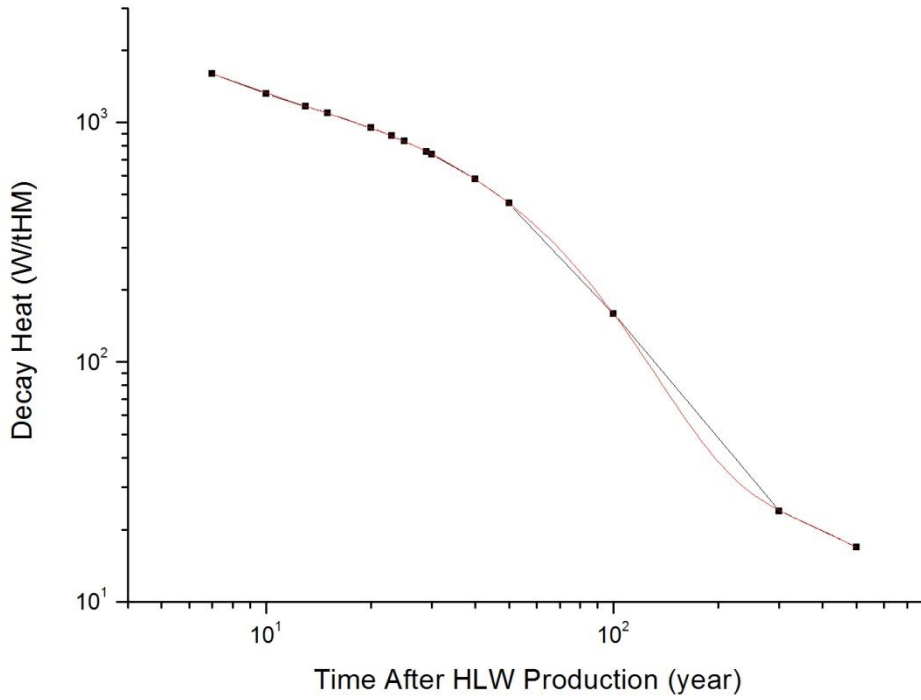


(a)

Equation	$y = A*\exp(-B*x)+C*\exp(-D*x)+E*\exp(-F*x)+G*\exp(-H*x)$		
Adj. R-Square	1		
		Value	Standard Error
B	A	3047,96803	111,97519
B	B	0,39371	0,00848
B	C	157,3909	9,96525
B	D	0,08421	0,01
B	E	30,13551	2,04952
B	F	0,00154	1,74127E-4
B	G	1115,03422	12,34931
B	H	0,02386	2,2812E-4

(b)

Figure A.II.5. (a) Exponential fit of decay heat of HLW with 40000 MWd/tHM, (b) Values of coefficients in Put's Formula



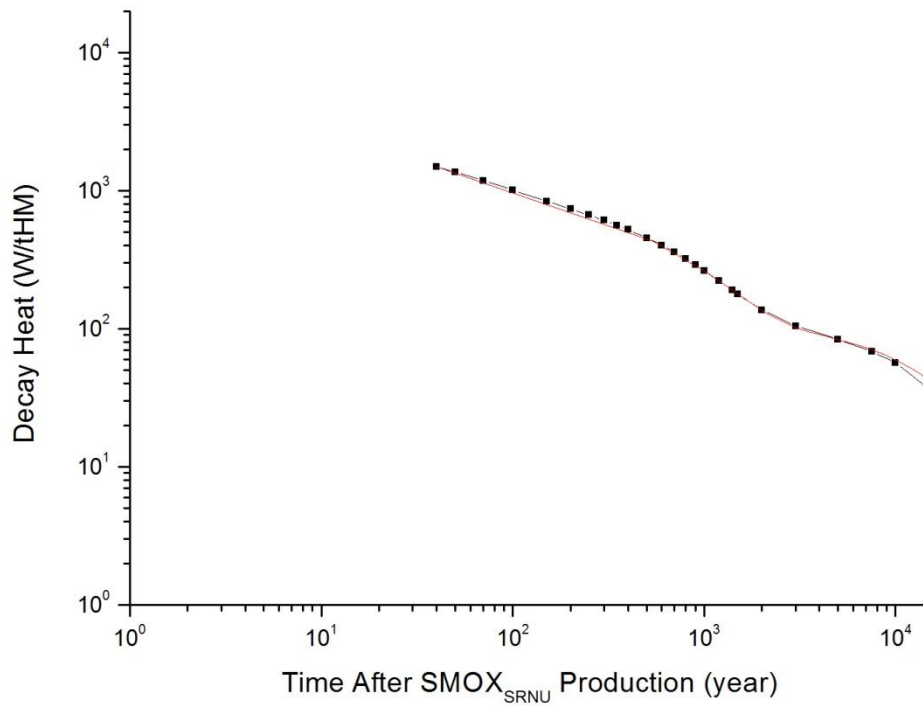
(a)

Equation	$y = A*\exp(-B*x)+C*\exp(-D*x)+E*\exp(-F*x)+G*\exp(-H*x)$		
Adj. R-Square	0,99999		
		Value	Standard Error
B	A	4507,79847	529,83586
B	B	0,43267	0,02618
B	C	285,92595	37,34775
B	D	0,09953	0,01933
B	E	1415,01852	26,23018
B	F	0,02409	4,72542E-4
B	G	37,13	5,98304
B	H	0,00159	4,14928E-4

(b)

Figure A.II.6. (a) Exponential fit of decay heat of HLW with 50000 MWd/tHM, (b) Values of coefficients in Put's Formula

SMOX_{SRNU}

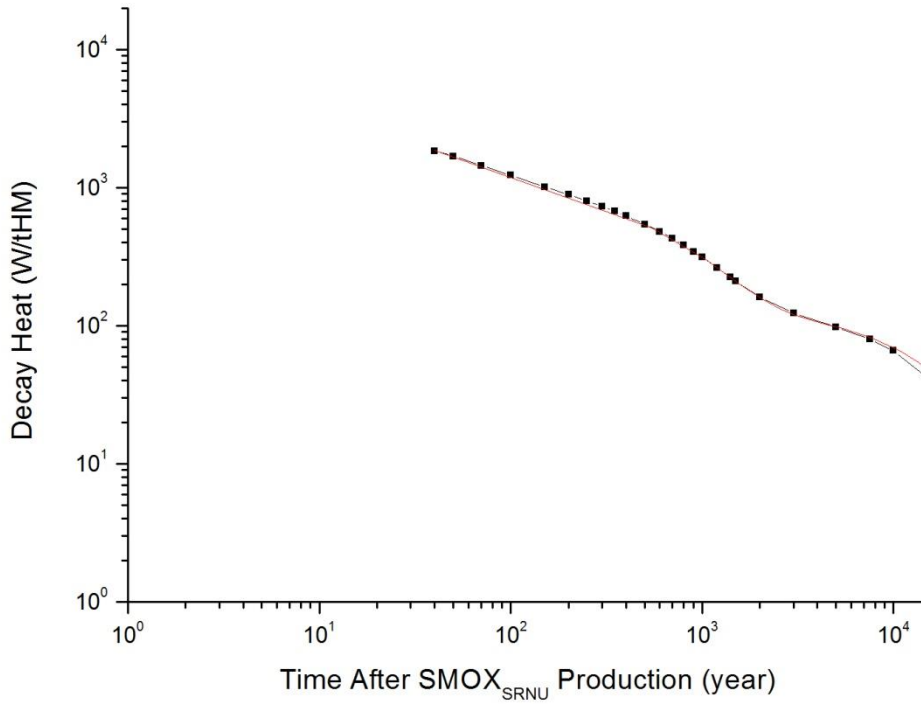


(a)

Equation	$y = A \cdot \exp(-B \cdot x) + C \cdot \exp(-D \cdot x) + E \cdot \exp(-F \cdot x) + G \cdot \exp(-H \cdot x)$		
Adj. R-Square	0,99999		
		Value	Standard Error
B	A	1131,78089	28,59233
B	B	0,02503	0,00106
B	C	390,09129	30,74987
B	D	0,00692	7,27714E-4
B	E	703,28263	16,67366
B	F	0,00152	3,30473E-5
B	G	116,67991	2,55861
B	H	6,75808E-5	3,02405E-6

(b)

Figure A.II.7. (a) Exponential fit of decay heat of SMOX_{SRNU} with 33000 MWd/tHM, (b) Values of coefficients in Put's Formula

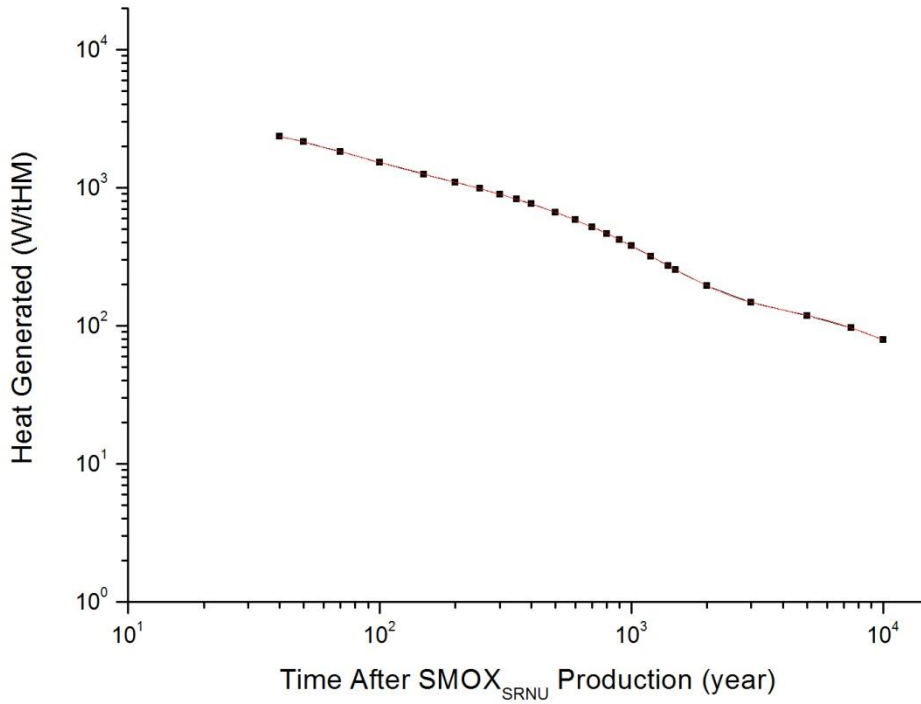


(a)

Equation	$y = A*\exp(-B*x)+C*\exp(-D*x)+E*\exp(-F*x)+G*\exp(-H*x)$		
Adj. R-Square	0,99997		
		Value	Standard Error
B	A	1495,35603	54,33027
B	B	0,02745	0,0018
B	C	552,24788	66,64929
B	D	0,00788	0,00103
B	E	865,25193	23,58283
B	F	0,00155	4,31095E-5
B	G	138,58239	4,44415
B	H	6,96081E-5	4,5723E-6

(b)

Figure A.II.8. (a) Exponential fit of decay heat of SMOX_{SRNU} with 40000 MWd/tHM, (b) Values of coefficients in Put's Formula



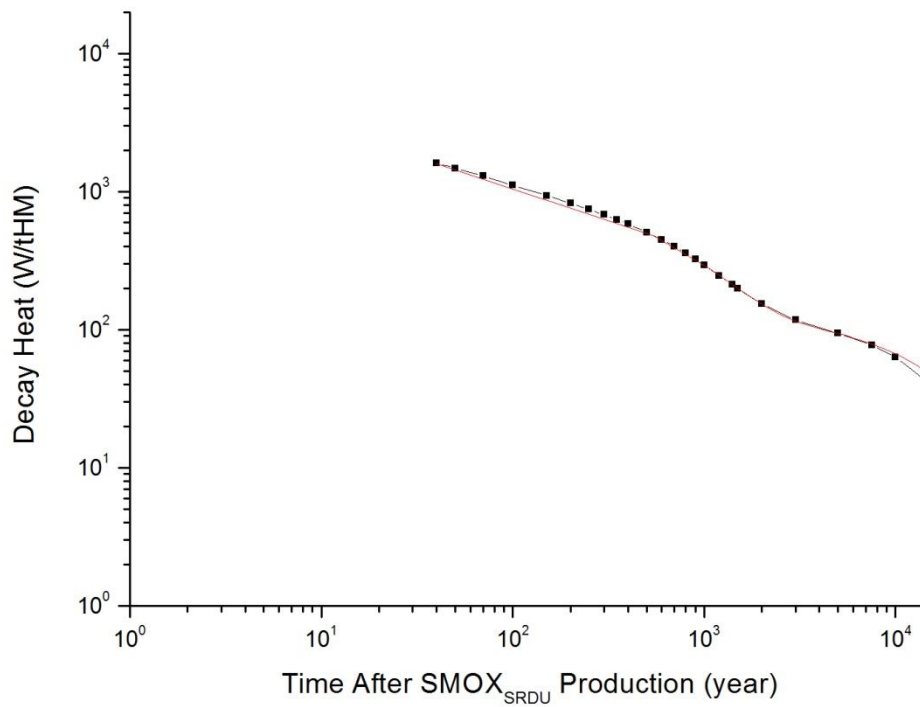
(a)

Equation	$y = A*\exp(-B*x)+C*\exp(-D*x)+E*\exp(-F*x)+G*\exp(-H*x)$		
Adj. R-Square	1		
		Value	Standard Error
B	A	660,44428	30,63831
B	B	0,00765	4,42275E-4
B	C	2100,53089	26,59086
B	D	0,02728	6,24574E-4
B	E	177,22131	3,0666
B	F	8,09547E-5	2,82806E-6
B	G	1058,92073	13,88441
B	H	0,00159	2,25067E-5

(b)

Figure A.II.9. (a) Exponential fit of decay heat of SMOX_{SRNU} with 50000 MWd/tHM, (b) Values of coefficients in Put's Formula

SMOX_{SRDU}:

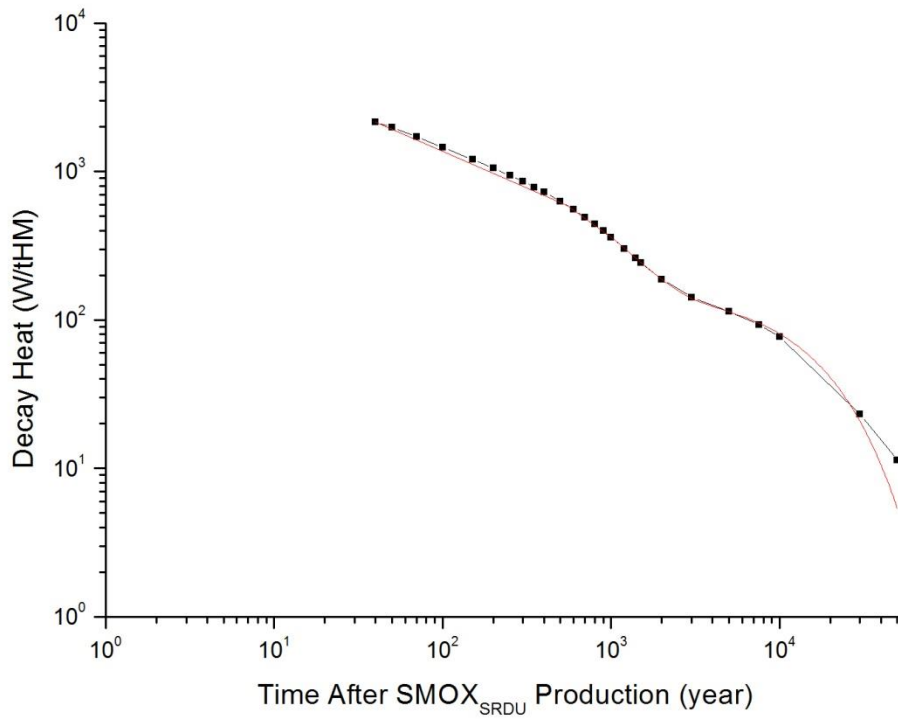


(a)

Equation	$y = A*\exp(-B*x)+C*\exp(-D*x)+E*\exp(-F*x)+G*\exp(-H*x)$		
Adj. R-Square	0,99998		
		Value	Standard Error
B	A	1093,45705	33,42312
B	B	0,02393	0,00116
B	C	415,85548	33,88342
B	D	0,00662	7,65091E-4
B	E	130,61779	2,94607
B	F	6,71871E-5	3,08341E-6
B	G	778,84497	20,94939
B	H	0,00151	3,57553E-5

(b)

Figure A.II.10. (a) Exponential fit of decay heat of SMOX_{SRDU} with 33000 MWd/tHM, (b) Values of coefficients in Put's Formula

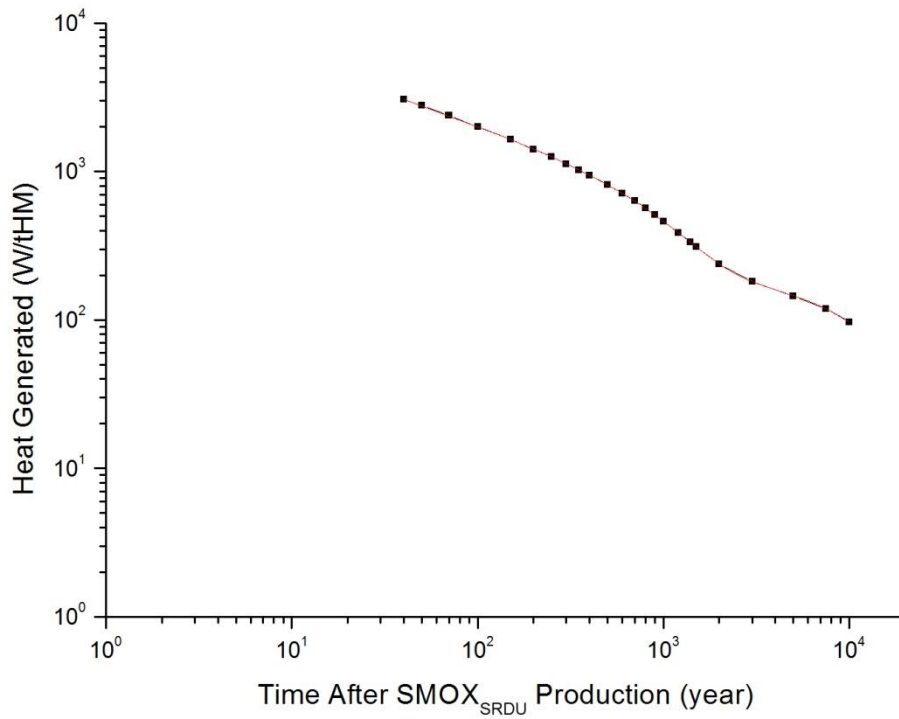


(a)

Equation	$y = A*\exp(-B*x)+C*\exp(-D*x)+E*\exp(-F*x)+G*\exp(-H*x)$		
Adj. R-Square	0,99998		
		Value	Standard Error
B	A	1566,19256	44,04776
B	B	0,02479	0,00117
B	C	672,91991	46,75599
B	D	0,00682	6,46126E-4
B	E	158,43793	4,02064
B	F	6,77711E-5	3,49345E-6
B	G	963,9444	26,40878
B	H	0,00151	3,77603E-5

(b)

Figure A.II.11. (a) Exponential fit of decay heat of SMOX_{SRDU} with 40000 MWd/tHM, (b) Values of coefficients in Put's Formula



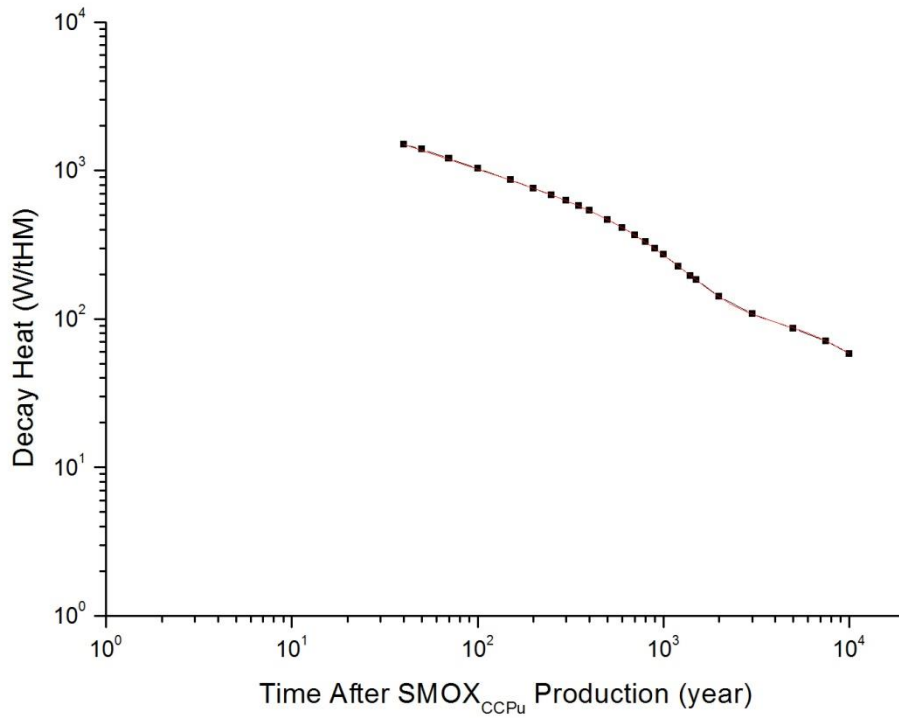
(a)

Equation	$y = A*\exp(-B*x)+C*\exp(-D*x)+E*\exp(-F*x)+G*\exp(-H*x)$		
Adj. R-Square	0,99999		
		Value	Standard Error
B	A	2193,85302	39,02964
B	B	0,02814	9,39049E-4
B	C	1251,58873	46,99468
B	D	0,00794	3,50629E-4
B	E	1290,68602	18,82225
B	F	0,0016	2,59635E-5
B	G	217,53033	4,40908
B	H	8,10007E-5	3,32962E-6

(b)

Figure A.II.12. (a) Exponential fit of decay heat of SMOX_{SRDU} with 50000 MWd/tHM, (b) Values of coefficients in Put's Formula

SMOX_{CCPu}

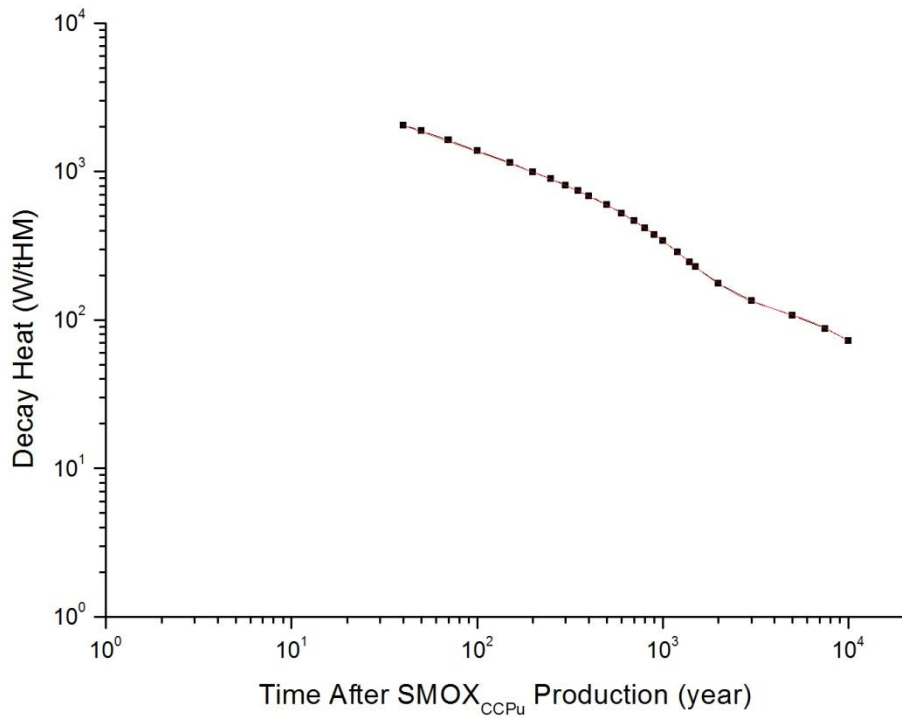


(a)

Equation	$y = A*\exp(-B*x)+C*\exp(-D*x)+E*\exp(-F*x)+G*\exp(-H*x)$		
Adj. R-Square	1		
		Value	Standard Error
B	A	128,56999	1,79072
B	B	7,93082E-5	2,24726E-6
B	C	737,67956	9,27425
B	D	0,00158	1,99798E-5
B	E	367,05245	20,99619
B	F	0,00725	4,90561E-4
B	G	1056,07985	20,75138
B	H	0,02377	6,0478E-4

(b)

Figure A.II.13. (a) Exponential fit of decay heat of SMOX_{CCPu} with 33000 MWd/tHM, (b) Values of coefficients in Put's Formula

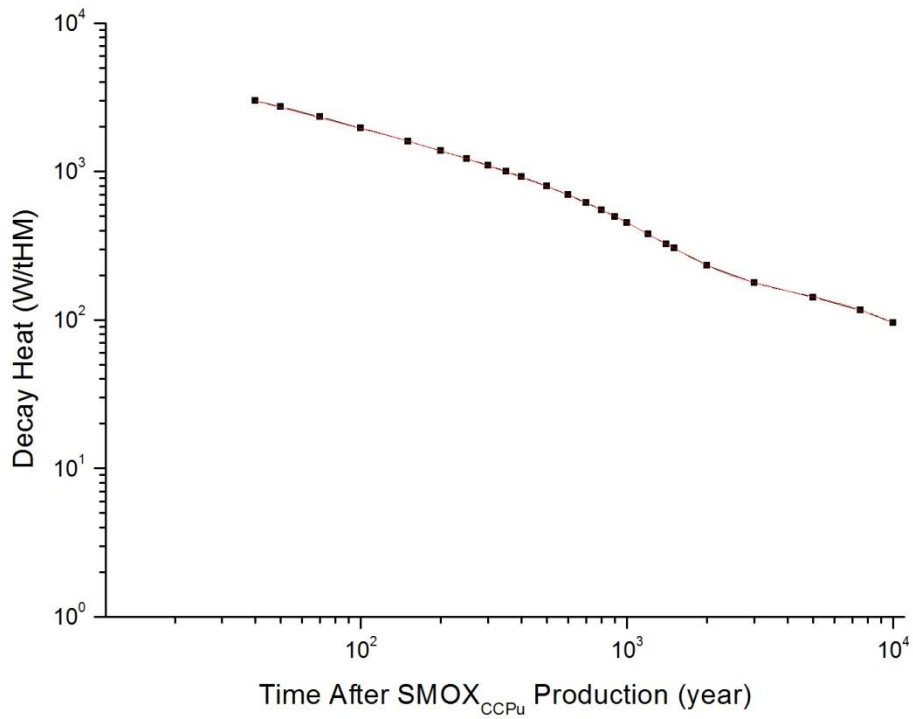


(a)

Equation	$y = A*\exp(-B*x)+C*\exp(-D*x)+E*\exp(-F*x)+G*\exp(-H*x)$		
Adj. R-Square	1		
		Value	Standard Error
B	A	678,93336	18,33464
B	B	0,00795	2,35674E-4
B	C	1492,73492	15,74687
B	D	0,02682	4,56802E-4
B	E	950,20825	6,61148
B	F	0,0016	1,22527E-5
B	G	160,72524	1,51436
B	H	8,0658E-5	1,54515E-6

(b)

Figure A.II.14. (a) Exponential fit of decay heat of SMOX_{CCPu} with 40000 MWd/tHM, (b) Values of coefficients in Put's Formula



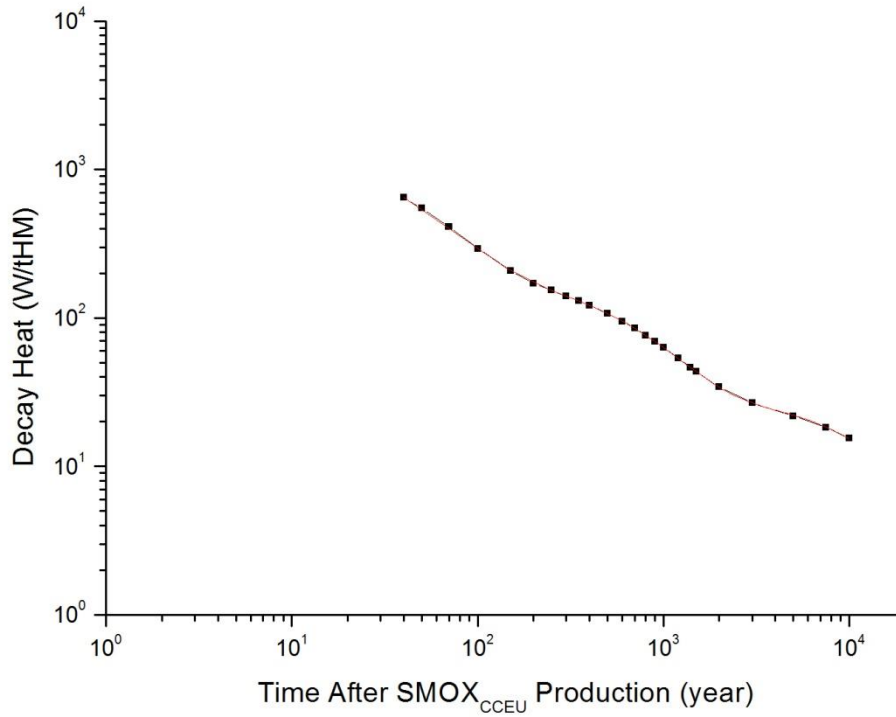
(a)

Equation	$y = A*\exp(-B*x)+C*\exp(-D*x)+E*\exp(-F*x)+G*\exp(-H*x)$		
Adj. R-Square	1		
		Value	Standard Error
B	A	1248,24918	28,72501
B	B	0,0081	2,15556E-4
B	C	214,12842	2,65905
B	D	8,10973E-5	2,04725E-6
B	E	2206,31367	23,28486
B	F	0,02884	5,95541E-4
B	G	1259,50842	11,03381
B	H	0,0016	1,59077E-5

(b)

Figure A.II.15. (a) Exponential fit of decay heat of SMOX_{CCPu} with 50000 MWd/tHM, (b) Values of coefficients in Put's Formula

SMOX_{CCEU}

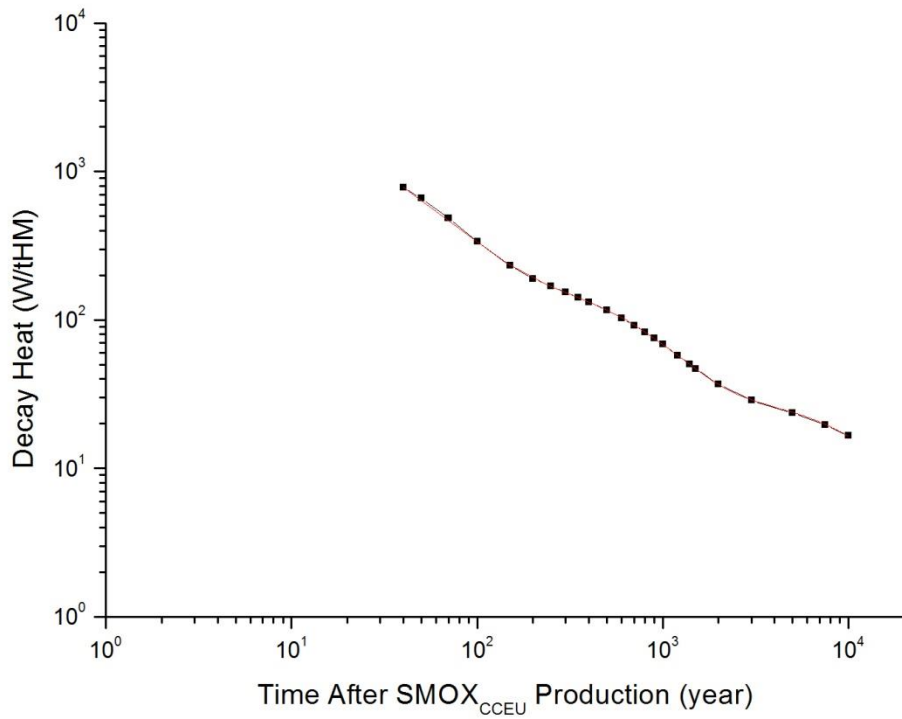


(a)

Equation	$y = A \cdot \exp(-B \cdot x) + C \cdot \exp(-D \cdot x) + E \cdot \exp(-F \cdot x) + G \cdot \exp(-H \cdot x)$		
Adj. R-Square	1		
		Value	Standard Error
B	A	1083,29112	29,51808
B	B	0,0257	5,00502E-4
B	C	170,73947	1,79464
B	D	0,00162	2,32427E-5
B	E	104,17979	32,95249
B	F	0,0112	0,00168
B	G	31,71382	0,5867
B	H	7,281E-5	3,0786E-6

(b)

Figure A.II.16. (a) Exponential fit of decay heat of SMOX_{CCEU} with 33000 MWd/tHM, (b) Values of coefficients in Put's Formula

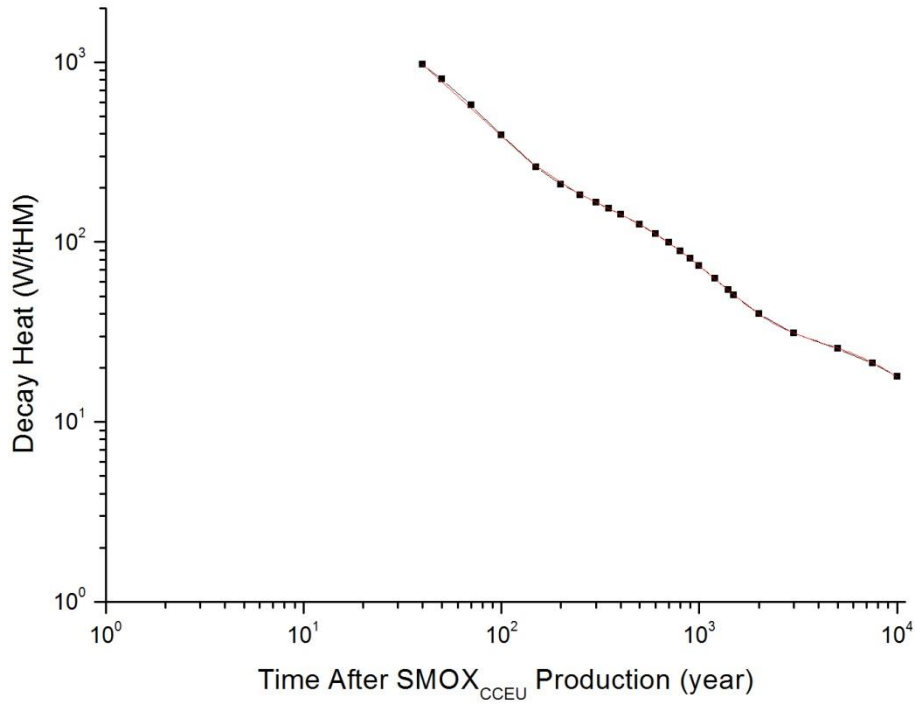


(a)

Equation	$y = A*\exp(-B*x)+C*\exp(-D*x)+E*\exp(-F*x)+G*\exp(-H*x)$		
Adj. R-Square	1		
		Value	Standard Error
B	A	187,5834	1,87312
B	B	0,00164	2,30975E-5
B	C	154,97712	42,31997
B	D	0,01187	0,00144
B	E	1381,86816	37,66505
B	F	0,02652	5,01194E-4
B	G	34,46063	0,64663
B	H	7,43116E-5	3,16262E-6

(b)

Figure A.II.17. (a) Exponential fit of decay heat of SMOX_{CCEU} with 40000 MWd/tHM, (b) Values of coefficients in Put's Formula



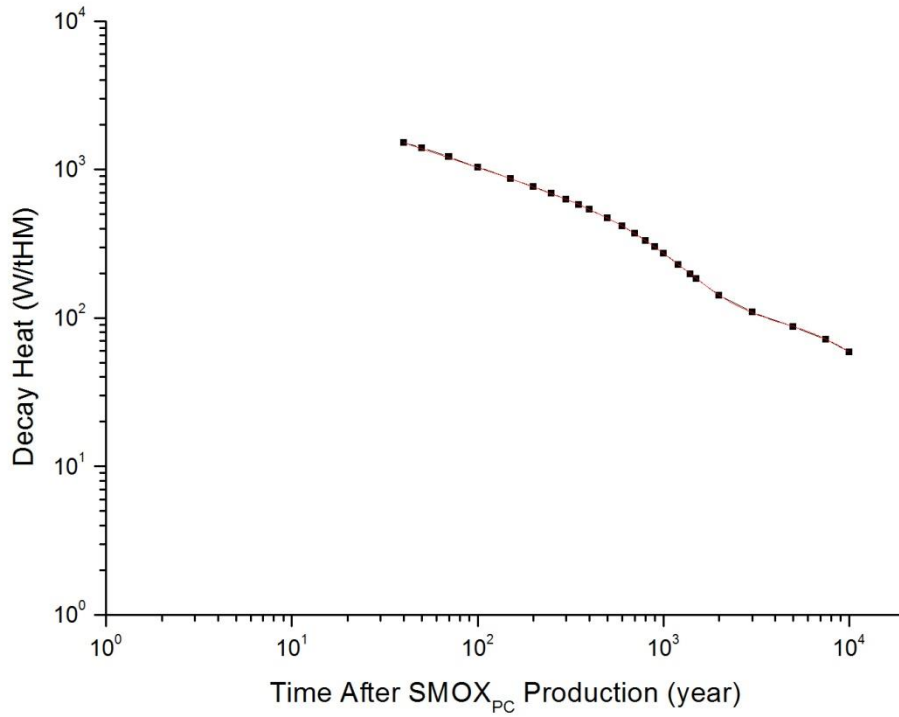
(a)

Equation	$y = A*\exp(-B*x)+C*\exp(-D*x)+E*\exp(-F*x)+G*\exp(-H*x)$		
Adj. R-Square	1		
		Value	Standard Error
B	A	266,15884	40,3381
B	B	0,01259	8,09811E-4
B	C	200,75838	1,48465
B	D	0,00163	1,81203E-5
B	E	37,15266	0,57264
B	F	7,39182E-5	2,60533E-6
B	G	1781,35842	35,14326
B	H	0,02789	3,93147E-4

(b)

Figure A.II.18. (a) Exponential fit of decay heat of SMOX_{CCEU} with 50000 MWd/tHM, (b) Values of coefficients in Put's Formula

SMOX_{PC}:

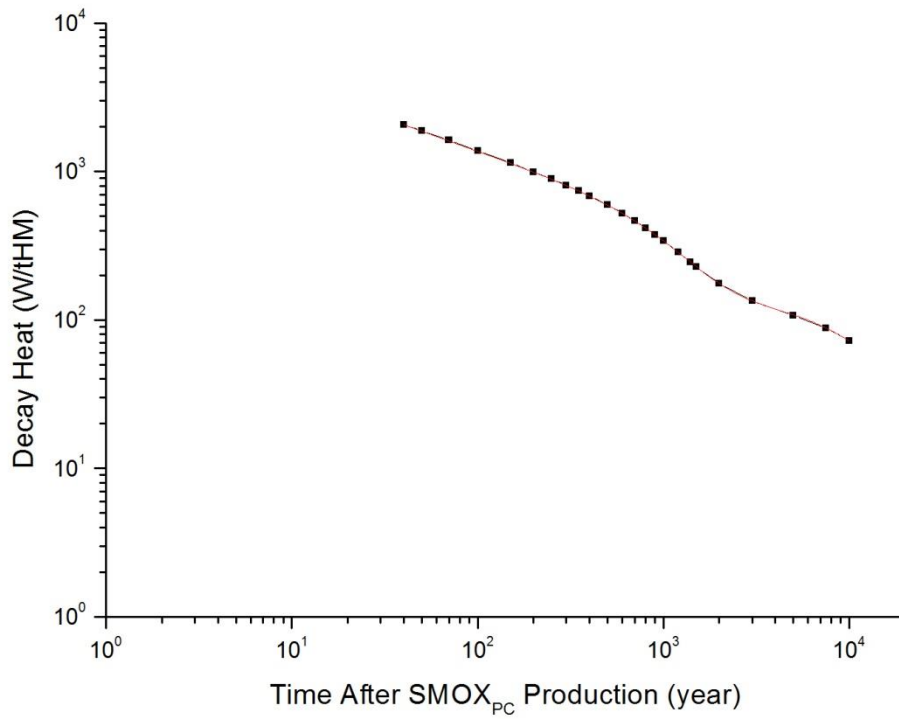


(a)

Equation	$y = A \cdot \exp(-B \cdot x) + C \cdot \exp(-D \cdot x) + E \cdot \exp(-F \cdot x) + G \cdot \exp(-H \cdot x)$		
Adj. R-Square	0,99999		
		Value	Standard Error
B	A	129,05522	2,65549
B	B	7,84108E-5	3,26883E-6
B	C	731,02655	16,47033
B	D	0,00157	3,21365E-5
B	E	1101,45583	26,16255
B	F	0,02241	6,93725E-4
B	G	324,27548	23,60064
B	H	0,0065	7,10228E-4

(b)

Figure A.II.19. (a) Exponential fit of decay heat of SMOX_{PC} with 33000 MWd/tHM, (b) Values of coefficients in Put's Formula

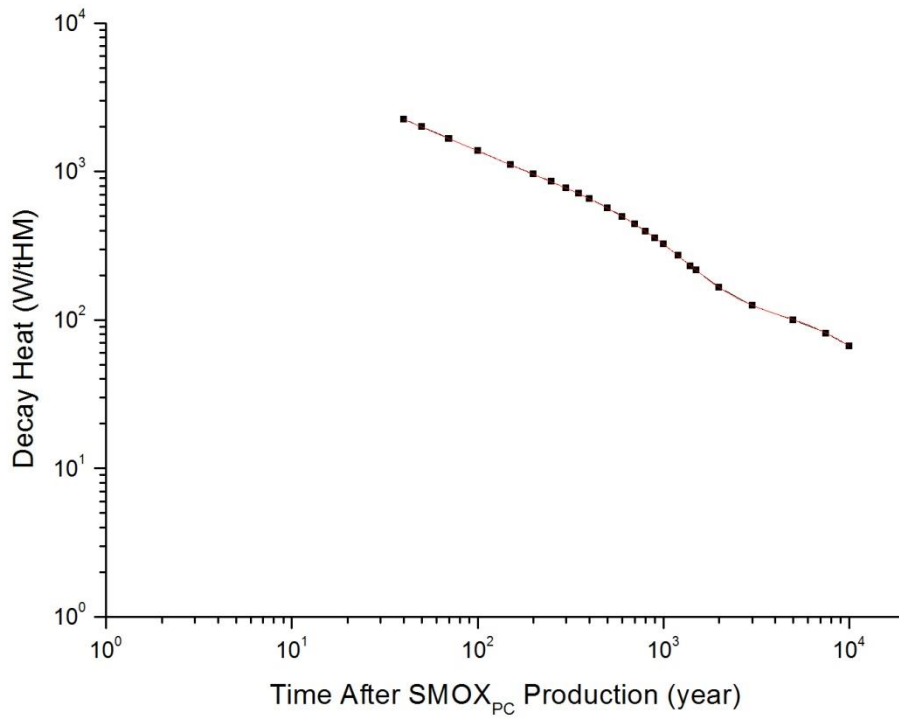


(a)

Equation	$y = A*\exp(-B*x)+C*\exp(-D*x)+E*\exp(-F*x)+G*\exp(-H*x)$		
Adj. R-Square	1		
		Value	Standard Error
B	A	755,41084	16,4869
B	B	0,00863	1,9233E-4
B	C	1529,50989	12,62952
B	D	0,02964	4,72949E-4
B	E	962,42604	4,9076
B	F	0,00161	9,77583E-6
B	G	161,82376	1,28075
B	H	8,11982E-5	1,31651E-6

(b)

Figure A.II.20. (a) Exponential fit of decay heat of SMOX_{PC} with 40000 MWd/tHM, (b) Values of coefficients in Put's Formula



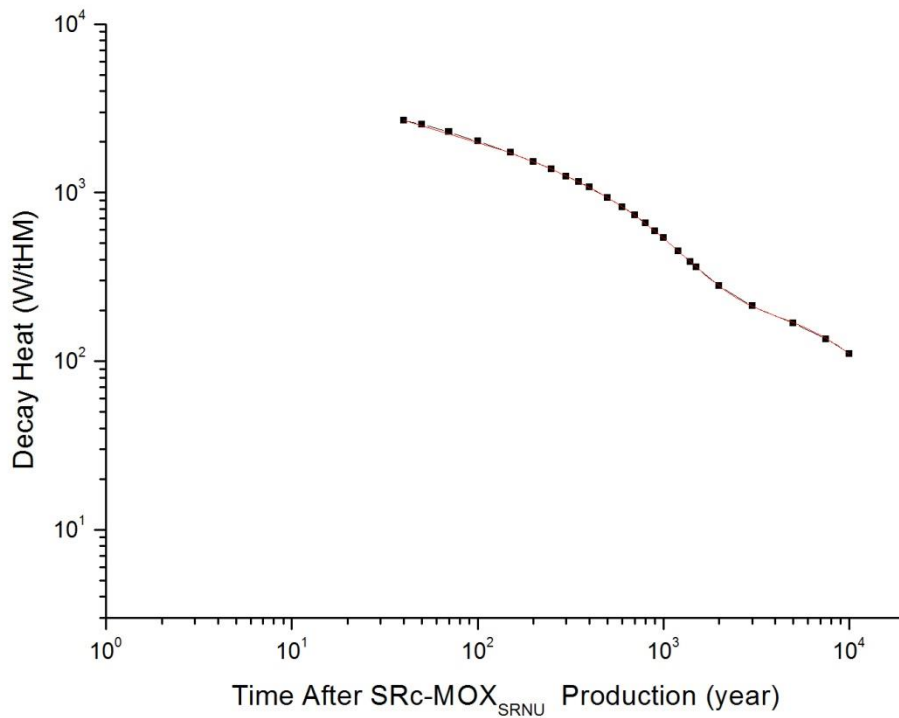
(a)

Equation	$y = A*\exp(-B*x)+C*\exp(-D*x)+E*\exp(-F*x)+G*\exp(-H*x)$		
Adj. R-Square	0,99999		
		Value	Standard Error
B	A	909,70663	14,79368
B	B	0,0016	2,95117E-5
B	C	151,0485	3,58275
B	D	8,21702E-5	3,91425E-6
B	E	718,1544	39,85459
B	F	0,00809	5,08899E-4
B	G	2223,52442	32,50108
B	H	0,0284	7,78551E-4

(b)

Figure A.II.21. (a) Exponential fit of decay heat of SMOX_{PC} with 50000 MWd/tHM, (b) Values of coefficients in Put's Formula

SRc-MOX_{SRNU}

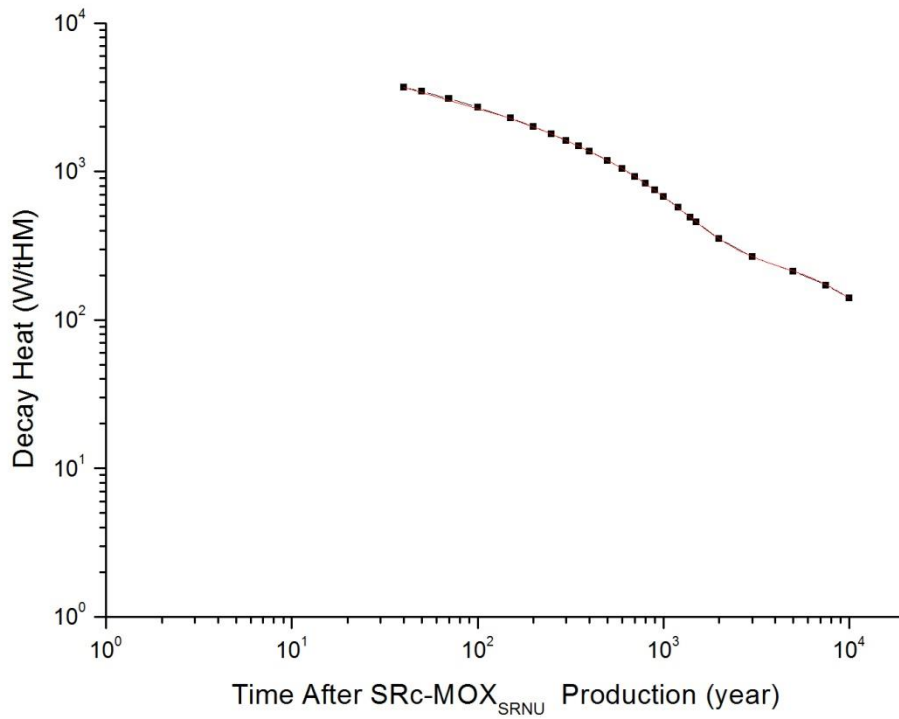


(a)

Equation	$y = A \cdot \exp(-B \cdot x) + C \cdot \exp(-D \cdot x) + E \cdot \exp(-F \cdot x) + G \cdot \exp(-H \cdot x)$		
Adj. R-Square	0,99999		
		Value	Standard Error
B	A	749,90228	76,09082
B	B	0,00713	7,12156E-4
B	C	1476,81458	25,93436
B	D	0,00159	2,66658E-5
B	E	1098,36528	81,57999
B	F	0,02053	0,00134
B	G	257,07455	4,58817
B	H	8,47362E-5	2,89642E-6

(b)

Figure A.II.22. (a) Exponential fit of decay heat of SRc-MOX_{SRNU} with 33000 MWd/tHM, (b) Values of coefficients in Put's Formula

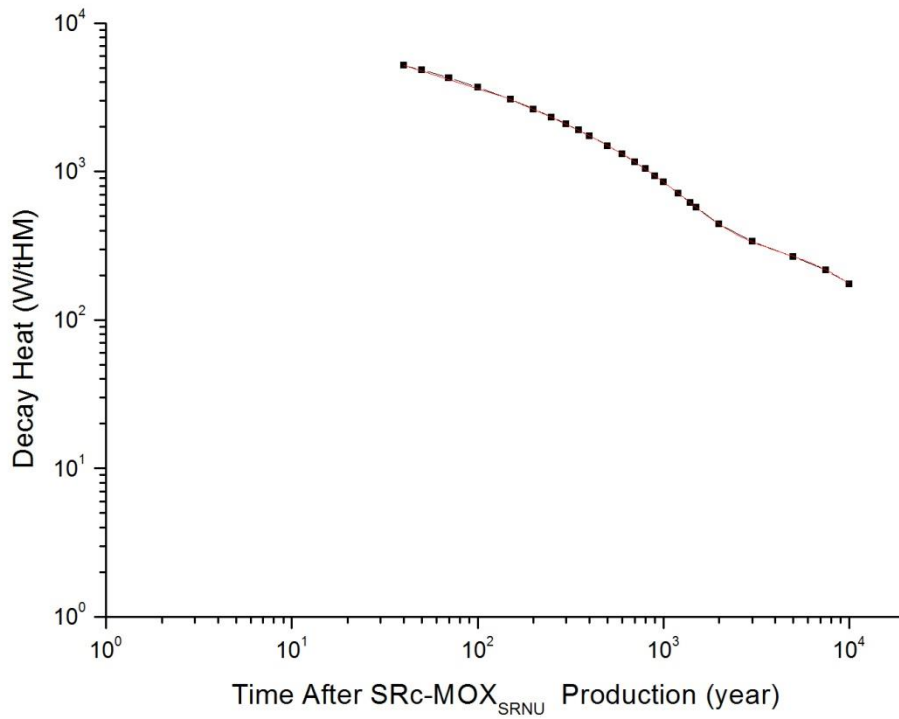


(a)

Equation	$y = A*\exp(-B*x)+C*\exp(-D*x)+E*\exp(-F*x)+G*\exp(-H*x)$		
Adj. R-Square	1		
		Value	Standard Error
B	A	1445,82779	44,6923
B	B	0,00772	2,40548E-4
B	C	1462,83341	42,49898
B	D	0,024	8,34107E-4
B	E	1863,09203	14,4737
B	F	0,00159	1,31304E-5
B	G	323,96699	3,13351
B	H	8,4374E-5	1,58565E-6

(b)

Figure A.II.23. (a) Exponential fit of decay heat of SRC-MOX_{SRNU} with 40000 MWd/tHM, (b) Values of coefficients in Put's Formula



(a)

Equation	$y = A*\exp(-B*x)+C*\exp(-D*x)+E*\exp(-F*x)+G*\exp(-H*x)$		
Adj. R-Square	1		
		Value	Standard Error
B	A	407,82061	4,87633
B	B	8,47325E-5	1,96293E-6
B	C	2321,52698	22,20413
B	D	0,00159	1,62693E-5
B	E	2444,18247	56,8206
B	F	0,00764	2,01022E-4
B	G	2183,31287	51,92109
B	H	0,02545	8,83924E-4

(b)

Figure A.II.24. (a) Exponential fit of decay heat of SRC-MOX_{SRNU} with 50000 MWd/tHM, (b) Values of coefficients in Put's Formula

**APPENDIX III: THERMAL ANALYSES AND DISPOSAL DENSITY
CALCULATIONS FOR 100 YEARS COOLING TIME**

Cooling time affects the heat generation rate of the waste loaded in to disposal canister and hence the disposal area needed. For this reason, thermal analyses are repeated for 100 years cooling time and total disposal area needed for each fuel cycle is determined. Canister spacing and disposal area needed for one ton of each waste type are given in Table A.III.1. Results of disposal density calculations for fuel cycles are given in Table A.III.2.

Table A.III.1. Minimum distance between canisters and disposal area needed per ton of each waste type (100 years cooling time)

Waste form	Burnup (MWd/tHM)	Canister spacing (m)	Disposal area per canister (m ² /canister)	Disposal area per ton of waste (m ² /t)
SUOX	33000	1.60	64.0	33.12
	40000	2.06	82.4	42.64
	50000	2.60	104.0	53.82
VHLW	33000	4.44	177.6	222.00
	40000	4.30	172.0	215.00
	50000	4.20	168.0	210.00
SMOX _{SRNU}	33000	2.10	84.0	173.87
	40000	3.00	120.0	248.39
	50000	5.12	204.8	423.92
SMOX _{SRDU}	33000	2.40	96.0	198.71
	40000	3.42	136.8	283.17
	50000	5.90	236.0	488.50
SMOX _{CCPu}	33000	2.18	87.2	180.50
	40000	3.16	126.4	261.64
	50000	5.60	224.0	463.66
SMOX _{CCEU}	33000	2.42	96.8	50.09
	40000	2.80	112.0	57.96
	50000	3.44	137.6	71.20
SMOX _{PC}	33000	2.16	86.4	178.84
	40000	3.08	123.2	255.01
	50000	5.42	216.8	448.76
SRC-MOX _{SRNU}	33000	6.10	244.0	505.06
	40000	14.60	584.0	1208.83
	50000	-	-	-

Table A.III.2. Results of disposal density calculations for fuel cycles (100 years cooling)

Burnup (MWd/tHM)	Electricity in MWe-yr produced (based on one ton of fresh fuel loaded) per unit area in m ² of disposal area required for all the SF/VHLW arising in that fuel cycle (MWe-yr/m ²)			Disposal-Area Advantage Factor (DAAF)		
	33000	40000	50000	33000	40000	50000
OT	7770.35	7242.38	7246.89	1	0.9321	0.9326
SRNU	6077.05	5872.74	5504.02	0.7821	0.7562	0.7083
SRDU	5957.59	5863.51	5390.04	0.7667	0.7546	0.6937
CCPu	2527.32	2129.33	1556.58	0.3252	0.2740	0.2003
CCEU	6775.52	6878.95	6941.71	0.8720	0.8853	0.8934
PC	5894.39	5691.41	5261.46	0.7586	0.7325	0.6771
SRc-MOX	5702.36	3954.78	-	0.7339	0.5090	-

APPENDIX IV: RESULTS OF THERMAL ANALYSIS FOR VHLW DISPOSAL CANISTER LOADED WITH % 15 WASTE AND 3 VHLW CYLINDERS

For the reference VHLW packages used in the study, the percentage of HLW in glass frit is 10 w/o and only 2 VHLW cylinders are put into a disposal canister. In order to assess the effect of concentration of waste loaded into canister on needed disposal area, thermal analysis are repeated for waste packages containing 15 w/o HLW in glass frit and 3 VHLW cylinders.

When percentage of HLW in glass frit in a disposal canister is increased to % 15, temperature limits are exceeded quickly. Results of thermal analysis performed for 15 w/o HLW in glass frit are given in Figures A.IV.1 through A.IV.3.

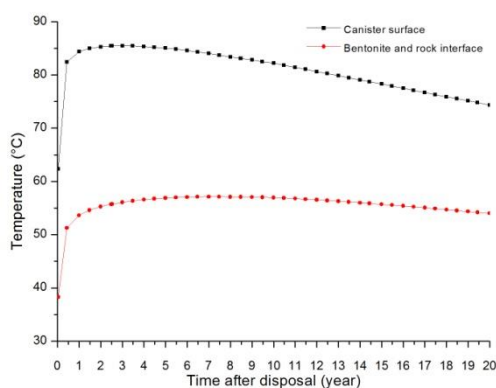


Figure A.IV.1. Temperature as a function of time on the canister surface and at the interface between bentonite and rock, spacing 10 m, % 15 w/o HLW in glass frit from reprocessing of 33000 MWd/tHM burnup SUOX

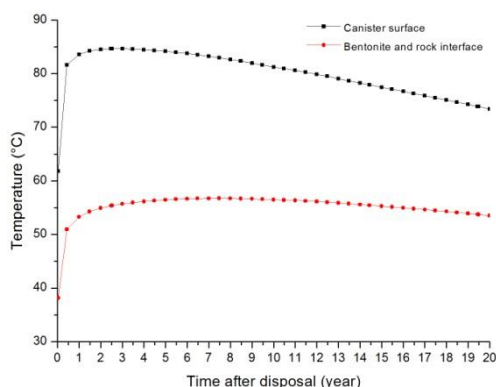


Figure A.IV.2. Temperature as a function of time on the canister surface and at the interface between bentonite and rock, spacing 10 m, % 15 w/o HLW in glass frit from reprocessing of 40000 MWd/tHM burnup SUOX

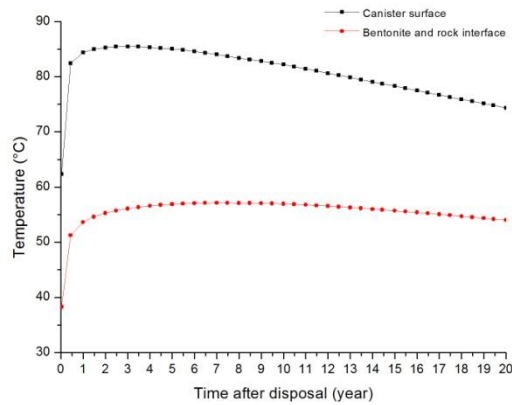


Figure A.IV.3. Temperature as a function of time on the canister surface and at the interface between bentonite and rock, spacing 10 m, % 15 w/o HLW in glass frit from reprocessing of 50000 MWd/tHM burnup SUOX

For disposal canisters loaded with 3 VHLW cylinders, the minimum distance required between 2 boreholes increase to 7, 6.7 and 6.7 meter for 33000, 40000 and 50000 MWd/tHM burnup values respectively. Results of thermal analysis for disposal canisters loaded with 3 VHLW cylinders are presented in Figures A.IV.4, A.IV.5 and A.IV.6. As a result, increasing VHLW cylinder number in a disposal canister does not change the results for disposal area calculations in favour of VHLW.

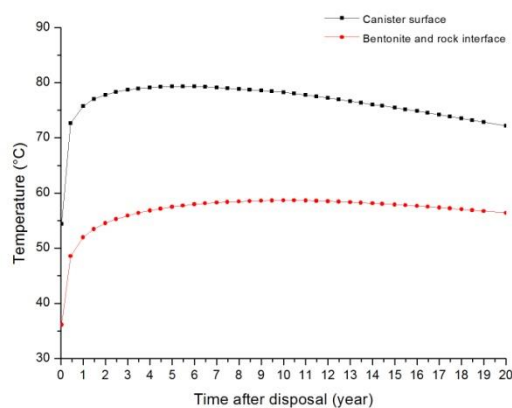


Figure A.IV.4. Temperature as a function of time on the canister surface and at the interface between bentonite and rock, spacing 7 m, 3 VHLW cylinders in disposal canister, 33000 MWd/tHM burnup

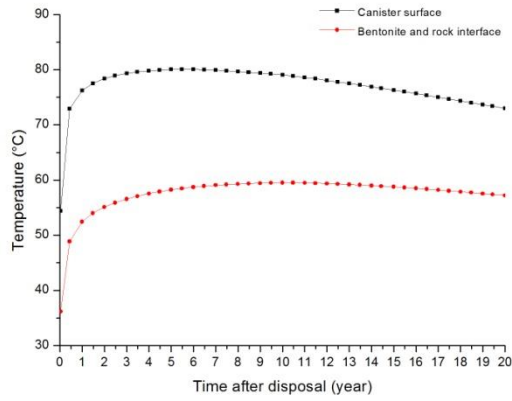


Figure A.IV.5. Temperature as a function of time on the canister surface and at the interface between bentonite and rock, spacing 6.7 m, 3 VHLW cylinders in disposal canister, 40000 MWd/tHM burnup

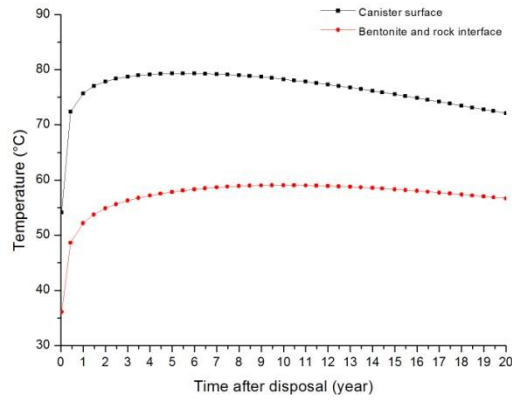


Figure A.IV.6. Temperature as a function of time on the canister surface and at the interface between bentonite and rock, spacing 6.7 m, 3 VHLW cylinders in disposal canister, 50000 MWd/tHM burnup

APPENDIX V: SENSITIVITY ANALYSIS FOR ROCK THERMAL PROPERTIES

Thermal properties of the host rock such as thermal conductivity and specific heat are the main effective factors for disposal area calculations. In order to calculate the effect of variation of host rock thermal properties, thermal analyses are repeated for conductivity and heat capacity values % 20 lower and higher than reference host rock thermal properties given in Table 6.1.

Thermal analyses are repeated for SUOX, VHLW and SMOX_{SRNU} wastes with 33000 MWd/tHM burnup. Table A.V.1 shows the canister spacing and needed disposal area for each waste type. Results of disposal density calculations for fuel cycles are given in Table A.V.II.

Table A.V.1. Disposal area needed per ton of waste (sensitivity analysis)

Waste form	Thermal property	Canister spacing (m)	Disposal area per canister (m ² /canister)	Disposal area per ton of waste (m ² /t)
SUOX	k (- % 20)	4.80	192.0	99.36
	k (+ % 20)	3.36	134.4	69.55
	c _p (- % 20)	4.10	164.0	84.87
	c _p (+ % 20)	3.76	150.4	77.83
VHLW	k (- % 20)	4.88	195.2	244.00
	k (+ % 20)	3.30	132.0	165.00
	c _p (- % 20)	4.10	164.0	205.00
	c _p (+ % 20)	3.74	149.6	187.00
SMOX _{SRNU}	k (- % 20)	3.68	147.2	304.69
	k (+ % 20)	2.60	104.0	215.27
	c _p (- % 20)	3.10	124.0	256.67
	c _p (+ % 20)	2.94	117.6	243.42

Table A.V.2. Disposal densities for OT and SRNU fuel cycles (sensitivity analysis)

Burnup (MWd/tHM)	Electricity in MWe-yr produced (based on one ton of fresh fuel loaded) per unit area in m ² of disposal area required for all the SF/VHLW arising in that fuel cycle (MWe-yr/m ²)			
	k (- % 20)	k (+ % 20)	c _p (- % 20)	c _p (+ % 20)
OT	2590.76	3700.13	3032.22	3306.49
SRNU	2438.08	3536.64	2894.48	3127.28

**APPENDIX VI: RESULTS OF THERMAL ANALYSIS FOR 100 °C
TEMPERATURE LIMIT**

In order to assess the effect of thermal limit on needed disposal area, thermal analyses are repeated for 100 °C thermal constraint. Results of thermal analyses and disposal density calculations are given in Table A.VI.1 and A.VI.2 respectively.

Table A.VI.1. Minimum distance between canisters and disposal area needed per ton of each waste type (100 °C thermal constraint)

Waste form	Burnup (MWd/tU)	Canister spacing (m)	Disposal area per canister (m ² /canister)	Disposal area per ton of waste (m ² /t)
SUOX	33000	2.40	96.0	49.67
	40000	3.08	123.2	68.41
	50000	4.20	168.0	86.94
SMOX _{SRNU}	33000	1.94	77.6	160.65
	40000	2.80	112.0	231.83
	50000	4.98	199.2	412.33
VHLW	33000	2.28	91.2	114.00
	40000	2.18	87.2	109.00
	50000	2.18	87.2	109.00

Table A.VI.2. Results for fuel cycles (100 °C thermal constraint)

Burnup (MWd/tHM)	Electricity in MWe-yr produced (based on one ton of fresh fuel loaded) per unit area in m ² of disposal area required for all the SF/VHLW arising in that fuel cycle (MWe-yr/m ²)			Disposal-Area Advantage Factor (DAAF)		
	33000	40000	50000	33000	40000	50000
OT	5181.08	4560.65	4485.66	1	0.8803	0.8658
SRNU	4969.86	4831.62	4446.85	0.9592	0.9326	0.8583

REFERENCES

- [1] Chapman, N., Hooper, A., The Disposal of Radioactive Wastes Underground, *Proceedings of the Geologists' Association*, 123, 46–63, **2012**.
- [2] Rosborg, B., Werme, L., The Swedish Nuclear Waste Program and the Long-term Corrosion Behaviour of Copper, *Journal of Nuclear Materials*, 379, 142-153, **2008**.
- [3] Cochran, R.G., Tsoulfanidis, N., *The Nuclear Fuel Cycle: Analysis and Management*, American Nuclear Society, **1990**.
- [4] Benedict, M., Pigford, T.H., Levi H.W., *Nuclear Chemical Engineering*, McGraw-Hill Book Company, **1983**.
- [5] Wolf, J.M., *History of the Eurochemic Company*, OECD, Paris, **1996**.
- [6] Zabunoğlu, O.H., Özdemir, L., Purex Co-processing of Spent LWR fuels: Fow sheet, *Annals of Nuclear Energy*, 32, 151-162, **2005**.
- [7] Karraker, D., *Radiation Chemistry of Acetohydroxamic Acid in the Urex Process*, Technical Report, Westinghouse Savannah River Company, **2002**.
- [8] Eccles, H., *Nuclear Fuel Cycle Technologies Sustainable in the Twenty first Century?*, *Solvent Extraction and Ion Exchange*, BNFL, 18(4), 633-654, **2000**.
- [9] Chandler, S.J., *Comparison of Reprocessing Methods for LWR Fuel*, Master Thesis, Georgia Institute of Technology, U.S.A, **2006**.
- [10] National Academy of Sciences, *The Disposal of Radioactive Waste on Land*, Publication 519, NAS Washington DC, **1957**.
- [11] EUR-9909 EN/FR, *Design Study on Containers for Geological Disposal of High Level Radioactive Waste*, Nuclear Science and Technology, **1985**.
- [12] EUR-8179 EN/FR, *Admissible Thermal Loading in Geological Formations Consequences on Radioactive Waste Disposal Methods*, Nuclear Science and Technology, **1982**.
- [13] Ringwood, A.E., *Safe Disposal of High Level Radioactive Wastes*, Australian National University Press, **1980**.
- [14] Ringwood, A.E., *Safe Disposal of High Level Radioactive Wastes: A New Strategy*, Australian National University Press, **1978**.
- [15] Thunvik, R., Braester, C., *Heat Propagation from a Radioactive Waste Repository, SKB 91 Reference Canister*, SKB Technical Report 91-61, Stockholm, **1991**.
- [16] Ahlstrom, P.E., Towards a Swedish Repository for Spent Fuel, *Nuclear Engineering and Design*, 176, 67–74, **1997**.
- [17] Pettersson, S., Widing, E., *Development of the Swedish Deep Repository for Spent Nuclear Fuel in Crystalline Host Rock*, WM'03 Conference, Tucson, **2003**.

- [18] Hopkirk, R.J., Wagner, W.H., *Thermal Loading in the Near Field Repositories for High and Intermediate Level Nuclear Waste*, NTB 85-54, Nagra Technical Report Series, Wettingen AG, **1986**.
- [19] Sasaki, T., Ando, K., Kawamura, H., Schneider, J.W., McKinley, I.G., *Thermal Analysis of Options for Spent Fuel Disposal in Switzerland*, Materials Research Society, 465, 1133-1141, **1997**.
- [20] Sigzek, G.D., Three-dimensional Thermal Analysis of In-floor Type Nuclear Waste Repository for a Ceramic Waste Form, *Nuclear Engineering and Design*, 235, 101-109, **2005**.
- [21] Moreno, L., Gylling, B., *Equivalent Flow Rate Concept in Near Field Transport Model COMP23*, SKB, Technical Report R-98-53, Stockholm, **1998**.
- [22] Bruno, J., Arcos, D., Duro, L., *Processes and Features Affecting the Near Field Hydrochemistry. Groundwater Bentonite Interaction*, SKB, Technical Report TR-99-29, Stockholm, **1999**.
- [23] Laaksoharju, M., *Groundwater Characterisation and Modeling: Problems, facts and possibilities*, SKB, Technical Report TR-99-42, Stockholm, **1999**.
- [24] Lindgren, M., Lindström, F., *SR-97 Radionuclide Transport Calculations*, SKB Technical Report TR-99-23, Stockholm, **1999**.
- [25] Ludvigson, J.E., Jönsson, S., *Forsmark Site Investigation. Hydraulic Interference Test, Boreholes HFM01, HFM02 and HFM03*, SKB, Technical Report P-03-35, Stockholm, **2003**.
- [26] Börgesson, L., Fälth, B., *Water Saturation Phase of the Tunnel Backfill in the KBS-3V Concept and its Influence on the Wetting of the Buffer*, Preliminary Report, Clay Technology AB, **2004**.
- [27] Hartley, L., Cox, I., Holton, D., Hunter, F., Joyce, S., Gylling, B., Lindgren, M., *Groundwater Flow and Radionuclide Transport Modeling Using CONNECTFLOW in Support of the SR Can Assessment*, SKB, Technical Report R-04-61, Stockholm, **2004**.
- [28] Laaksoharju, M., Gimeno, M., Auqué, L., Gómez, J., Smellie, J., Tullborg, E.L., Gurban, I., *Hydrogeochemical Evaluation of the Forsmark Site, Model Version, 1.1*. SKB, Technical Report R-04-05, Stockholm, **2004**.
- [29] Arcos, D., Grandia, F., Enviros, C.D., *Geochemical Evolution of the Near Field of a KBS-3 Repository*, SKB, Technical Report TR-06-16, Stockholm, **2006**.
- [30] Tarandi, T., *Calculated Temperature Field in and Around a Repository for Spent Nuclear Fuel*, SKB, Technical Report TR 83-22, Stockholm, **1983**.
- [31] Thunvik, R., Braester, C., *Heat Propagation from a Radioactive Waste Repository. SKB 91 Reference Canister*, SKB, Technical Report TR 91-61, Stockholm, **1991**.
- [32] Ageskog, L., Jansson, P., *Äspö Hard Rock Laboratory-Prototype Repository-Finite Element Analyses of Heat Transfer and Temperature Distribution in Buffer and Rock*, SKB, Technical Report HRL-98-20, Stockholm, **1998**.

- [33] *Outline Design for a Reference Repository Concept for UK High Level Waste/Spent Fuel*, Nirex Ltd. Technical Note, 502644, Didcot, **2005**.
- [34] Poston, D.I., Trellue, H.R., *User's Manual Version 2.0 for Monteburns, Version 1.0*, LA-UR-99-4999, Los Alamos National Laboratory, **1999**.
- [35] Chesson, K.E., *A One-Group Parametric Sensitivity Analysis for the Graphite Isotope Ratio Method and other Related Techniques Using Origen 2.2*, Master Thesis, Texas University, **2007**.
- [36] Özdemir, L., Acar Bulut, B., Zabunoğlu, O., Determination of Fissile Fraction in MOX (mixed U+Pu oxides) Fuels for Different Burnup Values, *Annals of Nuclear Energy*, 38(2-3), 540, **2011**.
- [37] Zabunoğlu, O., Determination of Enrichment of Recycle Uranium Fuels for Different Burnup Values, *Annals of Nuclear Energy*, 35, 285-90, **2008**.
- [38] Put, M., Henrion, P., *Modeling of Radionuclide Migration and Heat Transport from an HLW-Repository in Boom Clay*, EC, Report EUR 14156, Luxembourg, **1992**.
- [39] *Design Premises for Canister for Spent Nuclear Fuel*, SKB, Technical Report TR-98-08, Stockholm, **1998**.
- [40] IAEA, *Geological Disposal of Radioactive Waste: Technological Implications for Retrievability*, Nuclear Energy Series, Vienna, **2009**.
- [41] Anonym, <http://www.bfs.de/en/endlager/standortfindung> (Ocak, **2013**)
- [42] Huebner, K.H., Dewhirst, L.E., Byrom, G., *The Finite Element Method for Engineers*, John Wiley and Sons Ltd., **2001**.
- [43] Rao, S.S., *The Finite Element Method in Engineering*, Elsevier Butterworth Heinemann, **2005**.
- [44] Lewis, R.W., Nithiarasu, P., Seetharamu, K.N., *Fundamentals of the Finite Element Method for Heat and Fluid Flow*, John Wiley and Sons Ltd., **2004**.
- [45] Madenci, E., Güven, İ., *The Finite Element Method and Applications in Engineering Using Ansys*, Springer Science and Business Media, LLC, **2006**.
- [46] *ANSYS Modeling and Meshing Guide*, Ansys Inc., U.S.A., **2009**.
- [47] Choi, H.J., Choi, J., Double-layered Buffer to Enhance the Thermal Performance in a High-level Radioactive Waste Disposal System, *Nuclear Engineering and Design*, 238, 2815-2820, **2008**.
- [48] Lee, S.Y., Hensel, S.J., De Bock, C., *Thermal Analysis of Geologic High Level Radioactive Waste Packages*, SRNS-STI-2010-00244, Savannah River Nuclear Solutions LLC, **2010**.
- [49] *Heat Propagation in and Around the Deep Repository. Thermal Calculations Applied to Three Hypothetical Sites: Aberg, Beberg and Ceberg*, SKB Technical Report TR-99-02, Swedish Nuclear Fuel and Waste Management Co., Stockholm, **1999**.
- [50] IAEA, *Implications of Partitioning and Transmutation in Radioactive Waste Management*, Technical Report Series No.435, Vienna, **2004**.

- [51] Bergelson, B.R., Gerasimovi, A.S., Tikhomirovi, G.V., Radiotoxicity and Decay Heat Power of Spent Nuclear Fuel of VVER Type Reactors at Long-term Storage, *Radiation Protection Dosimetry*, 115, No.1-4, 445-447, **2005**.
- [52] Trellue, H.R., *Reduction of the Radiotoxicity of Spent Nuclear Fuel Using a Two-tiered System Comprising Light Water Reactors and Accelerator-Driven Systems*, LA-14052-T, Los Alamos National Laboratory, **2003**.

RESUME

Name Surname : Banu BULUT ACAR
Birth Place : Ankara, TURKEY
Birth Date : December 05, 1978
Marital Status : Married
e-mail : banubulut.acar@taek.gov.tr

Education

High School : İzmir A.A.S High School, 1994 - 1996
B.S. : Hacettepe University, Dep. of Nuclear Eng., 1996 - 2002
M.Sc. : Hacettepe University, Dep. of Nuclear Eng., 2002 - 2005
Ph.D. : Hacettepe University, Dep. of Nuclear Eng., 2005 – 2013

Language

English

Experience

2006 - today : Turkish Atomic Energy Authority, Ankara, Engineer.
2002 - 2006 : H.U. Nuclear Engineering Dept., Ankara, Research Assistant.

Area of Interests

Nuclear Fuel Cycle, Radioactive Waste Management, ANSYS, MonteBurns, Radiation Protection.

Publications

Özdemir, L., Acar Bulut, B., Zabunoğlu, H.O., Determination of Fissile Fraction in MOX (mixed U+Pu oxides) Fuels for Different Burnup Values, *Annals of Nuclear Energy*, 38(2-3), 540-546, 2011.

Acar Bulut, B., Zabunoğlu H.O., Comparison of the Once-Through and Closed Nuclear Fuel Cycles with Regard to Waste Disposal Area Required in a Geological Repository, *Annals of Nuclear Energy*, 60,172-180, 2013.

